Technical Reports   Arkansas Water Resources Center

1-1-1980

An Analysis of the Irreversible Thermodynaics Model for Coupled Heat and Moisture Transport Phenomena in Unsaturated Porous Media

J. A. Havens
University of Arkansas, Fayetteville

Recommended Citation

AN ANALYSIS OF THE
IRREVERSIBLE THERMODYNAMICS MODEL
FOR COUPLED HEAT AND MOISTURE TRANSPORT
PHENOMENA IN UNSATURATED POROUS MEDIA

by
J.A. Havens
Department of Chemical Engineering

UAWRRC

Arkansas Water Resources Research Center

PROJECT COMPLETION REPORT

PROJECT NO.   A-042-ARK   AGREEMENT NO.: 14-31-0001-6004

Starting Date: June, 1976   Ending Date: September, 1979

AN ANALYSIS OF THE IRREVERSIBLE THERMODYNAMICS MODEL
FOR COUPLED HEAT AND MOISTURE TRANSPORT
PHENOMENA IN UNSATURATED POROUS MEDIA

by

J. A. Havens
Department of Chemical Engineering

Arkansas Water Resources Research Center
UNIVERSITY OF ARKANSAS

in cooperation with

Engineering Experiment Station
UNIVERSITY OF ARKANSAS

Fayetteville, Arkansas   72701

January, 1980

i

ABSTRACT

The Irreversible Thermodynamics-based model for the description of coupled heat and moisture transfer, attributed to Cary and Taylor, was analyzed. The transport coefficients appearing in the model equations were independently determined, and the equations were numerically integrated to predict temperature and moisture content profiles for a closed system of water unsaturated glass beads.

An experimental investigation of the moist glass beads medium provided measurements of steady-state profiles of local temperatures and moisture content. These data, when compared with model predictions, indicated the validity of the Irreversible Thermodynamics approach. The coupling coefficient relating thermal gradients to moisture flux was found to be strongly moisture-dependent. The coupling coefficient which relates moisture content gradient to heat flux was found to be extremely small, and the heat flux associated with the moisture content gradient proved to be negligible.

ACKNOWLEDGEMENTS

TABLE OF CONTENTS

LIST OF TABLES

LIST OF FIGURES

CHAPTER 1

INTRODUCTION

Simultaneous transport of heat and mass in porous media occurs widely in natural and industrial processes. An understanding of the associated phenomenology is applicable, for example, to industrial processes such as recovery of petroleum from underground sources, process drying of granular materials, heat and mass transfer in packed beds, and in heat pipe technology. Simultaneous heat and moisture transport in soil occur as a result of diurnal and seasonal temperature fluctuations. Engineered systems involving soil heating with power plant condenser effluent for enhancing agricultural yields, and irrigation, particularly with warm water, portend a need for predictive theories for such processes.

Temperature gradients can induce water movement in porous media. For example, if a sealed column filled with an unsaturated porous medium of uniform moisture content is subjected to a temperature gradient, moisture movement occurs, and ultimately a steady-state moisture content profile is established in the column. Such a structure would not be anticipated from classical phenomenological relationships such as Darcy's Law. Thus, it is "observed" that moisture transfer in unsaturated porous media occurs in association with temperature gradients in addition to moisture content gradients. It is commonly asserted that the associated heat and mass transport processes are "coupled".

The Irreversible Thermodynamics (IT) theory which has been used to model coupled heat and moisture transfer processes was examined in

1

the present study. The coupled heat and moisture transfer equations attributed to Cary and Taylor [91] were numerically integrated to obtain temperature and moisture content profiles for a sealed, one-dimensional spherical system of water-unsaturated glass beads. A one-dimensional (spherical) water unsaturated glass bead medium was subjected to known heat flow rates, and the steady-state temperature and moisture content profiles were measured and compared with the Cary and Taylor model predictions.

CHAPTER 2

HISTORICAL AND LITERATURE REVIEW

The study of moisture transfer in porous media was initiated by Darcy [27] who observed that the flux of water through saturated soil is proportional to the imposed pressure gradient, an empirical relation now referred to as Darcy's Law. Buckingham [13] described the flow in an unsaturated porous medium occurring as a result of below-atmospheric water pressure and termed it capillary flow. Darcy's Law was later "extended" to include moisture flow in unsaturated porous media as well, and the coefficient of diffusivity of water in unsaturated media was defined [24]. Procedures for numerical treatment of the unsaturated flow Darcy equation with different kinds of boundary conditions have been proposed, and the literature is replete with examples of numerical solutions for various boundary conditions.

However, the work described above was restricted to consideration of moisture transfer under isothermal conditions. It was subsequently observed that temperature gradients can cause significant movement of moisture in soil [10, 11], and considerable research effort has been focused on the "energy status" of moisture in unsaturated porous media. Several authors have applied the theory of Equilibrium Thermodynamics to derive property relations among macroscopic variables in water-containing porous media [7, 32, 36, 108].

Simultaneously, efforts were made to establish transport equations for the transfer of heat in porous media and to determine the thermal properties of porous media. A complete theoretical

description is difficult, since a moist porous medium is a three-phase system (solid phase, liquid water, and a gas phase), and transfer of heat is invariably "coupled" to moisture movement. However, the special case of "pure" (Fourier) heat transfer has been considered, and the transport equations thus obtained have been solved for boundary conditions of practical interest [58, 59, 60, 95, 106]. Furthermore, experimental determination of the "effective" thermal conductivity of the porous medium, for use in these heat conduction equations, has been reported [46, 69, 70, 82].

In order to obtain a clearer understanding of the transport processes in a porous, three-phase system, it is necessary to formulate equations for describing the simultaneous or coupled transport of heat and mass species present. Research in this area has evolved along two paths: the classical Soil Physics approach and the phenomenological formalism of the Thermodynamics of Irreversible Processes.

The Soil Physics approach pioneered by Philip and deVries [78, 79, 97, 98, 99, 100] suggests modified forms of Fick's Law and Darcy's Law for vapor and liquid transfer of moisture in porous media. Philip and deVries developed equations for describing the coupled heat and moisture transfer phenomena from the theories of heat and mass transfer in soils and from a knowledge of the soil structure. This model, however, does not provide guidance for determining the transport coefficients appearing in the model equations. Numerous reports of application of the Philip and deVries model have been made. These include extensions of the model to different types of soils, attempts to estimate the transport coefficients, and solutions of the model equations for various boundary conditions [2, 23, 31, 33, 35, 40, 44,

45, 47, 51, 53, 55, 56, 61, 62, 64, 83, 84, 85, 88, 103, 105, 110].
However, these investigations have not established a conclusive quantita-
tive description in agreement with experimental evidence, primarily
because of the difficulty of determining the transport coefficients.

The Irreversible Thermodynamics approach, in contrast to the
Soil Physics approach, does not require as detailed an understanding of
the mechanism of heat and mass transfer or of the porous medium struc-
ture. It is a phenomenological theory, which postulates linear rela-
tions between "fluxes" of heat and mass and "thermodynamic forces" iden-
tified by the entropy production equation. This application of the
theory of Irreversible Thermodynamics was proposed by Cary and Taylor
as a special application of the general case involving transfers of heat
and several species in a porous medium system [20, 21, 22, 90, 91, 92].
It has since been extended by Cary to the consideration of the model's
limitations and its application to systems of practical interest [15,
16, 17, 18, 19]. One apparent advantage of the Cary and Taylor model
over the Philip and deVries model is that it provides definitions of the
coupling coefficients which facilitates their determination and subse-
quent use in the model equations. Other investigators have discussed
the determination of the phenomenological coefficients and the applica-
tion of the model to various porous media systems [1, 9, 14, 38, 41, 49,
55, 56, 81, 89]. To the author's knowledge, Gee [38] and Jury [55, 56]
have made the only experimental attempts to quantitatively determine the
coupling effects. Gee reported a significant increase in moisture
transfer when a temperature gradient was applied to a soil column. He
obtained values of the coupling coefficient relating the moisture flux
to the temperature gradient. Jury also reported a strong effect of

temperature gradient on moisture flux. Jury's data indicate negligible
heat flux associated with moisture content gradient. He performed two
experiments: a closed column one with zero net steady-state moisture
flux and an open column experiment with zero heat flux. Jury solved the
four simultaneous algebraic transport equations describing these two
experiments. The solution provided the values of the four phenomenolo-
gical coefficients in these equations. Jury also reported relations
between the coefficients appearing in the Cary and Taylor model equa-
tions and those in the Philip and deVries transport equations.

None of the work mentioned so far has, however, verified the
Cary and Taylor model by solving a boundary value problem involving the
phenomenological equations, conducting the corresponding laboratory
experiment with a porous medium system, and comparing the experimental
measurements with model predictions.

CHAPTER 3

THERMODYNAMICS OF IRREVERSIBLE PROCESSES

Irreversible Thermodynamics, the development of which is frequently associated with Onsager [74], Meixner [66], and Prigogine [39, 80], is a comparatively recent and developing subject. While Equilibrium Thermodynamics or "thermostatics", deals with the study of equilibrium states of physical and chemical systems, Non-equilibrium or Irreversible Thermodynamics attempts a phenomenological description of systems undergoing irreversible processes. Such processes are characterized by the presence of fluxes (transport) of mass and/or different forms of energy.

Although Irreversible Thermodynamics has recently been extended to the consideration of nonlinear system behavior [39, 63], the present discussion is limited to the theory of Linear Irreversible Thermodynamics, which has been described in several standard works [28, 34, 39, 43, 63, 80]. In this chapter, the basic principles of Linear Irreversible Thermodynamics are briefly summarized.

The entropy change of any system (defined by a closed surface in three-dimensional space) during an accounting period δt may be written as

$$dS = d_e S + d_i S, \qquad (3.1)$$

where

$d_e S$ is the total entropy transferred from the surroundings to system during the accounting period. The quantity $d_e S$, in

7

general, may be negative, zero or positive depending on the nature of the interactions of the system with its surroundings.

$d_i S$ is the entropy production within the system during the accounting period, which results from irreversible processes.

According to the Second Law of Thermodynamics,

$$d_i S > 0 \text{ for all real processes.} \tag{3.2}$$

Invoking the so-called assumption of "local equilibrium", the local (specific) entropy $\underline{S}$ is assumed related to the local values of the macroscopic state variables by the fundamental property relationship (Gibbs Equation) of Equilibrium Thermodynamics. The resulting equation, which relates the local entropy to internal energy, volume and composition, is

$$\frac{d\underline{U}}{dt} = T\frac{d\underline{S}}{dt} - P\frac{d\underline{V}}{dt} + \sum_i \mu_i \frac{dC_i}{dt} . \tag{3.3}$$

Application of balance (conservation) equations for mass and energy and subsequent utilization of Equation (3.3) leads to an entropy accountability relationship of the form

$$\frac{d\underline{S}}{dt} = \frac{d_e\underline{S}}{dt} + \sigma . \tag{3.4}$$

The local rate of entropy production σ is always nonnegative, and has the bilinear form

$$\sigma = \sum_i J_i X_i \qquad (3.5)$$

where J_i is the ith "thermodynamic flux",

$\quad\quad X_i$ is the ith "thermodynamic force".

The fluxes J_i appearing in the entropy production term are related to the familiar heat flux, mass flux, electrical current, etc., and the thermodynamic forces X_i are the gradients of intensive properties of the system (or functions thereof).

It has been experimentally observed that the thermodynamic fluxes and forces appearing in the entropy balance equation can be related by empirical rate expressions. In general, the fluxes and forces may be described by the phenomenological expressions [43]

$$J_i = \sum_k L_{ik} X_k , \qquad (3.6)$$

where L_{ik} are known as the phenomenological coefficients.

Equation (3.6) expresses the "Irreversible Thermodynamics" postulate that each thermodynamic flux is linearly related to all of the thermo-dynamic forces. The phenomenological coefficients may be functions of the intensive properties of the system such as temperature and pressure but not of the forces.

An important relation between the phenomenological coefficients, generally assumed valid within the linear region, is the Onsager reciprocal relation [74]

$$L_{ik} = L_{ki} . \qquad (3.7)$$

Equation (3.7) states that the matrix of phenomenological coefficients L_{ik} is symmetric, which reduces the number of unknowns in the transport equations.

Equation (3.7), which was derived by Onsager for a rather restricted class of relaxation processes using the principle of "microscopic reversibility" from statistical mechanics, has been verified experimentally for a large number of processes [67].

CHAPTER 4

DEVELOPMENT OF THE COUPLED HEAT AND

MOISTURE TRANSFER MODEL

The first development of an Irreversible Thermodynamics-based model for coupled heat and moisture transfer in unsaturated porous media is commonly attributed to Taylor and Cary [91]. In this chapter, the development by Taylor and Cary will be described to illustrate the Irreversible Thermodynamics theoretical approach to this problem. Concurrently, questions raised during the present work relating to the formulation of the entropy balance equation for this process and the identification of the associated thermodynamic "driving" forces for heat and mass fluxes are discussed.

The following simplifying assumptions are made in Taylor and Cary's development of the model equations for the coupled transfer of matter and energy in a continuous porous medium system:

1. The concept of "local equilibrium", which holds that the Gibbs equation of Equilibrium Thermodynamics (which provides an equation of state for entropy in equilibrium systems), applies <u>locally</u> in non-equilibrium or continuous systems. This is a fundamental, underlying assumption of the theory of Irreversible Thermodynamics.

2. An idealized, chemically inert, porous medium is considered, and effects other than heat and moisture transfers are neglected.

3. Moisture transfer is liquid phase, and the moisture content of the porous medium is sufficiently high that a continuous liquid phase exists. This assumption is implicit in Taylor and Cary's restriction of the "general" equations to the case with water being the only form of flowing matter, and in particular to single component flow (i.e., no diffusion).

4. The system is never "far" from equilibrium, so that the fluxes can be described by linear phenomenological equations.

5. The "water potential" is a unique function of the moisture content. (The identification of the water potential with local thermodynamic properties will be discussed below.)

6. Hysteresis effects are neglected.

Phenomenological equations are first developed for the transport of energy and several species in a general multicomponent system. These equations are then specialized to describe heat and liquid moisture transfer in porous media. Considering an open, multicomponent thermodynamic system but excluding chemical reaction, the equation of change for component mass is [43]

$$\rho \frac{DC_i}{Dt} = -\nabla \cdot J_i \, ,$$

(4.1)

where ρ is the total mass density of the system,

$\frac{D}{Dt}$ is the substantial derivative operator,

$C_i = \frac{\rho_i}{\rho}$ is the mass fraction of component i,

ρ_i is the mass density of component i,

J_i is the "diffusive" flux of component i,

or $\rho_i(v_i - v)$, v_i is the velocity of component i,

and v is the mass average velocity, or $\sum_i C_i v_i$,

and ∇ is the gradient operator.

The equation of change for total internal energy, neglecting external forces and viscous dissipation effects, is [43]

$$\rho \frac{DU}{Dt} = -\nabla \cdot J_Q - P \nabla \cdot v \; ,^*$$

(4.2)

where $\underline{U}$ is the specific internal energy,

J_Q is the thermodynamic heat flux,

and P is the pressure.

---

*It will be seen later that this form of the internal energy balance, when used in conjunction with Equations (4.1) and (4.3), leads to an entropy balance which requires a reinterpretation of "heat" transfer (defined in classical Equilibrium Thermodynamics as being strictly separable from energy transfers associated with mass transfer). This problem has been discussed and proposals for its clarification offered [111]. The application of the equations derived herein to a closed (zero mass flux) system renders these difficulties moot; however, verification of the Taylor and Cary model for open systems in which the mass flux is not zero requires attention to this problem.

The fundamental property relation, or Gibbs equation, which applies <u>locally</u>, is [43]

$$T \frac{DS}{Dt} = \frac{DU}{Dt} + P \frac{DV}{Dt} - \sum_{i=1}^{n} \mu_i \frac{DC_i}{Dt} , \qquad (4.3)$$

where $\underline{S}$ is the specific entropy,

$\quad\underline{V}$ is the specific volume, $1/\rho$,

and μ_i is the chemical potential of component i.

Combination of Equations (4.1), (4.2), and (4.3) gives, after some algebraic manipulations,

$$\rho \frac{DS}{Dt} = -\frac{1}{T} \nabla \cdot J_Q + \sum_{i=1}^{n} \frac{\mu_i}{T} \nabla \cdot J_i . \qquad (4.4)$$

Noting that

$$\frac{1}{T} \nabla \cdot J_Q = \nabla \cdot \frac{J_Q}{T} + \frac{J_Q}{T^2} \cdot \nabla T$$

and

$$\frac{\mu_i}{T} \nabla \cdot J_i = \nabla \cdot \frac{\mu_i J_i}{T} - J_i \cdot \nabla \frac{\mu_i}{T} , \qquad (4.5)$$

and utilizing the definition of the substantial derivative, Equation (4.4) can be rewritten as

$$\frac{\partial \rho \underline{S}}{\partial t} = -\nabla \cdot \left\{ \rho \underline{S} v + \frac{J_Q}{T} - \sum_{i=1}^{n} \frac{\mu_i J_i}{T} \right\}$$

(4.6)

$$- \left\{ \frac{J_Q}{T^2} \cdot \nabla T + \sum_{i=1}^{n} J_i \cdot \nabla \frac{\mu_i}{T} \right\} \quad .$$

Further, noting that

$$\mu_i = \overline{H}_i - T \overline{S}_i$$

(4.7)

where the overbar denotes partial properties, i.e.,

$$\overline{H}_i = \left(\frac{\partial H}{\partial m_i} \right)_{T,P,m_j} \quad ,$$

Equation (4.6) becomes

$$\frac{\partial \rho \underline{S}}{\partial t} = -\nabla \cdot \left\{ \rho \underline{S} v + \sum_{i=1}^{n} J_i \overline{S}_i - \sum_{i=1}^{n} \frac{J_i \overline{H}_i}{T} + \frac{J_Q}{T} \right\}$$

$$- \left\{ \frac{J_Q}{T^2} \cdot \nabla T + \sum_{i=1}^{n} J_i \cdot \nabla \frac{\mu_i}{T} \right\} \quad .$$

(4.8)

Since $\rho \underline{S} v + \sum_{i=1}^{n} J_i \overline{S}_i = \sum_{i=1}^{n} \rho_i v_i \overline{S}_i$, Equation (4.8) reduces to

$$\frac{\partial \rho S}{\partial t} = -\nabla \cdot \left\{ \sum_{i=1}^{n} \rho_i v_i \bar{S}_i - \sum \frac{J_i \bar{H}_i}{T} + \frac{J_Q}{T} \right\}$$

$$- \left\{ \frac{J_Q}{T^2} \nabla T + \sum_{i=1}^{n} J_i \cdot \nabla \frac{\mu_i}{T} \right\} \ . \tag{4.9}$$

The first term in the brackets on the RHS of Equation (4.9) is commonly interpreted as the <u>transfer</u> of entropy between the system and surroundings due to mass and heat transfers, while the second bracketed term represents the entropy <u>production</u> associated with irreversible processes taking place in the system. A redefinition of thermodynamic heat flux (see footnote, page 13) is then made as follows. Noting that

$$\nabla \frac{\mu_i}{T} = \frac{(\nabla \mu_i)_T}{T} - \frac{\bar{H}_i}{T^2} \nabla T \tag{4.10}$$

where $(\nabla \mu_i)_T$ denotes evaluation at a given temperature, and defining the calorimetric heat flux J_q as

$$J_q = J_Q - \sum_{i=1}^{n} J_i \bar{H}_i \ , \tag{4.11}$$

Equation (4.9) becomes

$$\frac{\partial \rho S}{\partial t} = -\nabla \cdot \left\{ \sum_{i=1}^{n} \rho_i v_i \bar{S}_i + \frac{J_q}{T} \right\}$$

$$- \left\{ \frac{J_q}{T^2} \cdot \nabla T + \sum_{i=1}^{n} \frac{J_i}{T} \cdot (\nabla \mu_i)_T \right\} \ . \tag{4.12}$$

The local volumetric rate of entropy production is therefore

$$\sigma' = - \frac{J_q}{T^2} \cdot \nabla T - \sum_{i=1}^{n} \frac{J_i}{T} \cdot (\nabla \mu_i)_T ,$$

and the dissipation function (rate of lost work) is

$$T\sigma' = -J_q \cdot \nabla \ln T - \sum_{i=1}^{n} J_i \cdot (\nabla \mu_i)_T . \tag{4.13}$$

The fluxes in Equation (4.13) are then assumed related to the associated forces identified in the equation by the linear phenomenological expressions

$$J_i = - \sum_{k=1}^{n} L_{ik}(\nabla \mu_i)_T - L_{iq} \nabla \ln T \tag{4.14}$$

and

$$J_q = - \sum_{k=1}^{n} L_{qk}(\nabla \mu_i)_T - L_{qq} \nabla \ln T , \tag{4.15}$$

where the phenomenological coefficients are related by the Onsager relations [74],

$$\left. \begin{array}{l} L_{ik} = L_{ki} \\[2em] \text{and} \\[2em] L_{iq} = L_{qi} \end{array} \right\} \tag{4.16}$$

Considering water the only species transferred, Equations (4.14) and (4.15) reduce to

$$J_w = -L_{ww} \, (\nabla \mu_w)_T - L_{wq} \, \nabla \ln T \tag{4.17}$$

and

$$J_q = -L_{qw} \, (\nabla \mu_w)_T - L_{qq} \, \nabla \ln T \ . \tag{4.18}$$

Following Taylor and Cary, the "water potential" ψ is defined as the difference in chemical potential between water in the porous medium and pure free water [91], i.e.,

$$\psi = \mu_w - \mu_w^0$$

where the chemical potential of pure free water, μ_w^0, is a constant; hence

$$\nabla \mu_w = \nabla \psi \ . \tag{4.19}$$

Substitution of Equation (4.19) in Equations (4.17) and (4.18) gives

$$J_w = -L_{ww} \nabla \psi - L_{wq} \nabla \ln T \quad ^* \qquad (4.20)$$

and

$$J_q = -L_{qw} \nabla \psi - L_{qq} \nabla \ln T \quad , \qquad (4.21)$$

which describe the coupled flows of heat and moisture in a porous medium.

When a sealed column of unsaturated porous medium is subjected to a constant temperature gradient, the steady-state moisture flux is zero, and Equation (4.20) reduces to

$$0 = -L_{ww} \nabla \psi - L_{wq} \nabla \ln T \quad , \qquad (4.22)$$

---

*The careful reader has noted that the isothermal gradient of the water potential, $(\nabla \psi)_T$, has been dropped in favor of $\nabla \psi$. Such an assumption appears justified in practice since the water potential is a much stronger function of moisture content than of temperature. This is probably more apparent from consideration of the temperature dependence of air-water surface tension which undoubtedly is a major component of the water potential as defined by Taylor and Cary.

which can be simplified to give

$$\frac{\nabla \psi}{\nabla \ln T} = -\frac{L_{wq}}{L_{ww}} = -\beta ,$$ (4.23)

which is to be considered the definition of the coefficient β.

Now, rewriting Equation (4.20,

$$J_w = -L_{ww} (\nabla \psi + \beta \nabla \ln T) ,$$ (4.24)

and using the Onsager relation [74], Equation (4.21) becomes

$$J_q = -L_{ww} \beta \nabla \psi - L_{qq} \nabla \ln T .$$ (4.25)

In order to use Equation (4.24) and (4.25) for systems of practical interest, it is necessary to relate ψ to a practically measurable variable. A single-valued functionality between ψ and water content is assumed, so that

$$J_w = -\rho_w D \nabla \theta - L_{wq} \nabla \ln T ,$$ (4.26)

where θ is the volumetric moisture content,

ρ_w is the density of water,

and $D = \frac{L_{ww}}{\rho_w} \frac{d\psi}{d\theta}$ is the coefficient of diffusivity.

At steady-state, in a sealed column, $J_w = 0$, and Equation (4.26) reduces to

$$\frac{\nabla \theta}{\nabla \ln T} = \frac{-L_{wq}}{\rho_w D} = -\beta^* ,\tag{4.27}$$

which is to be considered the definition of the coefficient β^*.

Applying the above relation to Equation (4.26),

$$J_w = -\rho_w D(\nabla \theta + \beta^* \nabla \ln T) ,\tag{4.28}$$

and similarly, using Equation (4.25) and the definition of D given in (4.26)

$$J_q = -\rho_w D \beta \nabla \theta - L_{qq} \nabla \ln T .\tag{4.29}$$

Equations (4.28) and (4.29) are known as the Cary and Taylor model.

CHAPTER 5

DISCUSSION OF TRANSPORT EQUATIONS AND

SOLUTION TECHNIQUE

The Cary and Taylor Irreversible Thermodynamics-based model for coupled heat and liquid moisture transfer in a three dimensional unsaturated porous medium is:

$$J_w = -\rho_w D(\nabla\theta + \beta^* \nabla \ln T) \tag{4.28}$$

$$J_q = -\rho_w D\beta\nabla\theta - L_{qq}\nabla \ln T, \tag{4.29}$$

where J_w is the flux of liquid water,

J_q is the flux of heat,

D is the coefficient of diffusivity of water in the
   unsaturated porous medium,

β^* is the coupling coefficient, defined as $-\nabla\theta / \nabla \ln T$
   at steady-state and zero moisture flux,

β is the coupling coefficient, defined as $-\nabla\psi / \nabla \ln T$
   at steady-state and zero moisture flux

L_{qq} is a phenomenological coefficient $= \lambda T$,

λ is the thermal conductivity of the porous medium,

T is the absolute temperature,

θ is the volumetric moisture content of the porous
   medium,

ρ_w is the density of water,

ψ is the water potential of liquid moisture in the
   porous medium, and

22

∇ is the gradient operator.

The transport coefficients D, β^*, β and L_{qq} have been reported to be strong functions of the volumetric moisture content [38, 50, 55, 91].

It is instructive to consider the case where only one of the gradients $\nabla\theta$ or $\nabla\ln T$ is present in the porous medium. For the case of isothermal equations ($\nabla\ln T = 0$), Equation (4.28) reduces to

$$J_w = -\rho_w D\nabla\theta \ , \tag{5.1}$$

which is a form of the classical Darcy's Law for movement of moisture in an isothermal unsaturated porous medium. Conversely, for heat conduction in a porous medium of uniform moisture content, $\nabla\theta$ is zero, and Equation (4.29) reduces to

$$J_q = -L_{qq}\nabla\ln T = -\lambda\nabla T \ , \tag{5.2}$$

which is the well known Fourier's law of heat conduction. It is thus seen that the theory of Irreversible Thermodynamics permits temperature gradients to be combined with moisture content gradients in the general flow equations of water and heat in unsaturated porous media in such a way that they reduce to the commonly used phenomenological equations under particular conditions.

Further, the general phenomenological Equations (4.28) and (4.29) provide information regarding the interaction between the coupled heat and moisture transfers and some insight into the nature of the phenomenological coefficients. For example, for the isothermal case,

$$J_q = -\rho_w D\beta\nabla\theta \tag{5.3}$$

represents the transport of heat associated with the gradient in moisture content. The magnitude of β will, in such a case, be a measure of the effect of coupling of the moisture content gradient on the heat flux. An evaluation of the coefficient $\rho_w D\beta^*$, or L_{wq}, which is the effect of the ln temperature gradient on the liquid moisture flow, will be considered later in this report. As described in the chapter on the development of the model equations, β^* is measured as the ratio $-\nabla\theta / \nabla \ln T$ in sealed steady-state experiments with zero net moisture flux. A large value of β^* indicates a strong influence of temperature gradient on moisture transfer in open systems.

Irreversible Thermodynamics is a phenomenological theory which does not explain the mechanism of coupling or the reasons for it, but several explanations have been proposed to account for the effects of the thermal gradient on moisture transfer [6, 18]. It has been suggested that since surface tension of an air-water interface decreases with increasing temperature, moisture in an unsaturated porous medium could flow from a warm region to a cooler region due to a surface tension gradient. Another proposed reason for coupled moisture flux is the effect of temperature on the adsorbed layer of moisture on the solid particles. The observation of coupled moisture transfer in a saturated medium has led to the proposal that transfer results from a net motion generated by random kinetic energy changes associated with the hydrogen bond distribution which develops under a thermal gradient [18].

It is possible that one or more of the above effects acts to cause coupling effects between heat and moisture. However, as Beatty [3] points out, it seems constructive to think of coupled heat and

mass transfers as "separable effect" processes. Beatty proposed that coupled processes are two or more macroscopically separable effects resulting from a single microscopic process in which the carrier molecules with higher kinetic energies than the average particles are transported as a result of two or more independently variable macroscopic potentials.

The thermal conductivity coefficient is a measure of the effect of the temperature gradient on the heat flux for the uncoupled case in the absence of moisture content gradients in the unsaturated porous medium. Porous medium thermal conductivity is a function of the moisture content, but its measurement as such is not straightforward since a moisture content gradient invariably accompanies steady state heat transfer.

The coefficient of diffusivity of liquid moisture in an unsaturated porous medium, D, is also a strong function of the moisture content. The coefficient of diffusivity is defined as $K\frac{d\psi}{d\theta}$, where K is the hydraulic conductivity of the porous medium and $d\psi / d\theta$ is the slope of the water potential versus moisture content (the so-called water retention curve), which is also a function of the moisture content.

A verification of the model Equations

$$J_w = -\rho_w D(\nabla\theta + \beta^*\nabla \ln T) \tag{4.28}$$

$$J_q = -\rho_w D\beta\nabla\theta - L_{qq}\nabla \ln T \tag{4.29}$$

can be carried out in the following manner. The transport coefficients D, β^*, β and L_{qq} can be determined independently from separate experiments. With proper initial and boundary conditions, Equations (4.28)

and (4.29) can be integrated, for steady-state conditions, yielding profiles of temperature and moisture contents. These profiles, when compared with experimentally observed temperatures and moisture content values for the system, provide a check of the validity of the model.

For the steady-state condition in a closed spherically symmetrical system of unsaturated porous medium indicated schematically in Figure 1, Equations (4.28) and (4.29) reduce to

$$J_w = 0 = -\rho_w D(\frac{d\theta}{dr} + \beta^* \frac{d \ln T}{dr}) \qquad (5.4)$$

$$J_q = \frac{Q}{4\pi r^2} = -\rho_w D\beta \frac{d\theta}{dr} - L_{qq} \frac{d \ln T}{dr}, \qquad (5.5)$$

where Q is the total steady state heat flow rate.

Equations (5.4) and (5.5) represent a set of nonlinear (due to the functionality of the coefficients) ordinary differential equations which, with two boundary conditions, can be integrated to give T and θ profiles in the annular region. A numerical integration technique utilizing the boundary value problem "shooting method" was used, with the temperature T_1 at radius R_1 as one of the boundary conditions and conservation of the total mass of water in the system as an additional equation of constraint. An initial value of moisture content θ_1, at radius R_1, was initially guessed to start the integration. After integration to the outside sphere radius R_2, the total mass of water in the system was calculated by integration of the predicted moisture profile. If the calculated mass of water was different from the initial mass of water in the system, the initial value θ_1 was iterated and the integration repeated. When the calculated and original masses of
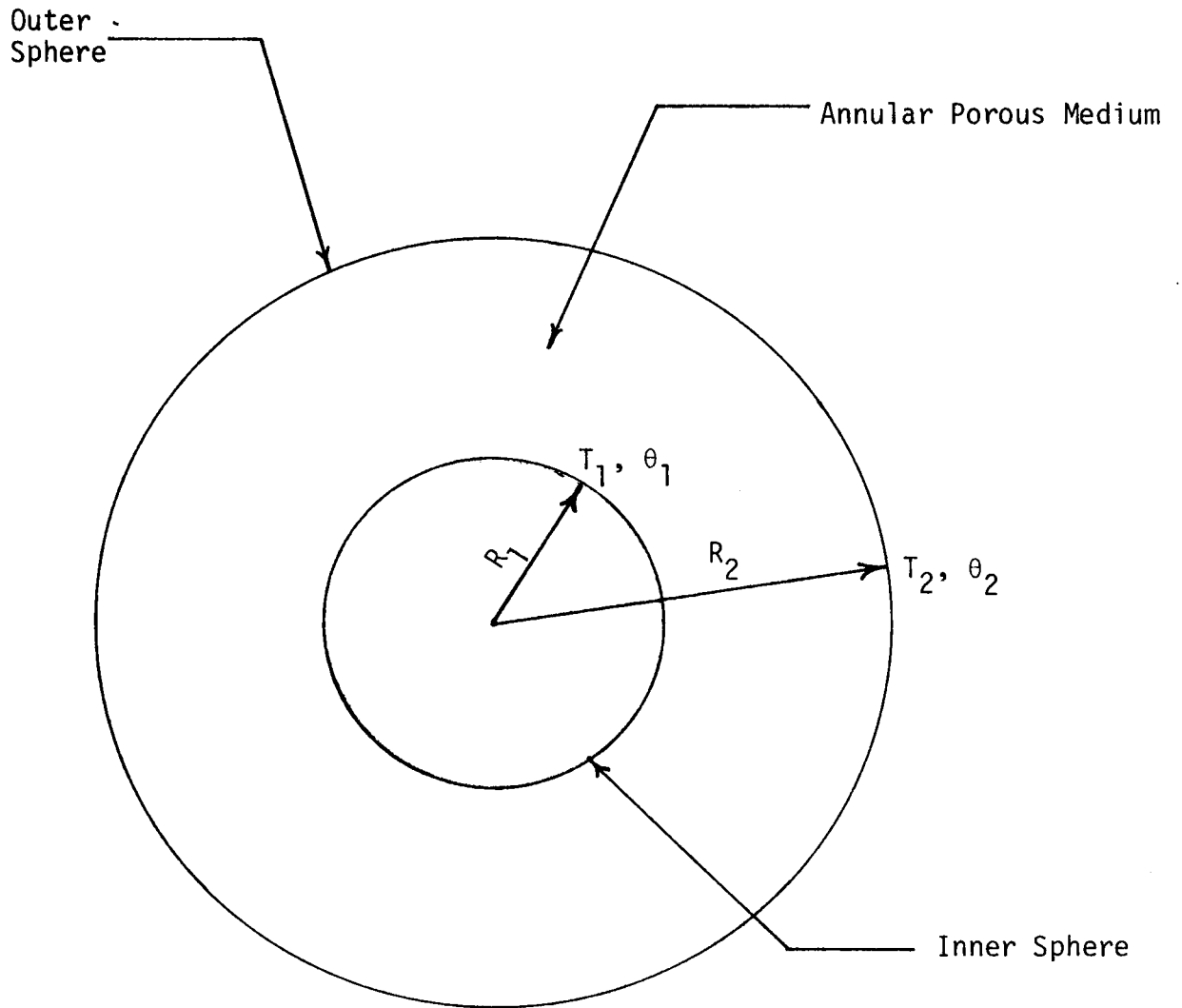
Figure 1. Spherical Porous Medium System

water agreed, the temperature and moisture content profiles thus obtained were the predicted steady-state distributions in these variables for the given system.

The Continuous System Modeling Program (CSMP)[1] was used for the numerical integration. A sample program is given in the Appendix.

---

[1] System 360 Continuous System Modeling Program (360-A-CS-16X), User's Manual, International Business Machines Corporation, Data Processing Division, White Plains, New York.

CHAPTER 6

MEASUREMENT OF TRANSPORT COEFFICIENTS

The transport coefficients thermal conductivity, diffusivity, and the two coupling coefficients were obtained independently from separate experiments, as functions of moisture content.

Thermal Conductivity, λ

The thermal conductivity of an unsaturated porous medium is an "overall" value for the three-phase solid-water-air system.

A steady-state determination of the thermal conductivity coefficient as a function of the volumetric moisture content of the porous medium, from heat flux and temperature gradient measurements, is not straightforward, since moisture transfer results from nonisothermal conditions in such a system. However, a transient method allows measurement of thermal diffusivity, from which thermal conductivity can be determined, before moisture migration occurs. An unsteady-state method for measuring thermal diffusivity of low thermal conductivity materials [25, 75] was used to determine the thermal diffusivity of moist porous media over a range of volumetric moisture contents.

The method is based on the solution of the differential equation for unsteady-state heat conduction in a cylinder,

$$\frac{\partial T}{\partial t} = \alpha \left[\frac{\partial^2 T}{\partial r^2} + \frac{1}{r} \frac{\partial T}{\partial r} \right] , \tag{6.1}$$

with the initial and boundary conditions

29

$T = T_0$ at $t = 0$

$\frac{\partial T}{\partial r} = 0$ at $r = 0$ for $t > 0$

and

$$\lim_{r \to r_m} \frac{\partial T}{\partial r} = -\frac{h}{\lambda}(T_a - T) \text{ for } t > 0$$

where T is the temperature,

T_0 is the initial uniform temperature of sample,

r is the radial distance from center of cylinder,

r_m is the radius of cylinder,

h is the surface heat transfer coefficient,

λ is the thermal conductivity,

T_a is the constant ambient temperature,

and t is the time.

The series solution to Equation (6.1) converges rapidly, and after a time of about one minute is well represented by the simple relation

$$Y = A \, 10^{-bt}, \tag{6.2}$$

$$\text{where } A = \frac{2 \, J_1(x_1)}{x_1 [J_0^2(x_1) + J_1^2(x_1)]} \left[J_0 \left(x_1 \frac{r}{r_m} \right) \right]$$

$$\text{and } b = \frac{-x_1 \alpha}{2.303 \, r_m^2} \tag{6.3}$$

where Y is the ratio of the temperature differences,

$(T_a - T) / (T_a - T_0)$,

A is a constant,

-b is an exponent; graphically, the slope of the

   log Y - t curve,

$J_0(x)$ is a Bessel function of first kind and zero order of x

$J_1(x)$ is a Bessel function of first kind and first order

   of x,

and α is the thermal diffusivity of the porous medium.

Equation (6.2) implies a linear relation between log Y and t with slope -b. For the experimental conditions used in this work, it can be shown that a limiting value of $x_1 = 2.405$ applies [25].

A diagram of the experimental apparatus is shown in Figure 2. Samples of the 210 - 297μ glass beads media were encased in thin-walled aluminum cylinders 15.2 cm long and 1.91 cm in diameter. A 0.1191 cm diameter two-bore ceramic thermocouple insulator supported a Chromel-Alumel thermocouple junction near the center of the sample. After allowing the sample temperature to equilibrate with the room temperature, T_0 (20°C), the cylinder was immersed in the constant temperature (T_a) water bath, and the thermocouple temperature, T, recorded as a function of time.

The recorded temperature was used in Equation (6.2) to graphically determine the slope, -b, from which the thermal diffusivity was calculated from Equation (6.3). Thermal conductivity was determined from the relation
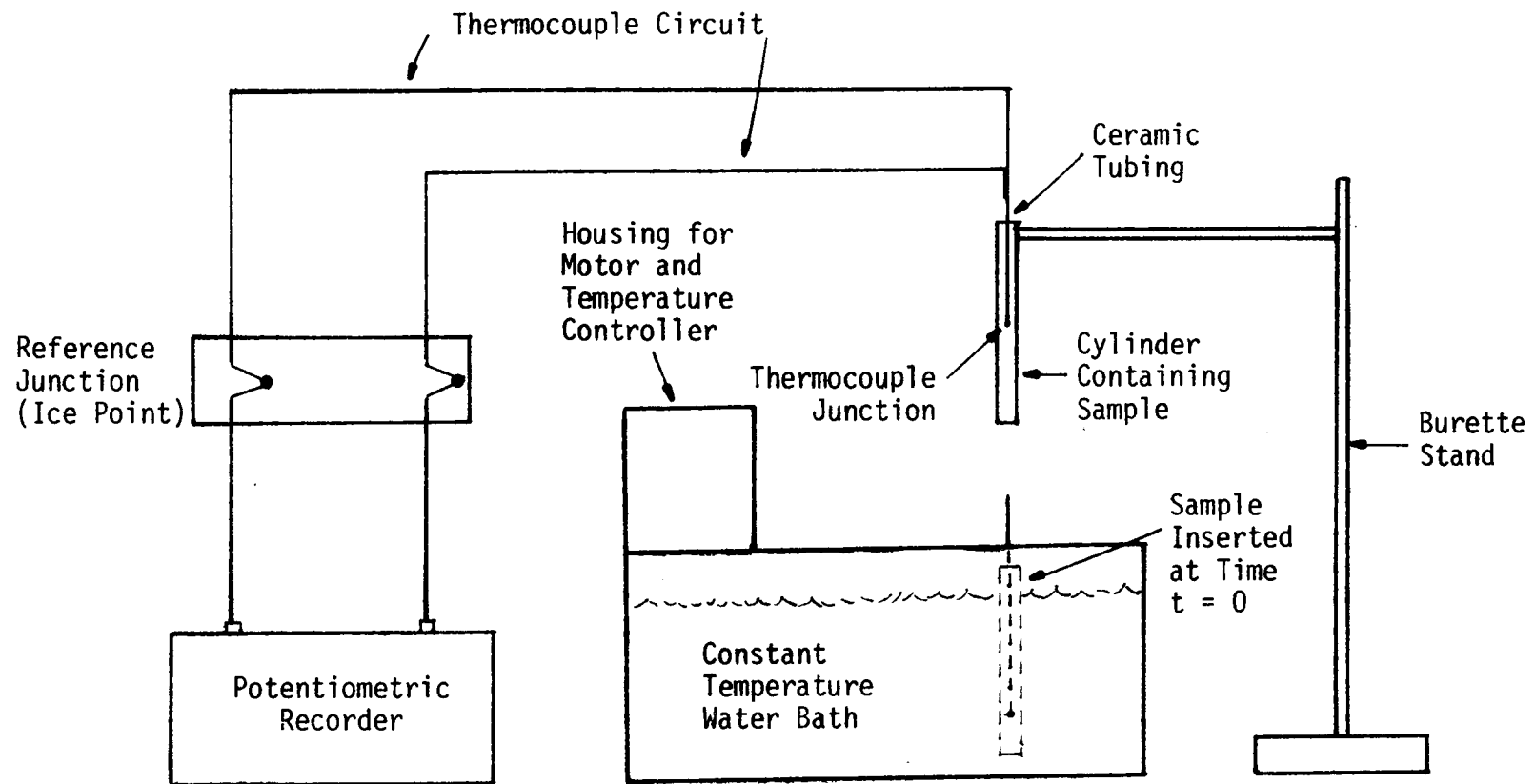
$$\lambda = \alpha \rho c \qquad (6.4)$$

Figure 2. Schematic of Experimental Apparatus for Thermal Conductivity Determination

where the volumetric heat capacity, ρc, was calculated as the volume weighted average of the heat capacities of the sample constituents, glass, water and air. Measurements were made with bath temperatures of 30° C, 35° C and 40° C. Thermal diffusivities calculated therefrom differed by less than 3%, which is within the expected experimental error.

A typical plot of log Y versus t for the moist glass beads medium is shown in Figure 3. The measured temperature approaches the final equilibrium value $Y \leq 0.05$ in about six minutes for the dry sample and three minutes for the moist sample. The transient period for the moist medium is long enough to satisfy the requirements for the model approximation (series convergence) but short enough to preclude significant moisture redistribution in the sample. Thermal diffusivities and conductivities for the glass bead medium are plotted as functions of volumetric moisture content in Figure 4. The thermal diffusivity of the beads was found to increase from 0.0013 cm^2/sec for dry beads to 0.003 cm^2/sec at 5% volumetric moisture content, above which it remains essentially constant with increasing moisture content, while the thermal conductivity of the porous medium increases from a value of 0.53 mcal/$^\circ$C cm sec for dry beads to 1.97 mcal/$^\circ$C cm sec for saturated beads.

Diffusivity, D

The diffusivity D of water in an unsaturated porous system is a strong function of the moisture content and is defined by the relationship

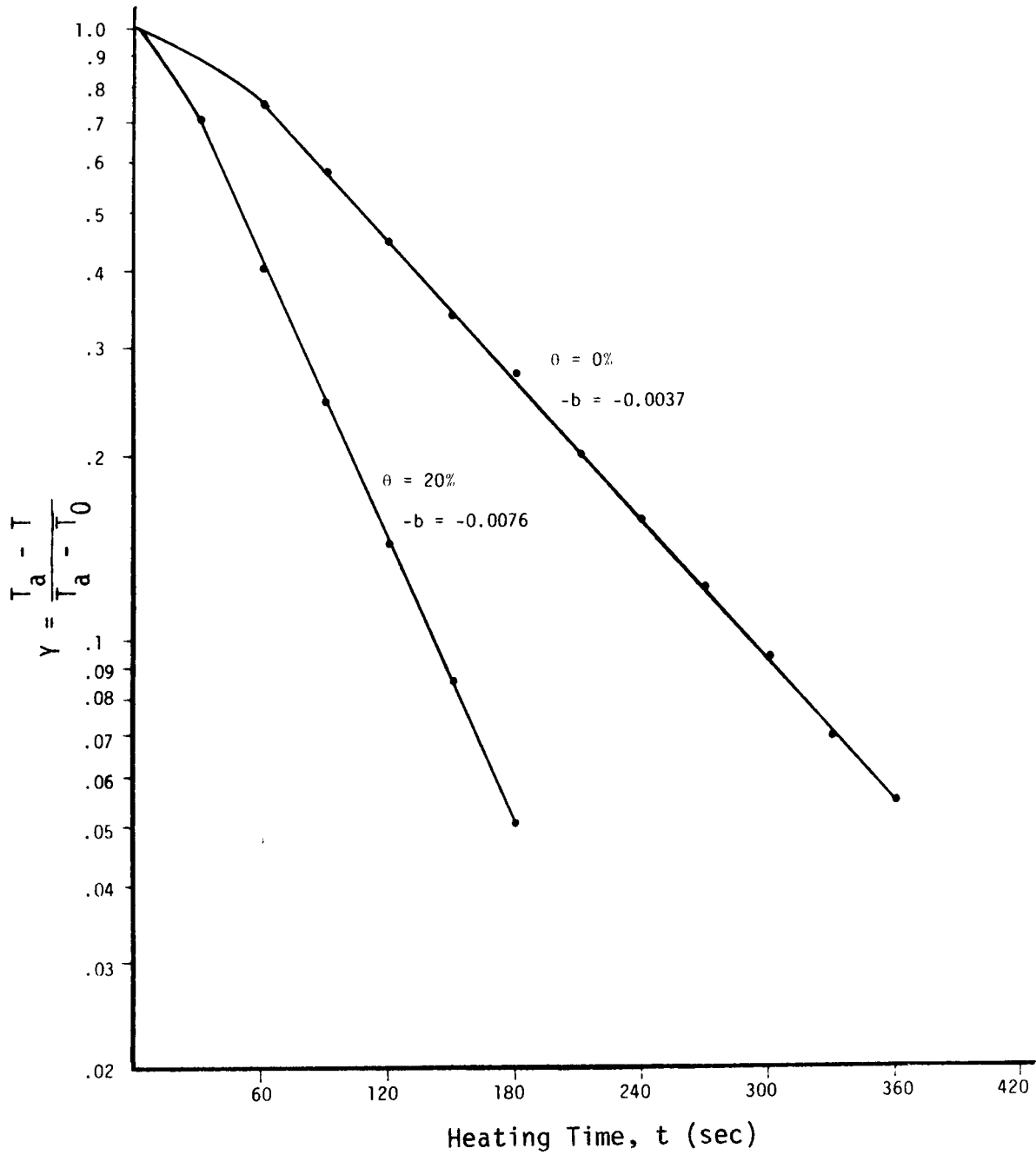$$D = K\frac{d\psi}{d\theta} \; , \tag{6.5}$$

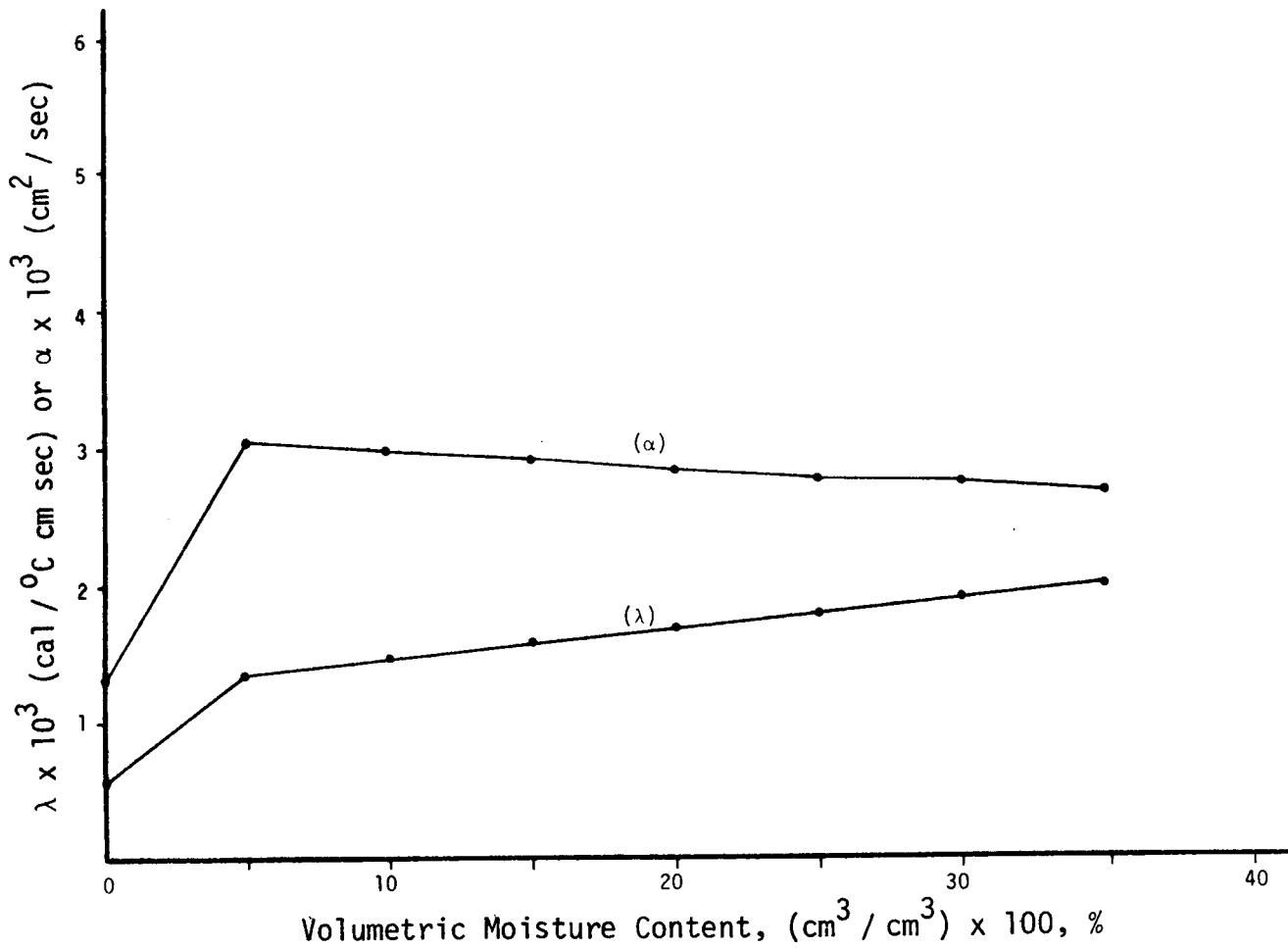Figure 3. Typical Heating Curves for Glass Beads

Figure 4.   Thermal Conductivity λ and Thermal Diffusivity α
            vs. Volumetric Moisture Content θ

where K is the unsaturated hydraulic conductivity,

ψ is the water potential,

and θ is the volumetric moisture content.

Independent determinations were made of K and $\frac{d\psi}{d\theta}$ over a wide range of moisture contents and were then substituted in Equation (6.5) to obtain values of D as a function of volumetric moisture content.

A predictive method which has been used by soil physicists to determine the hydraulic conductivities of glass beads and soils [42] was employed to obtain K values for the 210 - 297 μ glass beads - water system of the present study. The method involved experimental determination of the hydraulic conductivity value at one moisture content (the saturated hydraulic conductivity) and substitution into the following equation to calculate K values for other values of moisture content:

$$K(\theta)_i = \frac{K_s}{K_{sc}} \cdot \frac{30 \delta^2}{\rho_w g \eta} \cdot \frac{\varepsilon^p}{n^2} \sum_{j=1}^{m} [(2j + 1 - 2i)h_j^{-2})] \, ,$$

$$k = 1, 2, \ldots, m \qquad (6.6)$$

where $K(\theta)_i$ is the hydraulic conductivity for a specified water content or pressure,

θ is the moisture content,

i denotes the class of water content,

$\frac{K_s}{K_{sc}}$ is the matching factor (measured standard conductivity/ calculated saturated conductivity),

δ is the surface tension of water,

ρ_w is the density of water,

g is the gravitational constant,

η is the viscosity of water,

ε is the porosity of the medium,

p is the parameter that accounts for interaction of
   pore classes,

n is the total number of pore classes, and

h_j is the pressure for a given class of pores.

The saturated hydraulic conductivity K_s was measured in a laboratory experiment with a column of saturated glass beads medium. K_s was obtained from the Darcy's Law for flow in saturated media [27]:

$$Q_w = K_s A \frac{\Delta H}{L} ,$$ (6.7)

where Q_w is the volume of flow in time t,

A is the cross-sectional area of the column,

ΔH is the hydraulic head, and

L is the length of the column.

The value of saturated hydraulic conductivity thus obtained, along with Equation (6.6), gave the hydraulic conductivity, K, which is plotted as a function of volumetric moisture content in Figure 5.

The potential ψ of water in the porous medium is related to the water content θ, and the graphical relationship is usually referred to in Soil Physics literature as the water retention curve. The water retention curve for the glass beads - water system was measured using the pressure plate method [50]. Measurements were made over a wide
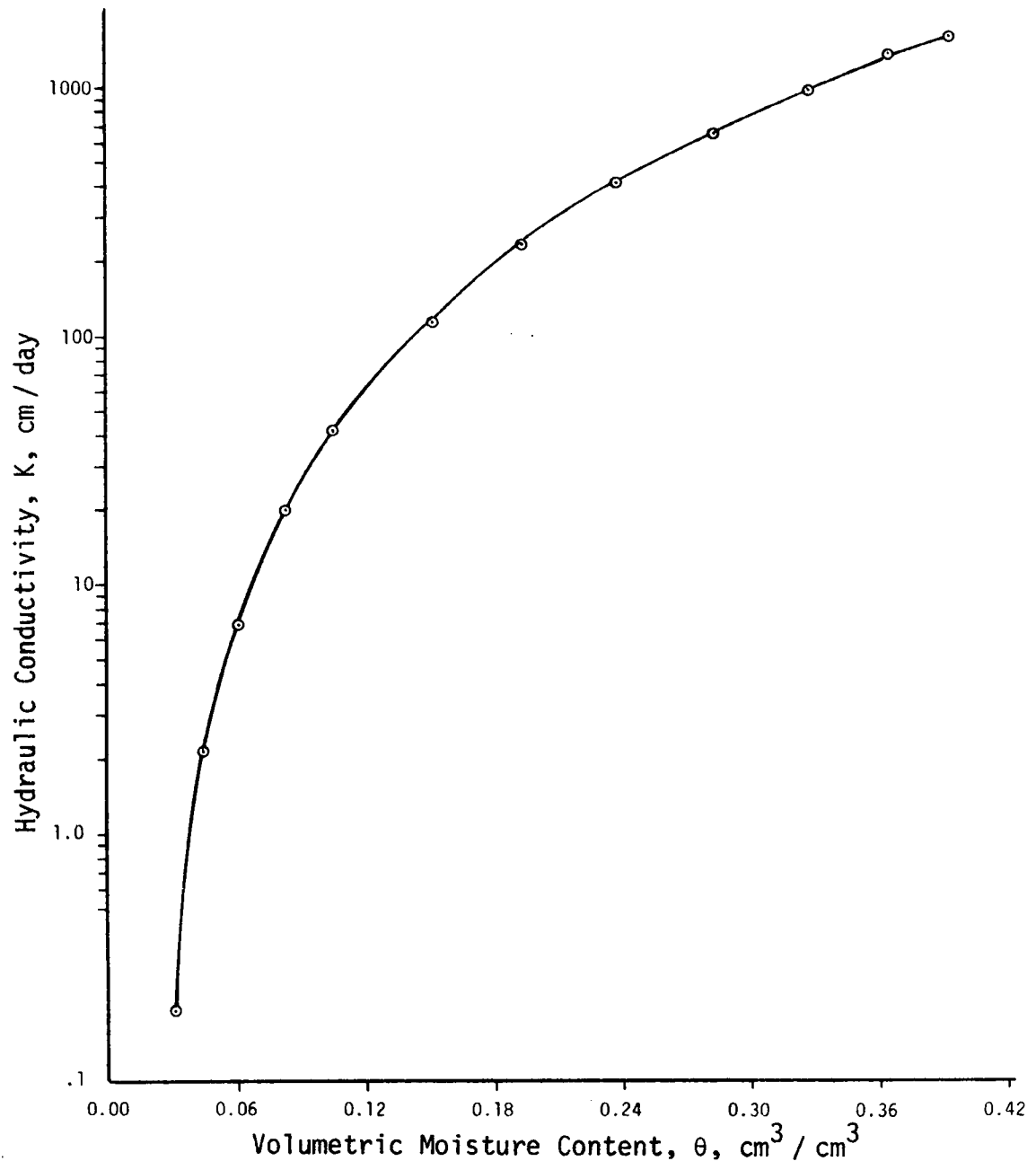
Figure 5. Hydraulic Conductivity K vs. Volumetric Moisture
Content θ

range of applied water potentials, and the relationship obtained between ψ and θ is plotted in Figure 6. As indicated in Figure 6, water potential decreases with increasing water content. Initially ψ decreases sharply for a slight change in θ near the dry region, followed by an almost linear relationship for a wide range of moisture content. Near saturation range, ψ again rapidly decreases with increasing moisture content. The slope $\frac{d\psi}{d\theta}$ of the water retention curve, at different values of moisture content, was obtained graphically by a method[1] which employs a French mirror to draw a normal to the curve at the point in question.

The values of $\frac{d\psi}{d\theta}$ obtained from the water retention curve and the hydraulic conductivities were substituted in Equation (6.5) to get the diffusivity D, which is shown in Figure 7 as a function of moisture content. The diffusivity is seen to be a strong function of moisture content; it increases with increasing moisture content at all moisture contents except a narrow range from $\theta = 0.18$ to $\theta = 0.21$, where D decreases with increasing θ.

Coefficient, β^*

The coupling coefficient β^* is a function of the moisture content, and is defined for the spherically symmetric one-dimensional system by the relation

$$\beta^* = - \left. \frac{d\theta \,/\, dr}{d \ln T \,/\, dr} \right|_{J_w = 0} . \tag{6.8}$$

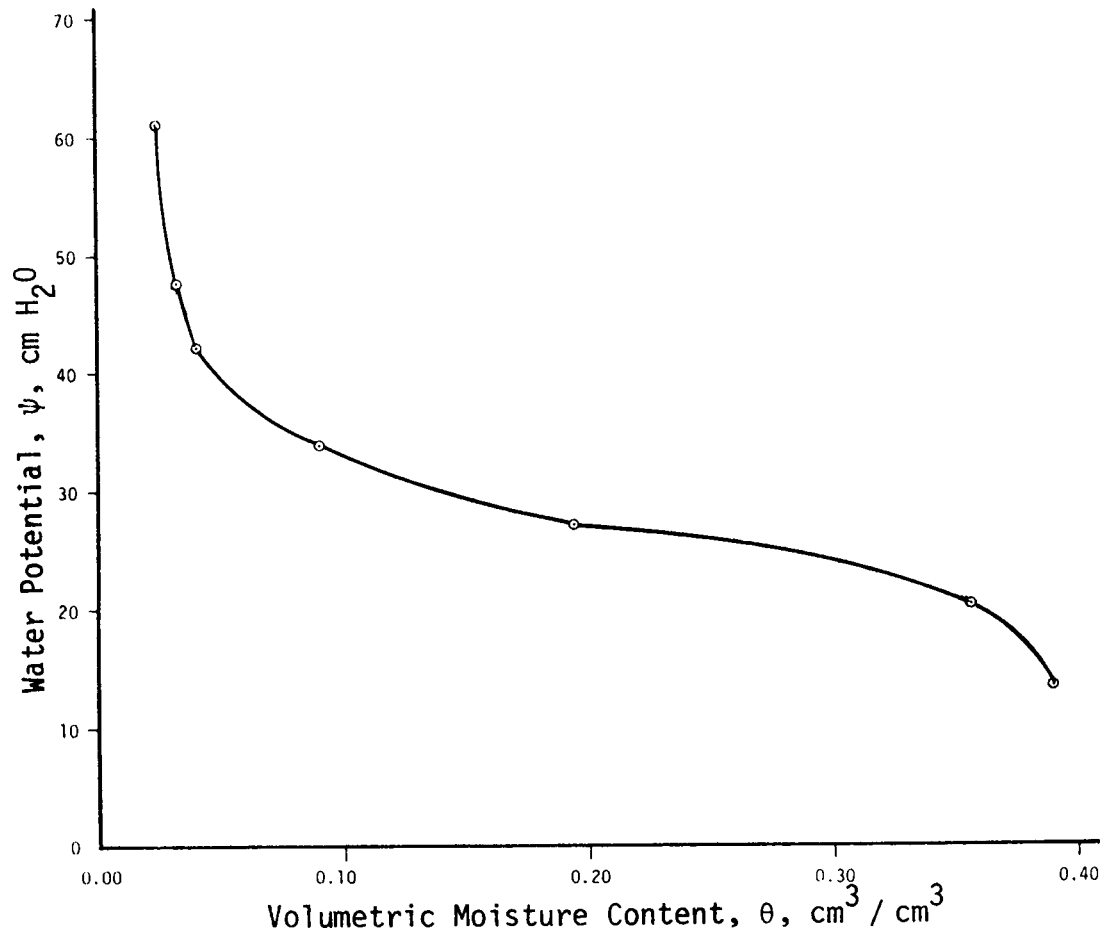[1]Kraus, M. N., "Drawing a Tangent to a Curve," Chemical Engineering, March 12, 1979.

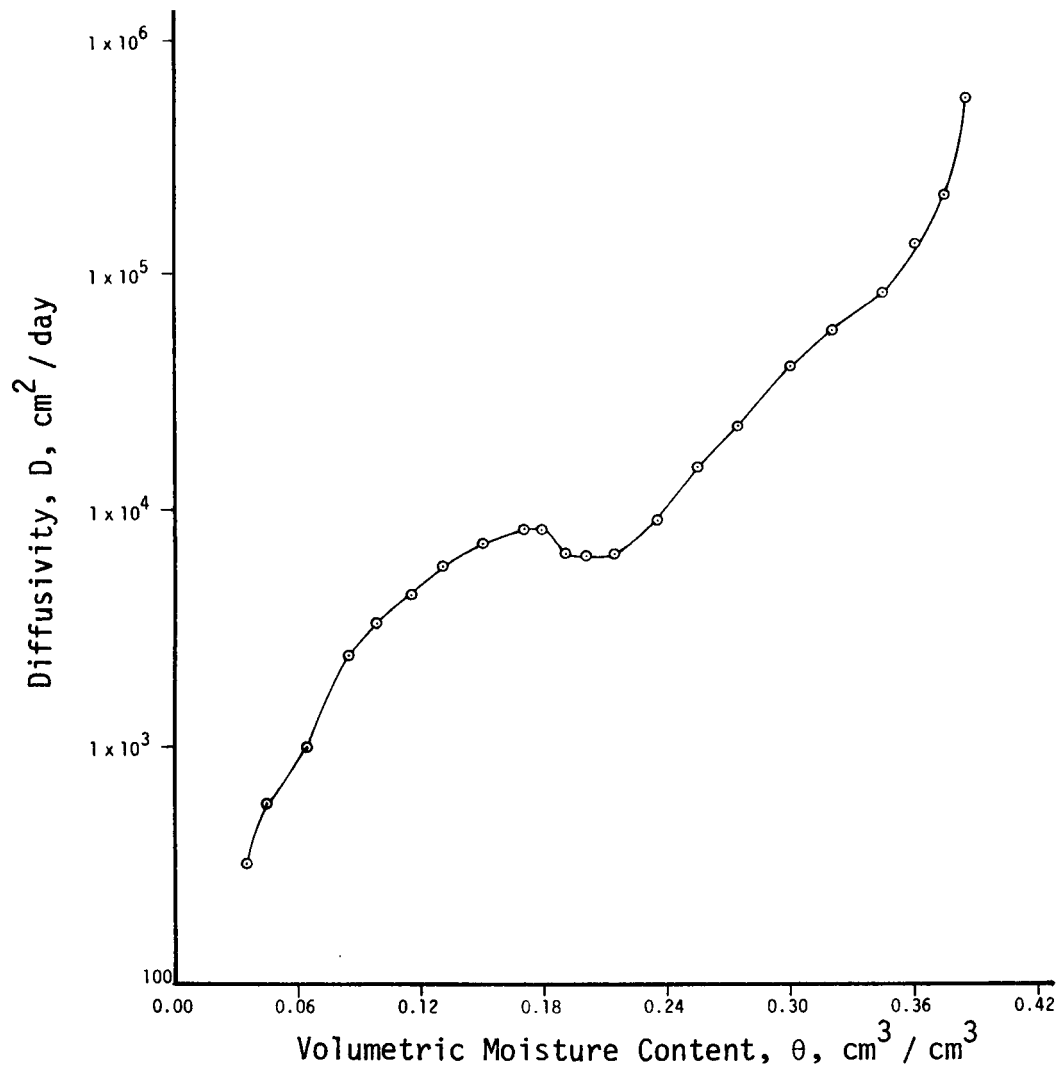Figure 6.   Water Potential ψ vs. Volumetric Moisture Content θ

Figure 7.   Diffusivity D vs. Volumetric Moisture Content θ

An evaluation of β^* from the above equation involves the experimental determination of the steady-state distributions of moisture content, θ, and temperature, T, in a sealed system of unsaturated porous medium (the spherical one-dimensional system in the present study). Slopes, or first derivatives of these distributions, $\frac{d\theta}{dr}$ and $\frac{d\ln T}{dr}$, are taken, and the negative of their ratio gives β^*. In order to obtain β^* as a function of θ over the entire range of moisture contents for which the model applies, it is necessary to carry out a closed experiment with a sufficiently large value of heat rate, Q, that results in a steady-state distribution of θ over the model range. As suggested by previous investigations [55, 91], a value of $\theta = 0.01$ was chosen as the lower limit for the range over which the model requirement of a continuous liquid phase applies. Experimental Run 2, described in Chapter 8 on results and discussion, exhibited such a wide range of moisture contents, and β^* calculations were made from data on T and θ distributions obtained from that run. The slopes $\frac{d\theta}{dr}$ and $\frac{d\ln T}{dr}$ were graphically obtained with the (French mirror) method described earlier. The values of β^* as function of moisture content, calculated from these data, are plotted in Figure 8. β^* increases with increasing moisture content until it reaches a maximum value at $\theta = 0.28$, after which it decreases as θ increases. A plot of the phenomenological coefficient $L_{wq} = D\beta^*$ is also shown as a function of θ in Figure 9. In order to ascertain that β^* is a single-valued function of θ, it is necessary to prove that β^* exhibits a unique relation with θ for several experiments with different values of the gradients $\nabla \ln T$ and $\nabla \theta$. This test will be examined in Chapter 8, where β^* values will be shown for some sample experimental runs.
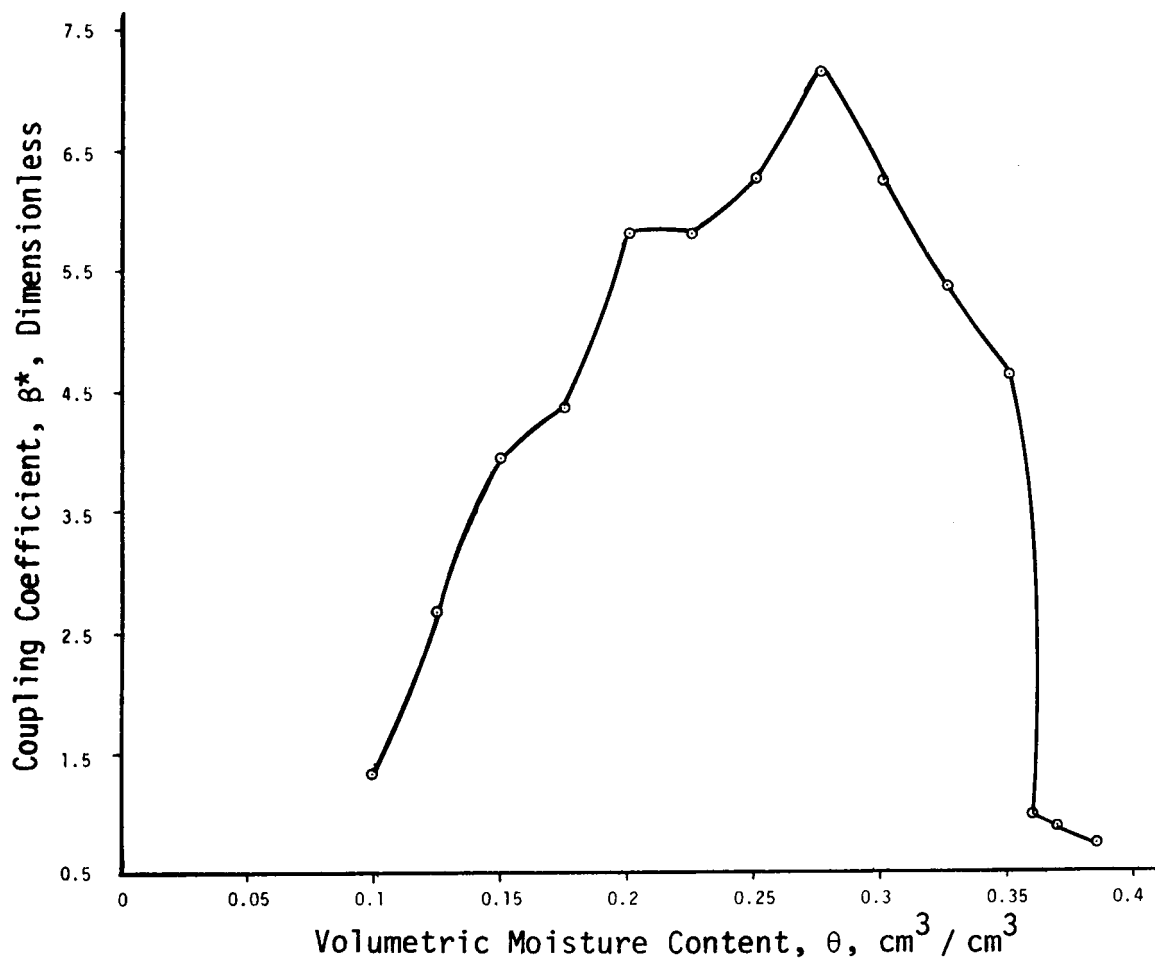
Figure 8. Coupling Coefficient β* vs. Volumetric Moisture
Content θ
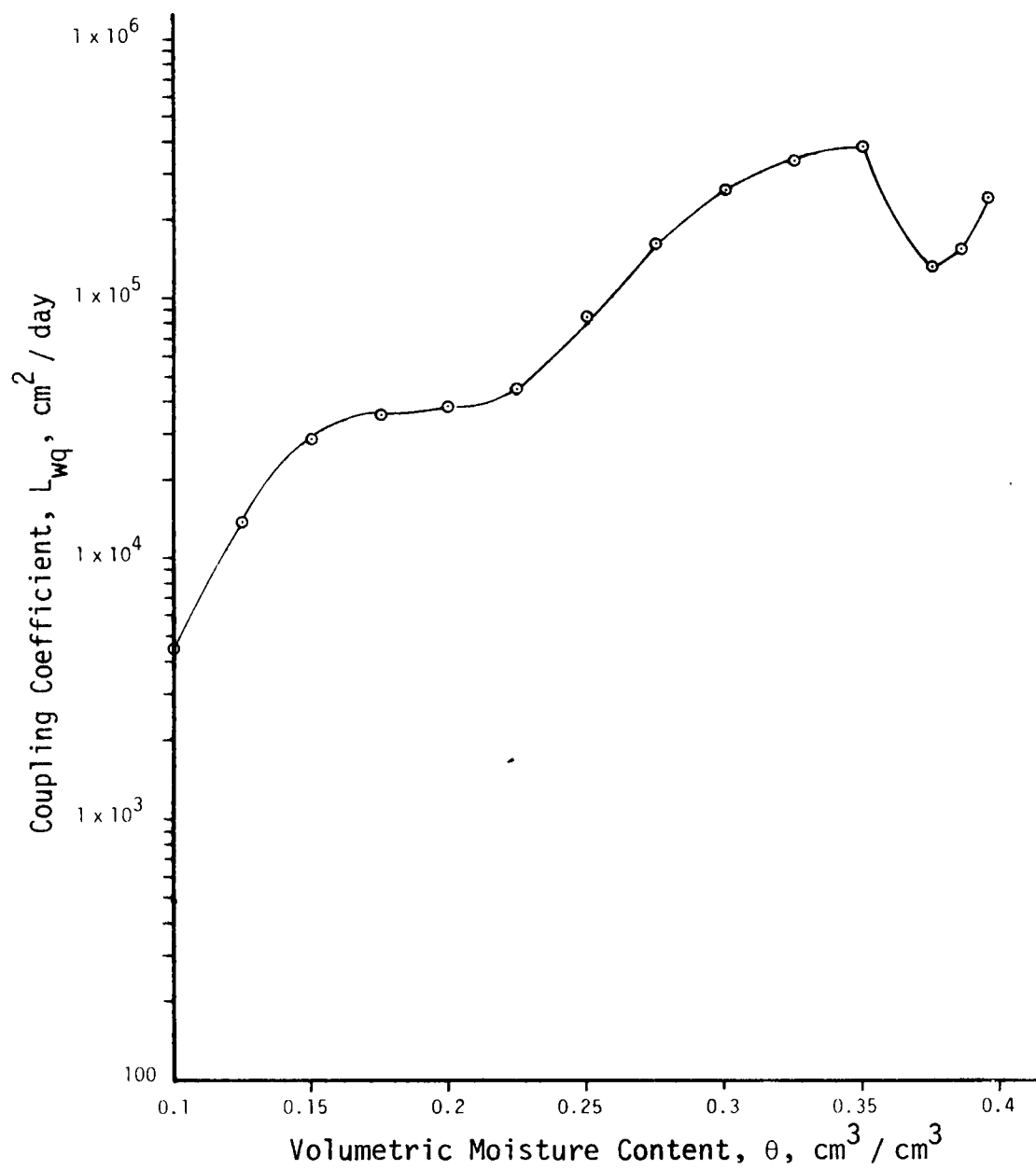
Figure 9.   Coupling Coefficient L_{wq} vs. Volumetric Moisture Content θ

Coefficient, β

The coupling coefficient, β, which denotes the effect of moisture content on the heat flux, is defined by the relation

$$\beta = - \left. \frac{d\psi / dr}{d \ln T / dr} \right|_{J_W = 0} = - \frac{\partial \psi}{\partial \theta} \frac{\partial \theta}{\partial \ln T} = \beta^\star \frac{\partial \psi}{\partial \theta} , \qquad (6.9)$$

and is a function of the moisture content, θ, since both $\beta^\star$ and $\frac{\partial \psi}{\partial \theta}$ are functions of θ.

A graph of β is shown in Figure 10. It is to be remembered that β and $\beta^\star$ are related through the Onsager reciprocal relation, and calculation of β from Equation (6.9) reflects this relationship. It has been suggested that β is too small to be calculated with sufficient accuracy from experimental data (or even zero) [12, 55]. This will be examined in Chapter 8.

Figure 10. Coupling Coefficient β vs. Volumetric Moisture
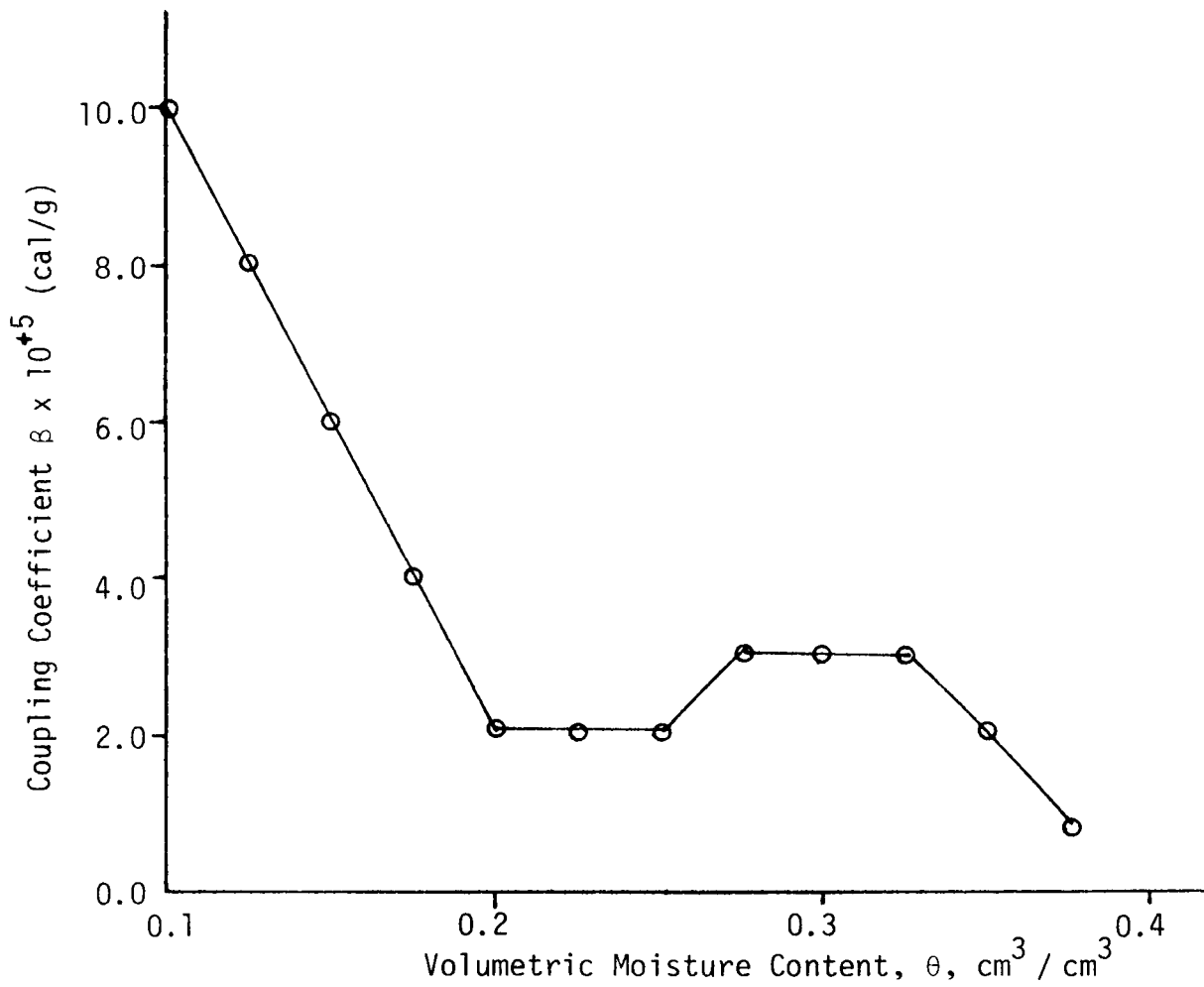Content θ

CHAPTER 7

DESCRIPTION OF EXPERIMENT

An open system experiment, in which heat and moisture fluxes
occur simultaneously as a result of coupling between the temperature
and moisture content gradients, could provide a test of the validity of
the Irreversible Thermodynamics model Equations (4.28) and (4.29).
However, the difficulties associated with the measurement of the small
values of moisture fluxes and the specification of exact boundary con-
ditions make such an open system experiment extremely difficult to
perform.

In light of these difficulties, it was decided to analyze in
this study a simpler, closed system that would provide a valid test of
the Cary and Taylor model.

The low values of thermal conductivity of porous media accentu-
ate errors due to heat losses. A spherical system in which the porous
medium is enclosed in the annular region between two concentric spheres
precludes heat losses. Using a high thermal conductivity material such
as copper as the sphere material provides an effective means for
applying constant and uniform temperature and heat rate boundary con-
ditions.

The choice of 210 - 298 μ glass beads and distilled water as
the unsaturated porous medium was made to minimize effects other than
coupled heat and moisture transfer, and to provide a system in which
measurements of the required properties and variables could be made
accurately enough to obtain a verification of the IT model.

The system that was designed to meet these objectives is indicated diagrammatically in Figure 11. The primary components of the assembly are two concentric spheres which are mounted on a support stand. A heater encased in the inner sphere provided the heat input to the system, and the system was enclosed in a constant temperature air-bath which provided the outer surface boundary condition. Guides located on the outer sphere were part of a moisture content sampling system for obtaining local measurements of moisture content. Local temperatures in the medium were monitored with thermocouples and a potentiometric recorder.

The sphere assembly, the thermocouple arrangement and the moisture content sampling system were used by Moore [70] and are described by him in thorough detail; however for the sake of continuity, and to make this study self-contained, the experimental set-up will be described in this chapter by considering each component assembly separately.

Outer Sphere

The outer sphere consisted of two copper hemispheres, 30.48 cm in diameter, spun from 0.47 cm thick copper sheet. The hemispheres were joined together at the bases with flanges extending 2.54 cm outward.

The top of each hemisphere had a hole, 9.86 cm in diameter, machined in it, and plugs, shown in Figure 12, were used to seal the openings. While the upper hemisphere opening had the plug permanently silver soldered to it, the lower hemisphere opening was threaded to
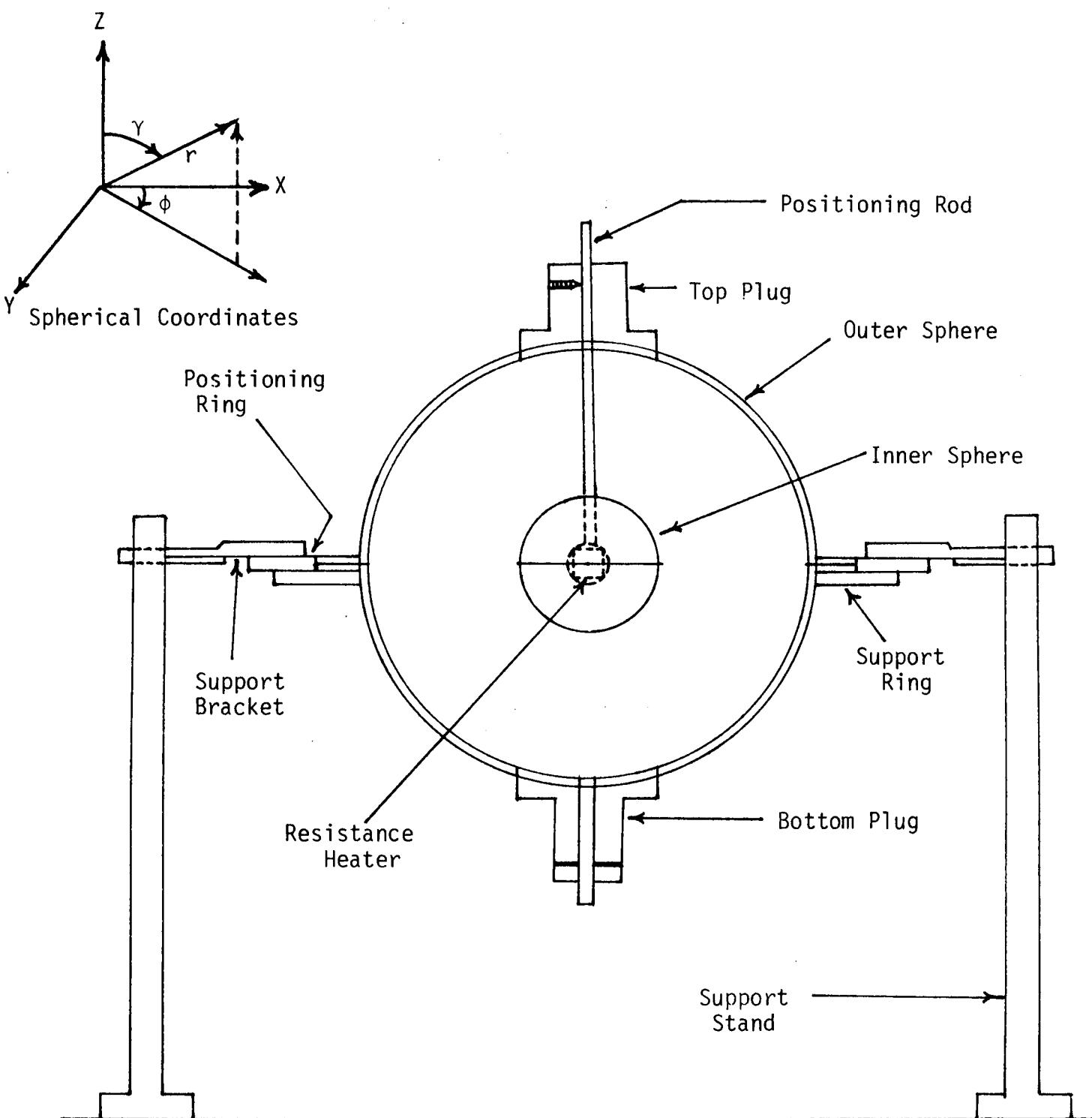
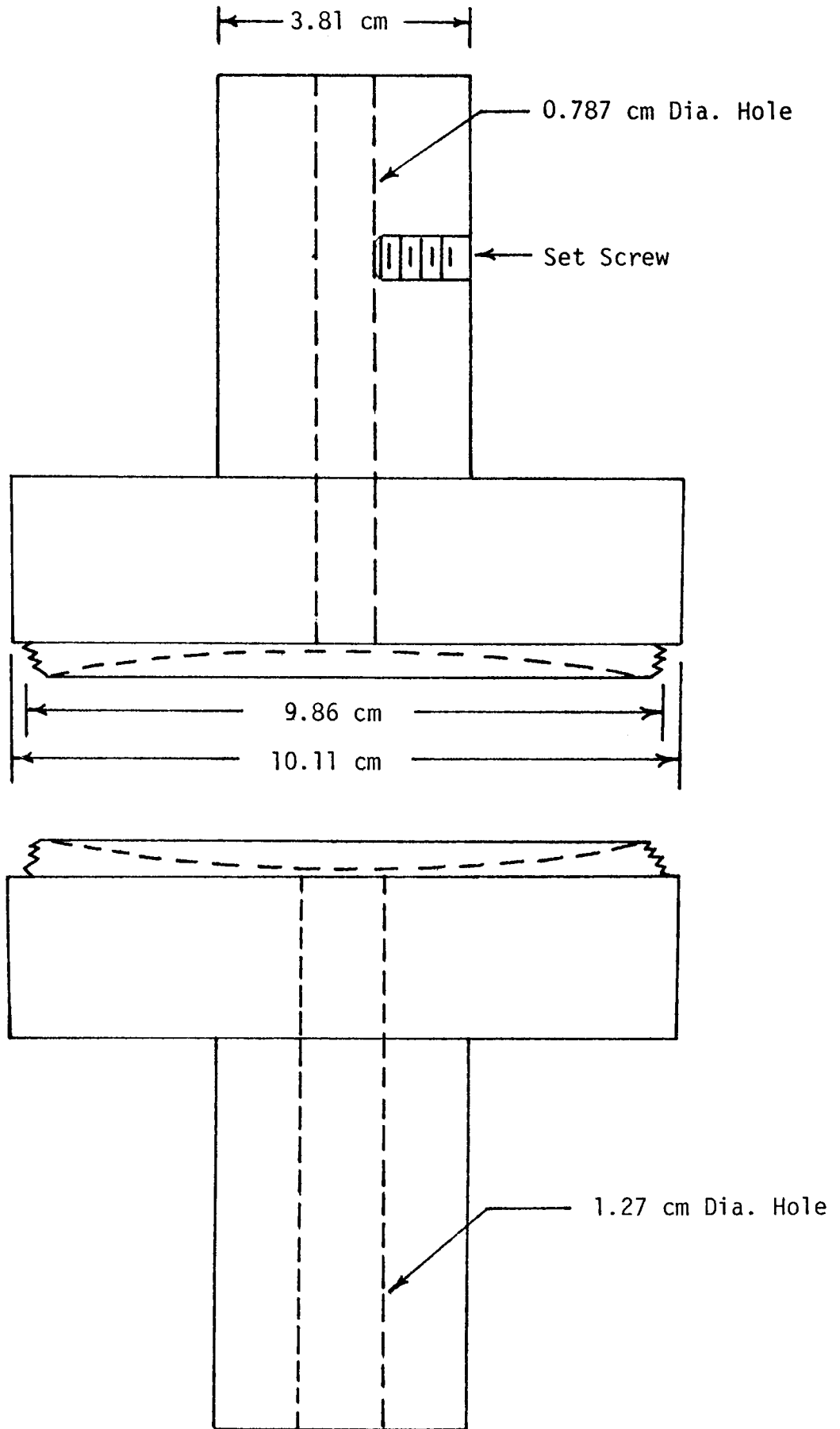Figure 11. Schematic of Apparatus

Figure 12. Top and Bottom Access Plugs

accept the threaded plug, which could be either screwed into position or removed for filling and emptying the porous medium.

Guides, through which the moisture content samples were extracted, are shown in Figure 13. These were aligned with 1.27 cm diameter holes in the outer sphere and bonded to the sphere surface which was flattened around the holes. The guides were then sealed by inserting 1.27 cm diameter stainless steel rods with copper plugs, having the same surface curvature as the outer sphere, silver soldered at the ends. A 1.27 cm diamter hole was also drilled in the center of the bottom plug and closed with a plug. This port served as another sampling lcoation.

The thermocouple supports, described later in this chapter, were positioned on their outer ends by nylon pins which were inserted in holes drilled in threaded copper bushings. These bushings, which screwed into 2.54 cm diameter holes in the outer sphere, are also shown in Figure 13.

Thermocouples made from 30 gage, glass-wrapped Chromel-Alumel wires were positioned at three locations on the inner surface of the outer sphere, to determine the temperature variation on the outer sphere. The thermocouple wires were bonded to the sphere surface with epoxy glue, and the junctions were left exposed.

Inner Sphere and Heater

The inner sphere and the heating element are shown schematically in Figure 14. The inner sphere consisted of two copper hemispheres, 10.0 cm in diameter, joined by an internal annular ring. The heater was potted in a 2.54 inch diameter cavity in the center of the sphere. A

1.27 cm

Locking Tab

Steel Collar

Set Screw

Set Screw

Stainless Steel Tube

Copper Plug Silver
Soldered to Tube

Guide Plug

2.22 cm

7.62 cm

1.27 cm Dia. Hole

3.175 cm

Wrench
Holes

2.54 cm Dia.

Thermocouple Support Bushing
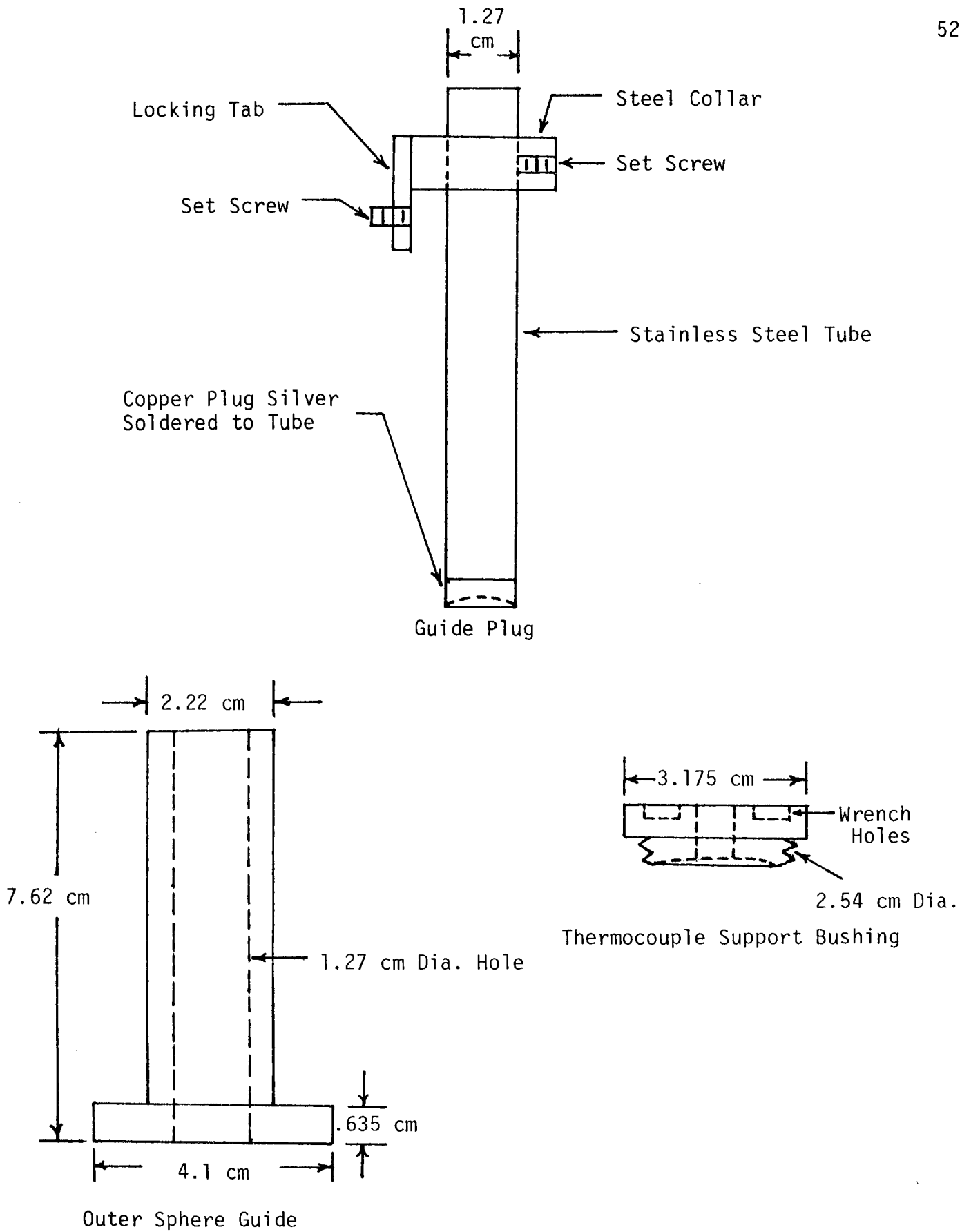
.635 cm

4.1 cm

Outer Sphere Guide
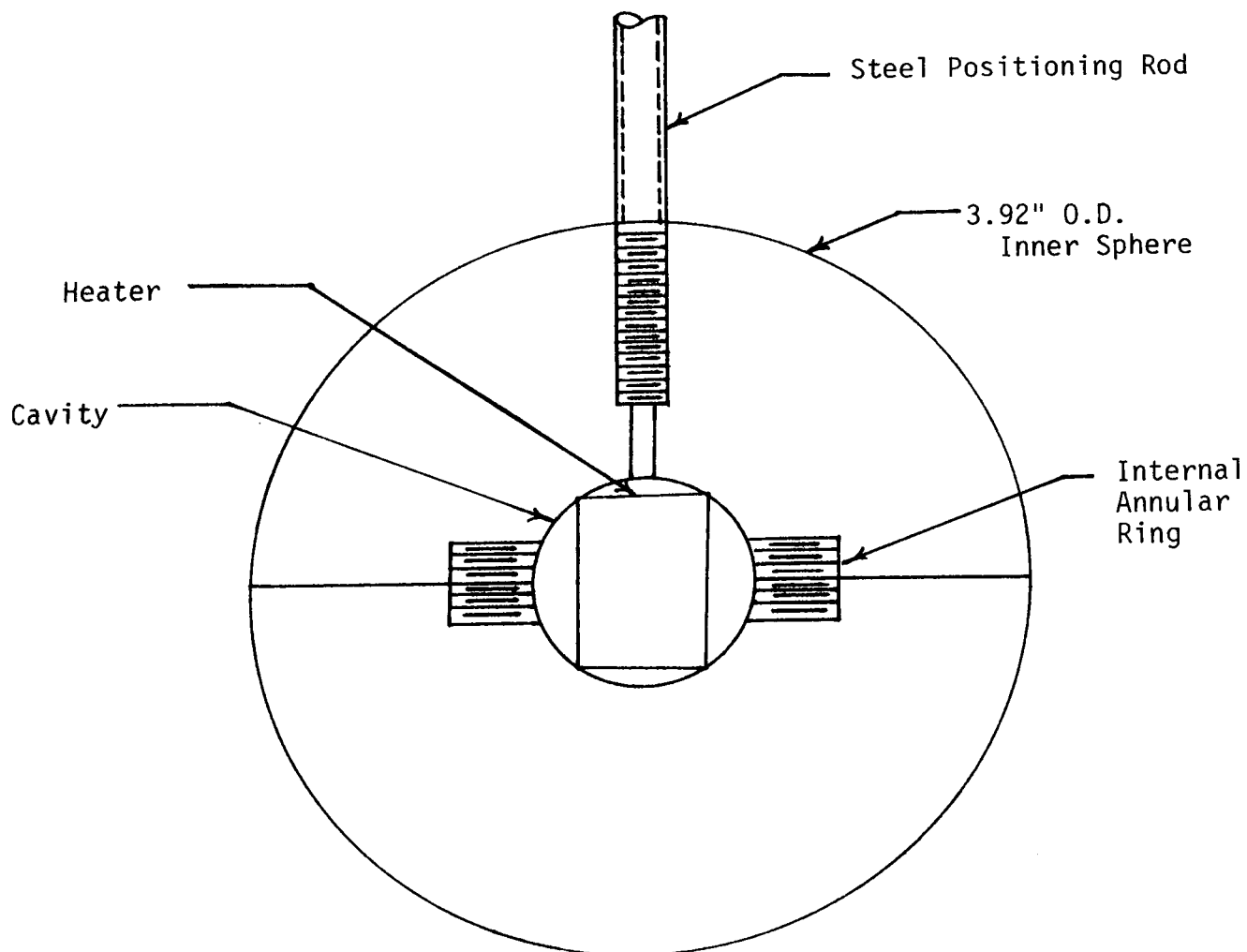
Figure 13. Sampling Guide, Plug, and Bushing

Figure 14. Cross-section of Inner Sphere

hole was drilled in the center of the top hemisphere to accept a 0.79 cm O.D., 0.47 cm I.D. steel rod which extended out from the outer sphere surface through a hole in the top plug. An O-ring was used to seal the clearance between the tube and the plug hole, and a set screw fixed the position of the rod in the plug, thus positioning the inner sphere in the center of the outer sphere.

0.32 cm deep holes were drilled on the outer surface of the inner sphere and small nylon pins fixed in them for positioning the inner ends of the thermocouple support tubes.

The resistance heating element consisted of a 1.27 cm diameter, 2.22 cm long, Firerod Cartridge heater[1] with a cold resistance of 3.67 ohms and a maximum rated power of 100 watts. The heater was potted in the inner sphere cavity with RTV encapsulant rubber.

Thermocouples used to determine the temperature variations on the outer surface of the inner sphere were made from 0.0127 cm Chromel-Alumel, Teflon-insulated wires, and the wires were bonded along their entire length on the sphere surface with epoxy. These thermocouple wires entered the inner sphere positioning tube through a small hole and extended out of the outer sphere, along with the heater leads, from the top end of the positioning tube.

Power for the heater was provided by a DC power supply and a constant voltage transformer connected to the house supply. The Lambda Model LP-531-FM[2] regulated DC power supply had a variable voltage range

---

[1]Manufactured by Watlow Electric Manufacturing Company, St. Louis, Missouri.

[2]Manufactured by Lambda Electronics, Melville, Long Island, New York.

of 0 - 20 volts and a current range of 45 mA - 5.7 A at ambient temperatures, and it regulated the output voltages to within 0.01% + 1 mv for line variations from 105 - 132 VAC or for load changes from no load to full load. Metered panels provided readings for both the voltage and the current. The AC input to the power supply was provided by a Sola CVS[3] constant voltage transformer connected to the house 125 VAC supply. The transformer had an output voltage of 118 VAC.

The power to the heater was also measured independently by current and voltage readouts on a Fluke Model 8010A[4] digital multimeter. The multimeter, when connected in series in the heater circuit, measured the DC current with an accuracy of $\pm$ (0.3% of reading + 1 digit) and a resolution of 1 mA, and when connected in parallel across the power supply output terminals, measured the DC voltage with an accuracy of $\pm$ (0.1% of reading + 1 digit) and a resolution of 10 mv on the 20 v range that was used.

Power supplied to the heater was varied for different experimental runs by adjusting the voltage until the desired power requirement was indicated by the voltage and current readouts on the meters.

Sphere Support Assembly

As described earlier, the inner sphere was supported at the center of the outer sphere by the positioning rod which extended out from a closely fitting hole in the outer sphere top plug.

----

[3]Manufactured by Sola Electric, Elk Grove Village, Illinois.

[4]Manufactured by John Fluke Manufacturing Company, Inc., Mountlake Terrace, Washington.

The outer sphere support assembly is shown in Figure 15. The hemispheres were joined at the flanges and positioned relative to each other by a 0.64 cm aluminum ring fitting closely around the outside surface of both flanges. The flange of the lower hemisphere rested on an aluminum supporting ring, which was clamped to the positioning ring above it with 0.64 cm bolts. The bolts were tightened by nuts on the positioning ring with the washers overlapping the surface of the upper hemisphere flange. A thin rubber gasket ring was placed between the two flanges in order to provide a vapor tight seal. Occlusive seals were also ensured at the clearances around the guide plug ends by bonding thin rubber wiper rings around the holes on the inside surface of the outer sphere.

The sphere assembly was supported on two rotatable brackets on opposite sides to which the positioning and supporting rings were secured with bolts and nuts. The support bracket rods rested in holes in two hexagonal support stands fabricated from angle irons and iron bars in the Engineering Instrument Shop. The stands were clamped to a bench top. Rotation of the sphere assembly along with the support brackets provided accessibility of the required sampling location on the outer sphere.

Temperature Measurement

The temperatures on the inner and outer spheres were measured by thermocouples positioned on their surfaces, as discussed earlier. The locations of these thermocouple junctions were as shown in Table 1. (See Figure 11 for details of angular coordinates γ and ϕ.)
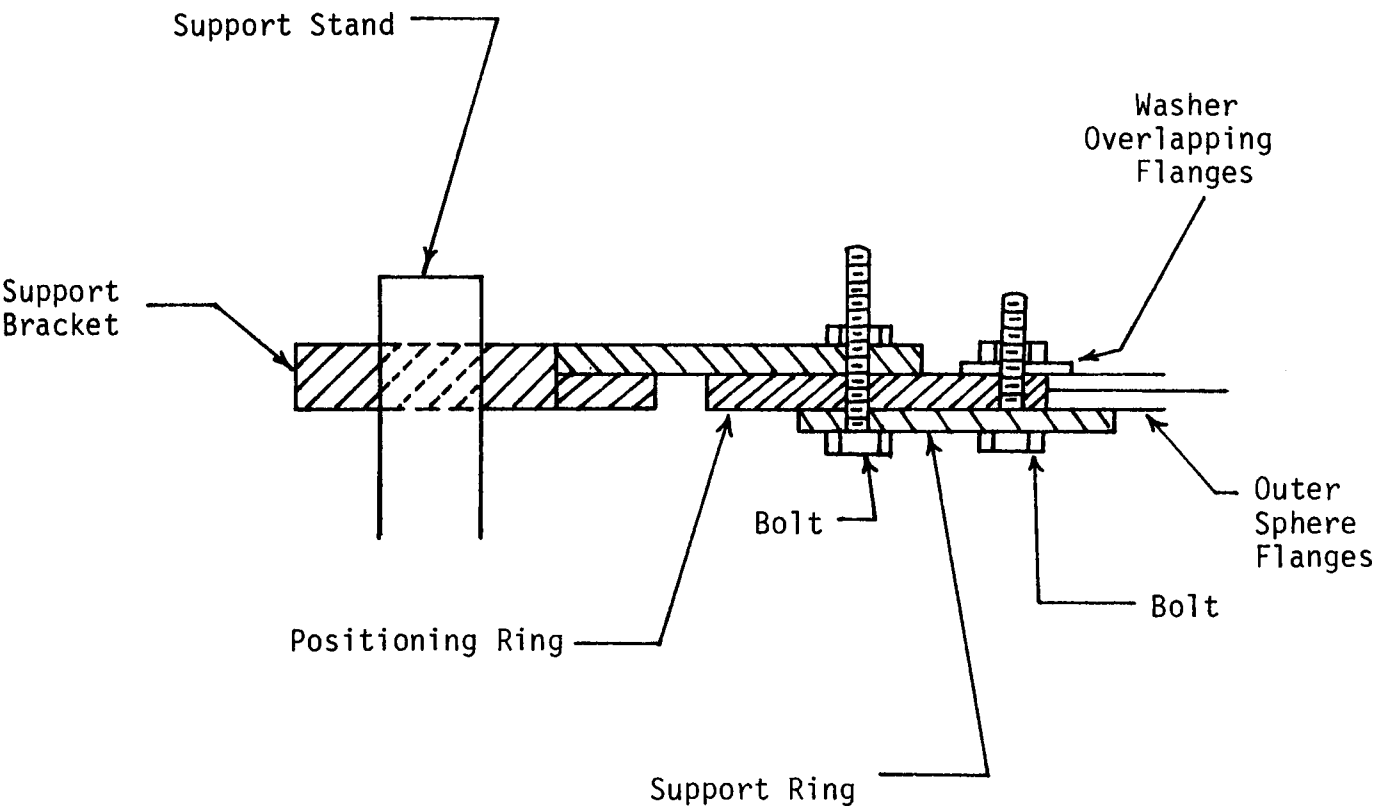
Figure 15. Outer Sphere Support Assembly

TABLE 1

LOCATIONS OF THERMOCOUPLES ON THE INNER
SURFACE OF THE OUTER SPHERE AND THE
OUTER SURFACE OF THE INNER SPHERE

Angular coordinates of thermocouple locations

	Inner Sphere Thermocouple Locations		
	$\phi = 54^o$	$\phi = 174^o$	$\phi = 294^o$
γ	32°	98°	153°

	Outer Sphere Thermocouple Locations		
	$\phi = 21^o$	$\phi = 141^o$	$\phi = 261^o$
γ	48°	111°	165°

Local temperatures in the medium were measured with thermocouples fabricated from 0.0127 cm Teflon-insulated Chromel-Alumel wires. The thermocouple junctions lay at 1.27 cm intervals along radial directions and were supported by 0.117 cm diameter, two bore, ceramic insulating tubes which were bonded to 0.318 cm O.D. ceramic insulators extending from the inner sphere to the outer sphere. A thermocouple support assembly is shown in Figure 16.

The thermocouple wires, after exiting the small diameter insulators, were bonded along the surface of the positioning insulator from which they passed through holes in the nylon pins and came out of the outer sphere.

The thermocouple supports, each with seven thermocouple junctions, were positioned at four different locations in the medium,
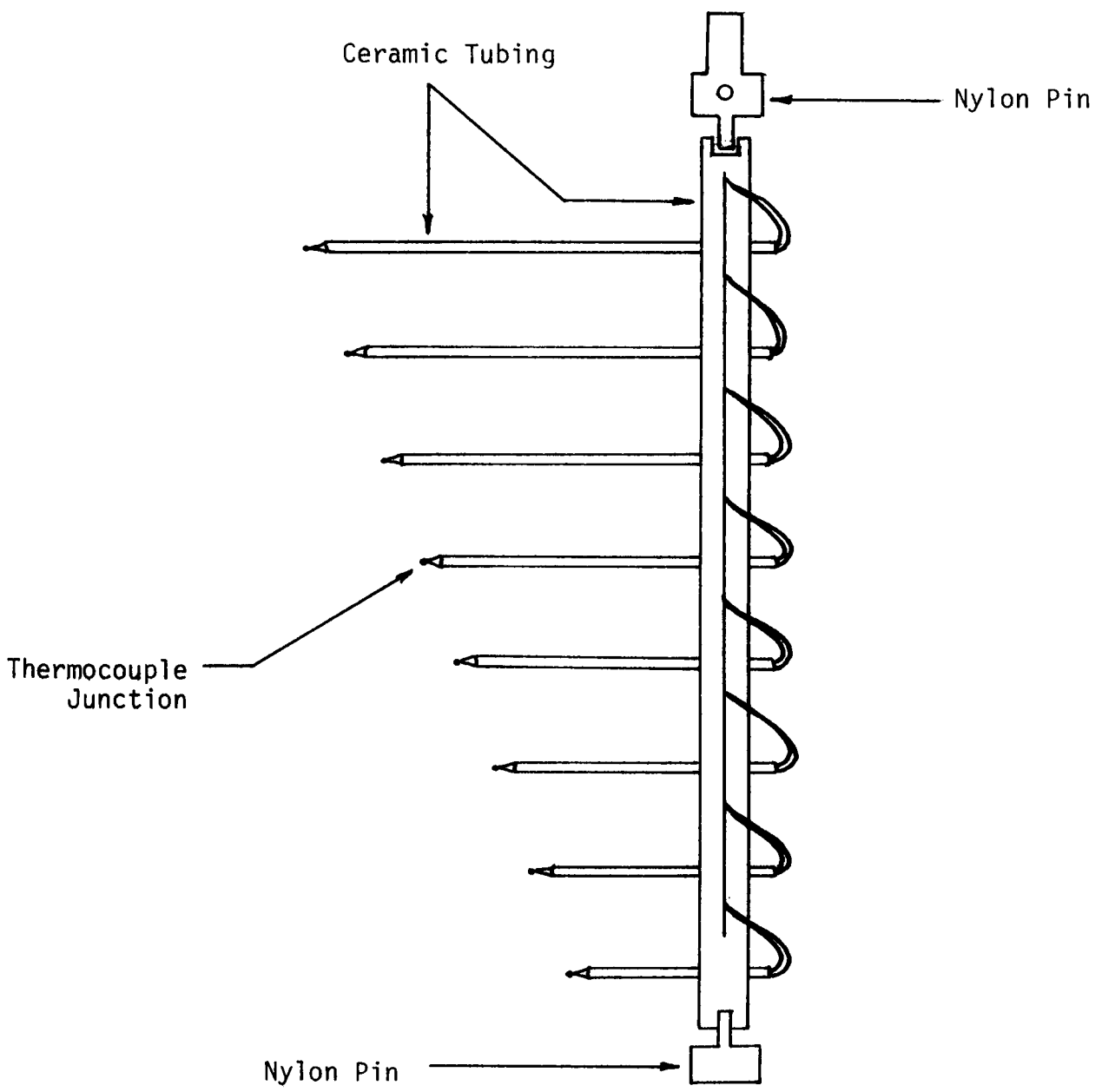
Figure 16. Thermocouple Support

and the angular coordinates of these measurement junctions are shown in Table 2.

TABLE 2

COORDINATES OF MEDIUM THERMOCOUPLES

Location	γ (degrees)	ϕ (degrees)
1	156	295
2	32	115
3	116	116
4	63	295

The accuracy of temperature measurement with the Chromel-Alumel thermocouples was verified by comparing the measured temperatures with those indicated by precision thermometers, and the uncertainties associated with the thermocouple measurements were found to be within the range of error introduced by linearly interpolating between EMF versus temperature values given in the thermocouple conversion tables. Therefore, no correction was applied to the temperatures indicated by the thermocouple EMF values.

Distortion of the temperature field caused by the presence of the thermocouple supports in the medium was found to be negligible by Moore [70], and was, therefore, not measured in the present study. Moore [70] also installed thermocouples in the wall of the inner sphere

positioning tube in order to measure the heat loss through the tube, and his results indicated a minimal heat loss through the tube for values of heat input greatly higher than those used in these experiments; therefore the positioning rod heat loss was assumed negligible.

The thermocouple circuit used to measure the thermocouple EMF's is shown schematically in Figure 17. The thermocouple wires, after coming out of the outer sphere, were connected to terminals on two aluminum panels which were clamped with L-joints to the top of the rotatable brackets. 20 gage, PVC-insulated, stranded copper extension wires leading from the terminal panels were connected to the terminals of a 40-position, rotary thermocouple selector switch[5], which permitted sequential connections of the thermocouples to a Laboratory Strip-Chart Potentiometric Recorder[6]. 34 thermocouples were connected to the recorder through the switch in this manner.

The single-pen strip-chart recorder, with a 250 mm chart width, had switch-selected input spans of 1 mv, 2 mv, 5 mv, 10 mv, 20 mv, 50 mv, 100 mv, 200 mv, 500 mv, 1 v, 2v, and 5v, and had chart speeds of 1, 2, 3, 4, 5, 6, 10, 12, 15, 20, and 30 cm/min and cm/hr. The zero was continuously adjustable from -100% to +100%. Most of the thermocouple EMF's were measured with the 1 mv span with the zero set at 1 mv, and with the 2 mv span with the zero set at 1 mv to obtain the proper range of voltages over the entire span.

---

[5] Model OSW5-40, manufactured by Omega Engineering, Inc., Stamford, Connecticut.

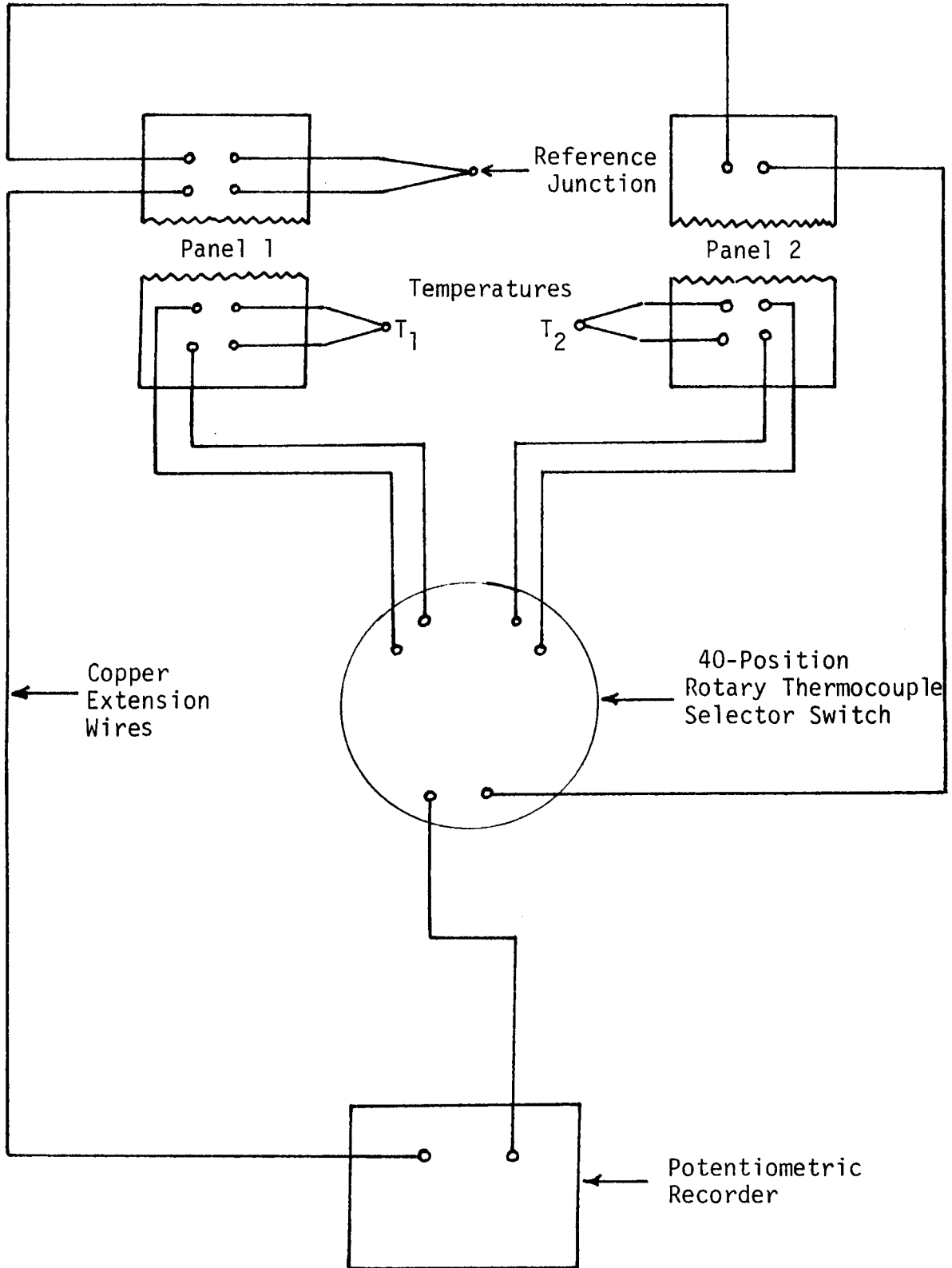[6] Model 8373-10, manufactured by Cole-Parmer Instrument Company, Chicago, Illinois.

Figure 17. Schematic of Thermocouple Circuit

The only likely source of error in the temperature measurement could have been due to a net EMF introduced in the circuit because of connections made between dissimilar wires. However, since connections between dissimilar wires were at the same temperature, and the reference junction was directly connected to the terminal panel, the possibility of such an error was minimized.

Moisture Content Measurement

Local moisture content values, along three radial directions in the medium, were determined from a gravimetric analysis of samples extracted from the three locations by a sampling device.

TABLE 3

COORDINATES OF MOISTURE CONTENT
SAMPLING GUIDES

Location	γ (degrees)	ϕ (degrees)
1	180	Bottom Plug
2	135	90°
3	45	90°

After steady-state was reached in an experimental run, a 1.27 cm core of the porous medium was removed along a radial line with a stainless steel tube inserted in the annular medium through the guide on the outer sphere. Then, the sampling device shown in Figure 18 was introduced through the guide to permit extraction of eight local samples of the medium at 1.27 cm intervals along the radial direction from the medium surrounding the core opening.
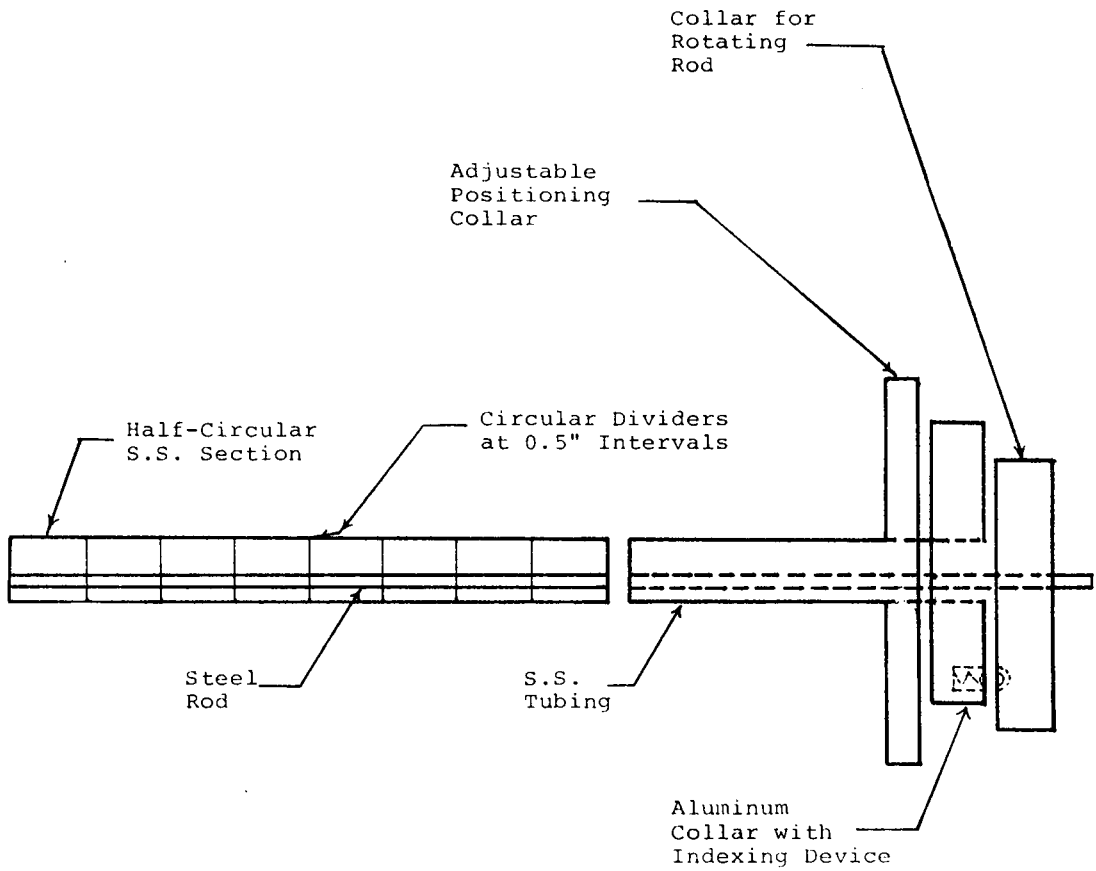
Figure 18. Moisture Content Sampling Device

The sampling device consisted of a 10.16 cm long, 1.27 cm O.D., and 0.071 cm wall thickness, half-cylindrical stainless steel tube, along the length of which circular dividers were welded at 1.27 cm intervals to permit extraction of eight local samples from the medium by the eight half-cylindrical buckets so formed. The half-cylindrical sampling tube was positioned by a 0.318 cm steel rod soldered along its inside surface and extending through a plastic bushing inside a section of stainless steel tubing. The stainless steel tubing closely fit the guide on the outer hemisphere. The outer end of this section extended beyond the end of the guide to allow the half-cylindrical buckets to be located and to provide for rotating the steel rod.

The samples were weighed with a Sartorius electronic balance.[7] The balance has a capacity of 160 g, readability to 0.1 mg, and a sensitivity of 0.5 mg.

The relative humidity in the laboratory was maintained close to saturation for a few hours prior to placing the medium in the sphere annulus at the beginning of a run or extracting the samples of the medium at the completion of a run, with a Sears Kenmore humidifier, in order to minimize loss of moisture by evaporation from the moist porous medium.

Temperature Control System

It was necessary to maintain a constant temperature on the outer sphere surface in order to implement the boundary conditions used for solving the model differential equations.

---

[7]Model No. 2842, manufactured by Brinkmann Instruments, Inc., Westbury, New York.

The constant temperature on the surface of the outer sphere was maintained by enclosing the equipment assembly during an experimental run in a 76 cm x 76 cm x 76 cm wooden cabinet in which the air was controlled at a uniform temperature with the help of a temperature control system. A block diagram of the control system used is shown in Figure 19. It consisted of a solid-state time proportioning temperature controller[8], with a 10-speed hot air blower[9] as the control element. An Iron-Constantan thermocouple provided measurement of the controlled air temperature to the controller, and four 100 CFM box fans mounted on the inside walls of the wooden cabinet maintained constant mixing of the air bath and uniformity of the controlled air temperature. A 43 CFM box fan mounted in the wall of the wooden cabinet, when used with a variable autotransformer, provided a constant air throughput of about 6 CFM, to remove the excess heat generated in the system. A room temperature control system maintained the air temperature variation in the laboratory within a 3° C range, and it was found that a temperature constancy of $\pm 0.15^\circ$ C for the air bath was achieved for the temperature controlled. However, the temperature of the outer sphere surface was held constant with a better uniformity because of its large thermal mass.

The air bath temperature was continuously recorded for the initial runs by a Chromel-Alumel thermocouple connected to a laboratory strip-chart potentiometric recorder[6] described earlier. A mercury

---

[8]Model No. 2179-10, manufactured by Cole-Parmer Instrument Company, Chicago, Illinois.

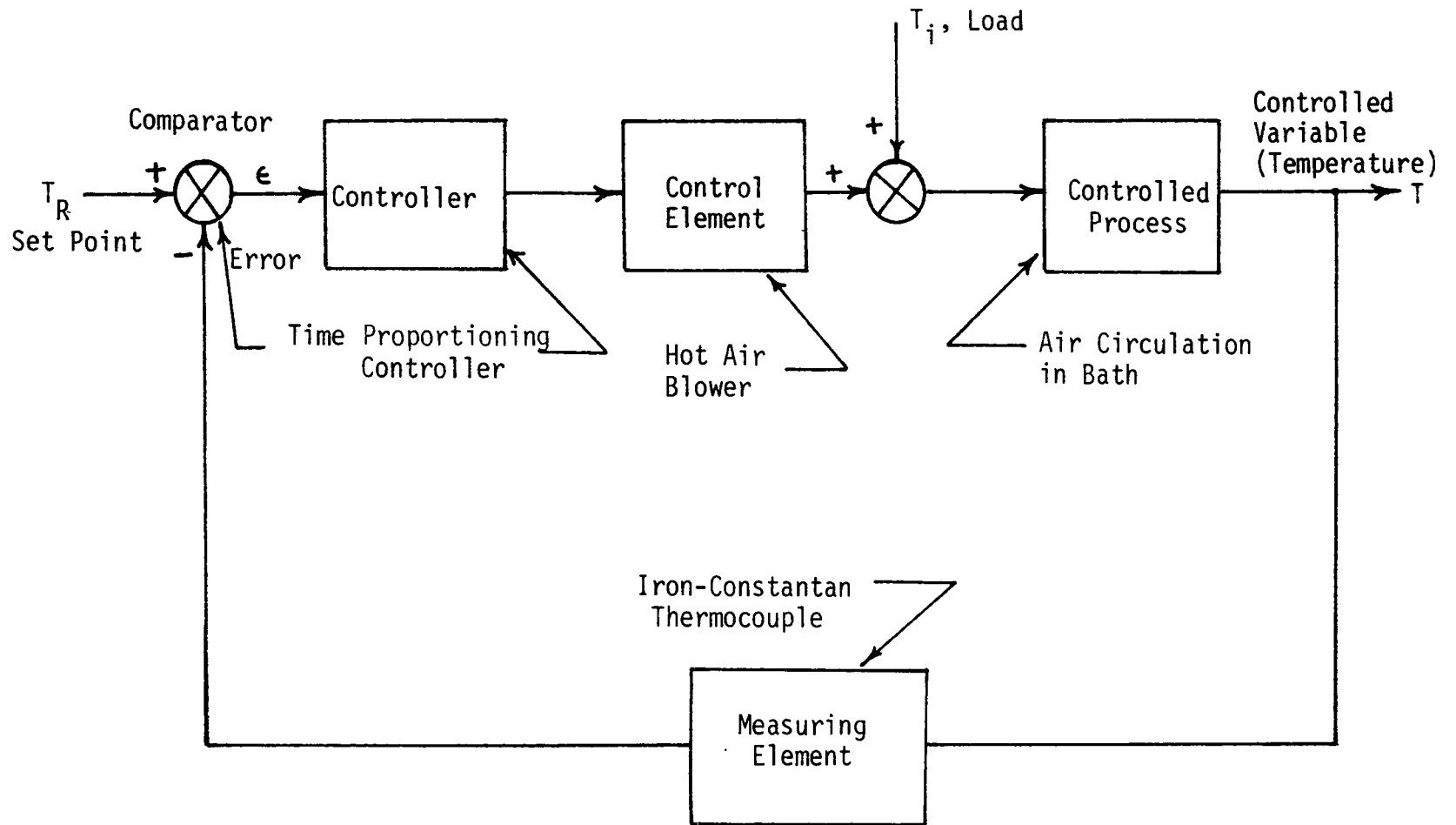[9]Manufactured by Montgomery Ward Company.

Figure 19.   Block Diagram of Temperature Control System

thermometer introduced in the top of the air bath provided independent measurement of the air temperature in the cabinet.

Experimental Procedure

The inner sphere was positioned at the center of the outer sphere, which was then mounted on the support stand assembly as described earlier. Thermocouple supports were installed in the annular space, and the leads extending out of the outer sphere, as well as the inner sphere thermocouple leads emerging from the positioning rod, were connected to the copper hook-up wires on the terminal panels. Plugs were introduced in the two outer sphere guides to seal the openings.

Porous medium was prepared by mixing required amounts of glass beads and distilled water in eight 1 gallon glass jars which were then allowed to stand for a period of 48 hours in order for the moisture content to attain uniformity in each jar. The sphere assembly was rotated until the port in the lower hemisphere was at the top for filling.

Small quantities of the moist glass beads were introduced in the annulus, with constant tapping on the outer sphere with a rubber hammer and evenly spreading out the filled medium with a spatula, in order to pack the medium uniformly. The filling procedure required about four hours, and samples of the medium were taken periodically during the filling procedure to accurately determine the initial uniform moisture content of the medium.

The start-up of the experiment was effected by first placing the wooden cabinet on the equipment assembly and activating the air

bath temperature control system. After the air temperature had been controlled at a uniform value for a period of 2 to 3 hours, the heater power supply was turned on. The current through the heater was increased slowly to avoid breakage due to thermal shock. The temperature at a location in the medium was recorded continuously by the potentiometric recorder, with a chart speed of 1 cm/hr. Steady-state was reached in 24 - 48 hours, depending on experimental conditions. After this temperature had remained constant for several hours, temperatures at all the locations in the medium and the inner and outer sphere surface temperatures were recorded by switching with the thermocouple selector switch, a process that took about 15 minutes to complete.

The heater power supply and the temperature control system were then deactivated and the wooden cabinet lifted from over the equipment to begin the moisture content sampling of the medium. The sampling technique consisted of removing a core of the medium with a stainless steel tube and then rotating the sphere until the guide was in a horizontal position. The sampling device was then introduced into the opening from which the core had been removed, and the buckets rotated in a counter-clockwise direction for collecting local samples of the medium around the opening. The sampler was then pulled out with its open face vertically upward and the samples transferred with a spatula to 10 ml sealable vials. This procedure was repeated for all the three sampling locations. After all the samples were collected, the vials were wiped clean from the outside and weighed. They were then placed, after removing the caps, in a drying oven[10] at 105° C,

---

[10]Model Stabil-Therm, manufactured by Blue M Electric Company, Blue Island, Illinois.

for about one hour. The vials were then removed from the oven, allowed to attain room temperature, and weighed after replacing the caps. The porous medium samples were then removed from the vials, which were again weighed in the empty state. This procedure allowed a gravimetric determination of the local moisture content values in the medium, which were then converted to volumetric measurements from a knowledge of the medium density.

The time period, from the moment the heating and temperature control systems were deactivated to the time when sampling of the medium from the three locations was completed, was 15 - 20 minutes, an interval which was short enough to preclude more than a negligible moisture redistribution in the annular medium, after the 24 - 40 hours required for the system to reach steady state. Thus, possible errors in the steady-state moisture content values determined for the samples must be attributed to collection and handling of the samples only.

The procedure was repeated for other runs with the same initial moisture content but different heater outputs. After a series of such runs was completed, the bottom plug was removed and the porous medium emptied from the annular space. The medium was placed in large trays and dried in the oven. Broken thermocouples were replaced, the sphere surfaces were thoroughly cleaned and dried, and the equipment was prepared for another series of runs with a different value of initial moisture content.

CHAPTER 8

RESULTS AND DISCUSSION

The results of eleven steady-state experimental runs are pre-
sented and analyzed. Porous media components for the runs were
nominally 250 μ (210 - 297 μ) spherical glass beads and distilled
water. The initial moisture contents of the media and the applied
heating rates are shown in Table 4. Excepting Run 1, three or more
runs with different heating rates were made for each of three initial
moisture contents. Steady-state temperature profiles measured on four
different radii along with inner and outer sphere temperatures, and
moisture content profiles measured along three different radii are
shown for the eleven runs in Figures 20 through 41.

TABLE 4

INITIAL MOISTURE CONTENTS AND HEATING RATES
FOR EXPERIMENTAL RUNS

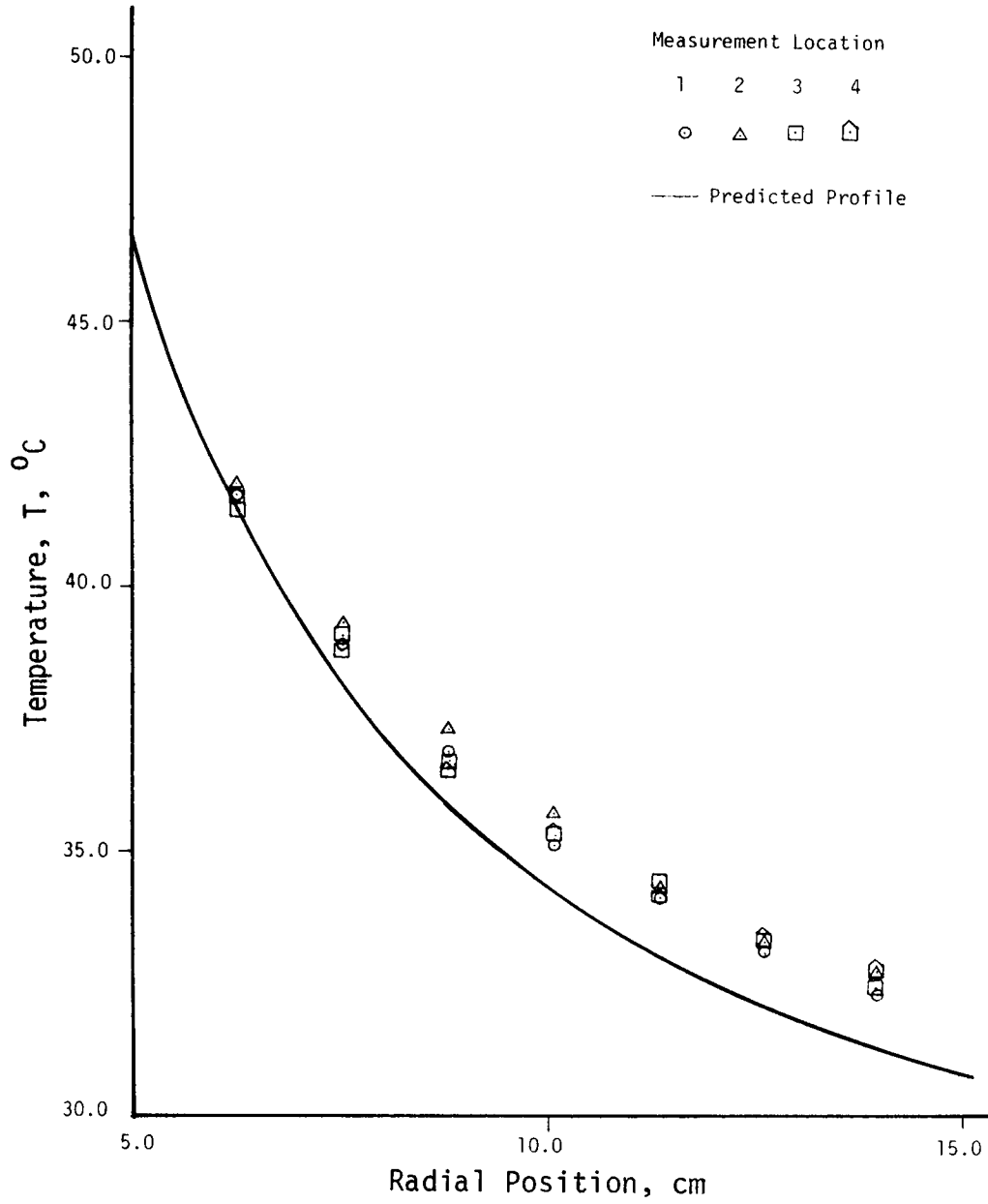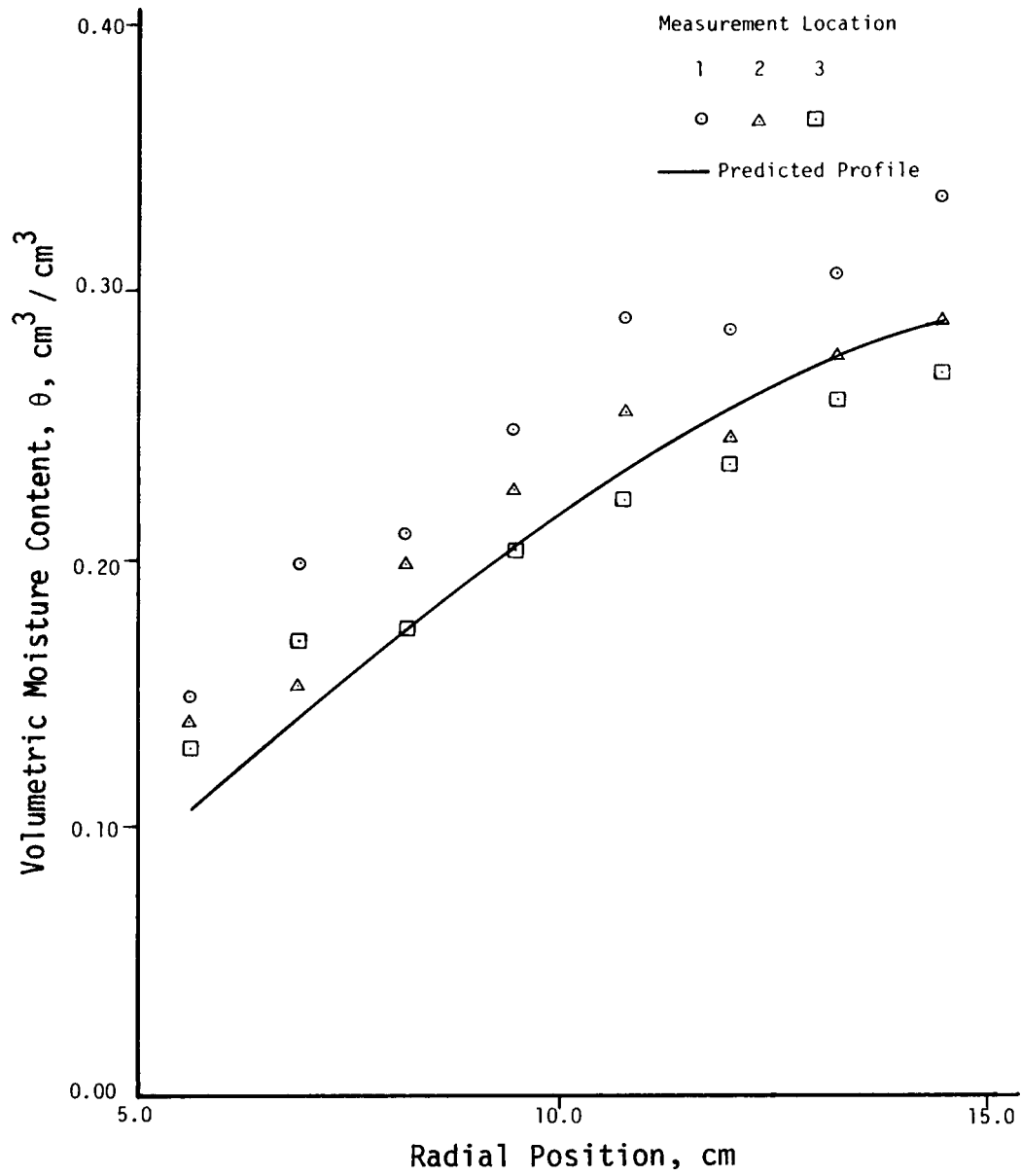| Run No.	Initial Moisture Content, cm^3/cm^3	Heating Rate, Q, cal/day
1	0.23	2.28×10^5
2	0.32	3.10×10^5
3	0.32	2.83×10^5
4	0.32	1.87×10^5
5	0.32	2.40×10^5
6	0.27	2.56×10^5
7	0.27	2.25×10^5
8	0.27	1.80×10^5
9	0.30	2.39×10^5
10	0.30	2.06×10^5
11	0.30	1.58×10^5

71

Figure 20. Local T vs. Radial Position--Run 1

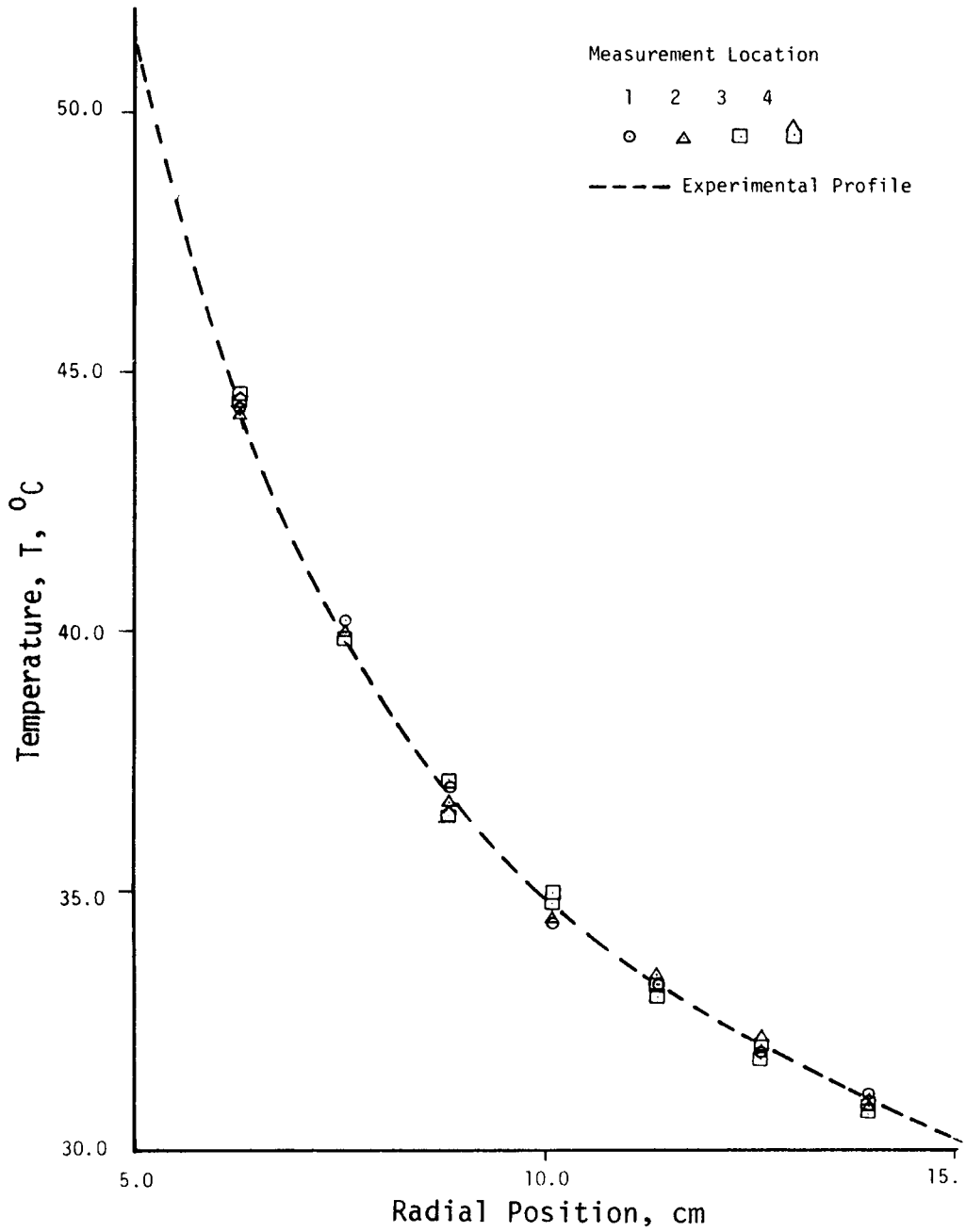Figure 21.   Local θ vs. Radial Position--Run 1

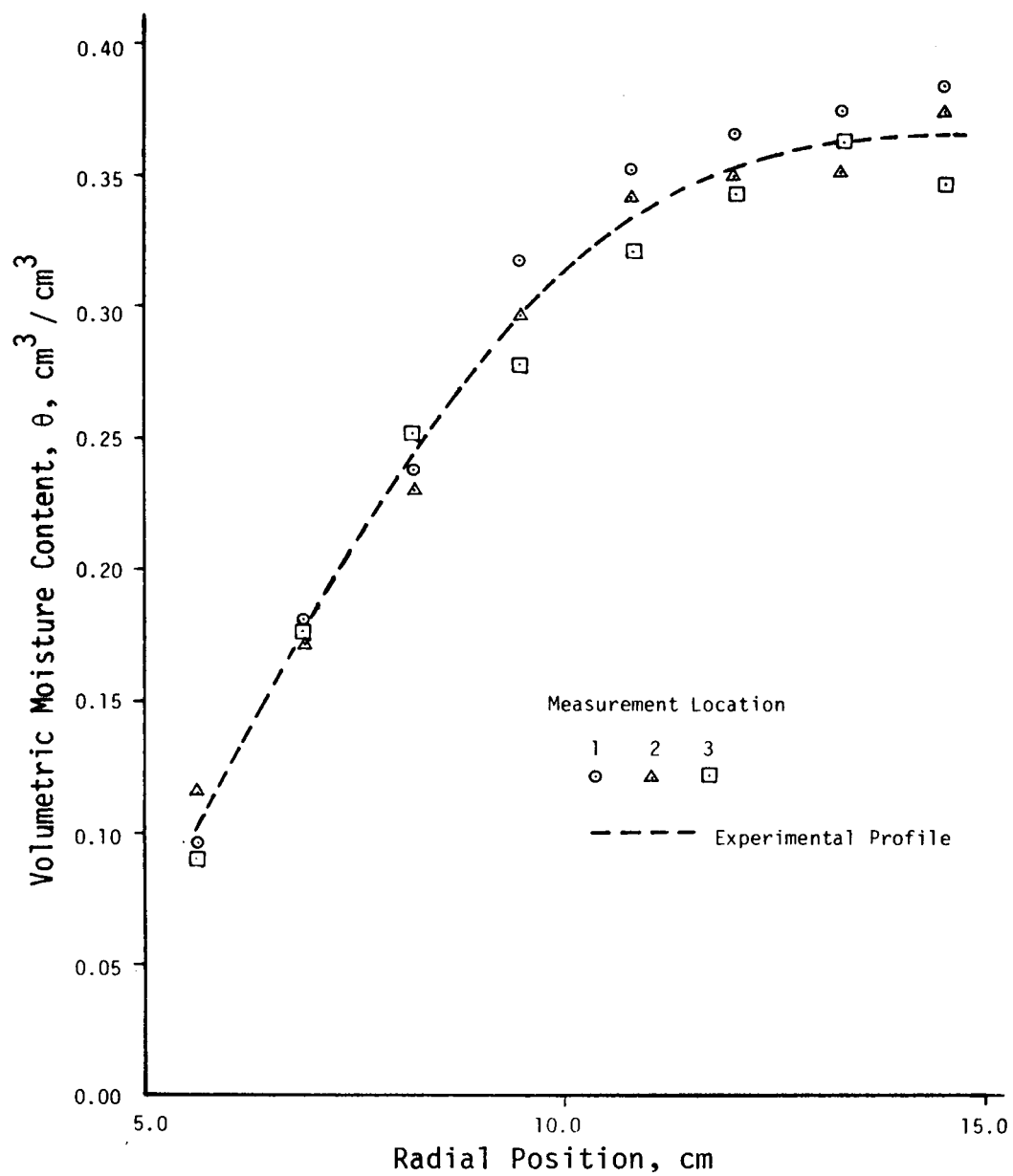Figure 22. Local T vs. Radial Position--Run 2

Figure 23. Local θ vs. Radial Position--Run 2

Figure 24.   Local T vs. Radial Position--Run 3

Figure 25. Local θ vs. Radial Position--Run 3

Figure 26. Local T vs. Radial Position--Run 4

Figure 27. Local θ vs. Radial Position--Run 4

Figure 28. Local T vs. Radial Position--Run 5

Figure 29. Local θ vs. Radial Position--Run 5

Figure 30.   Local T vs. Radial Position--Run 6

Figure 31. Local θ vs. Radial Position--Run 6

Figure 32. Local T vs. Radial Position--Run 7

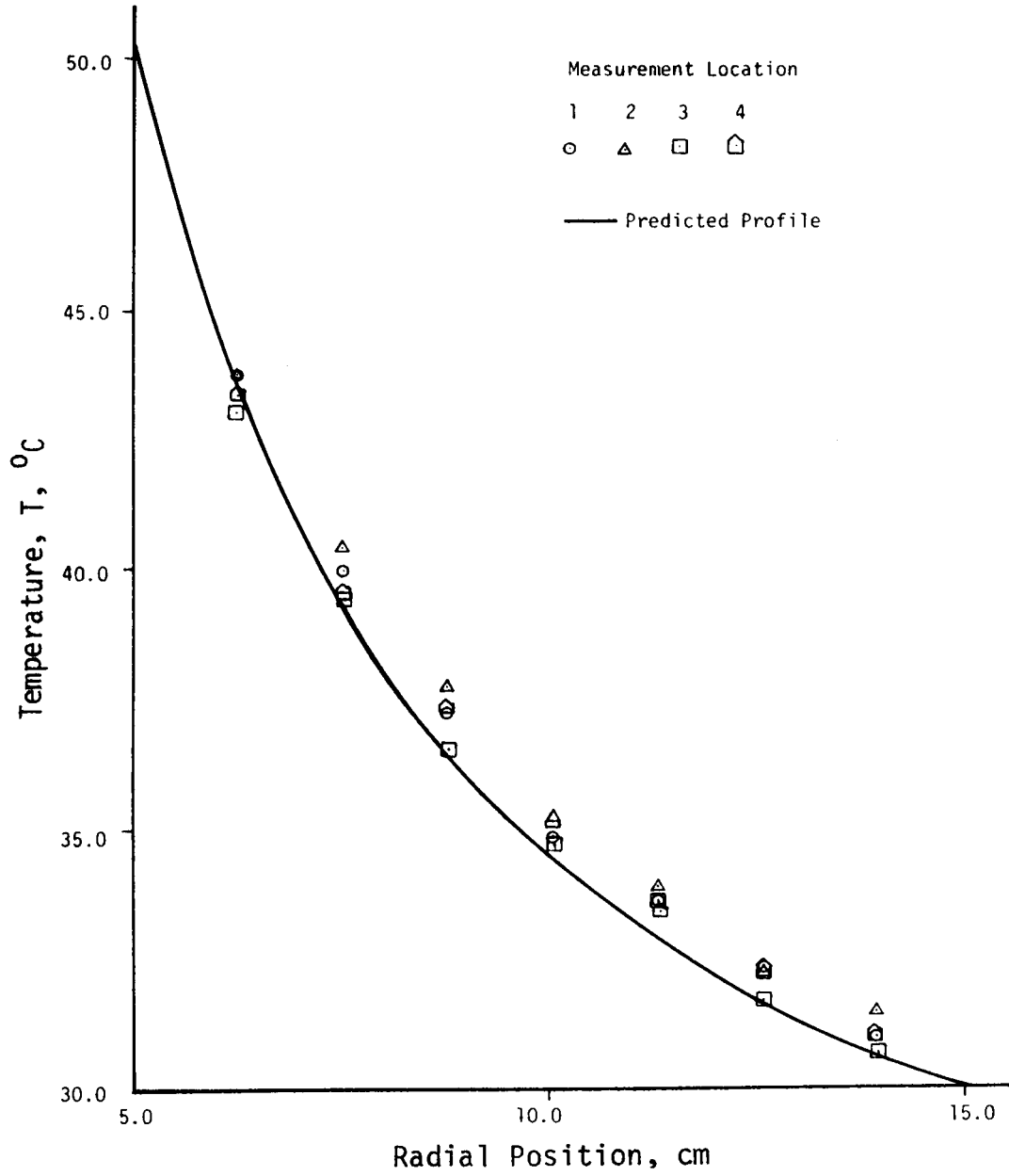Figure 33. Local θ vs. Radial Position--Run 7

Figure 34. Local T vs. Radial Position--Run 8
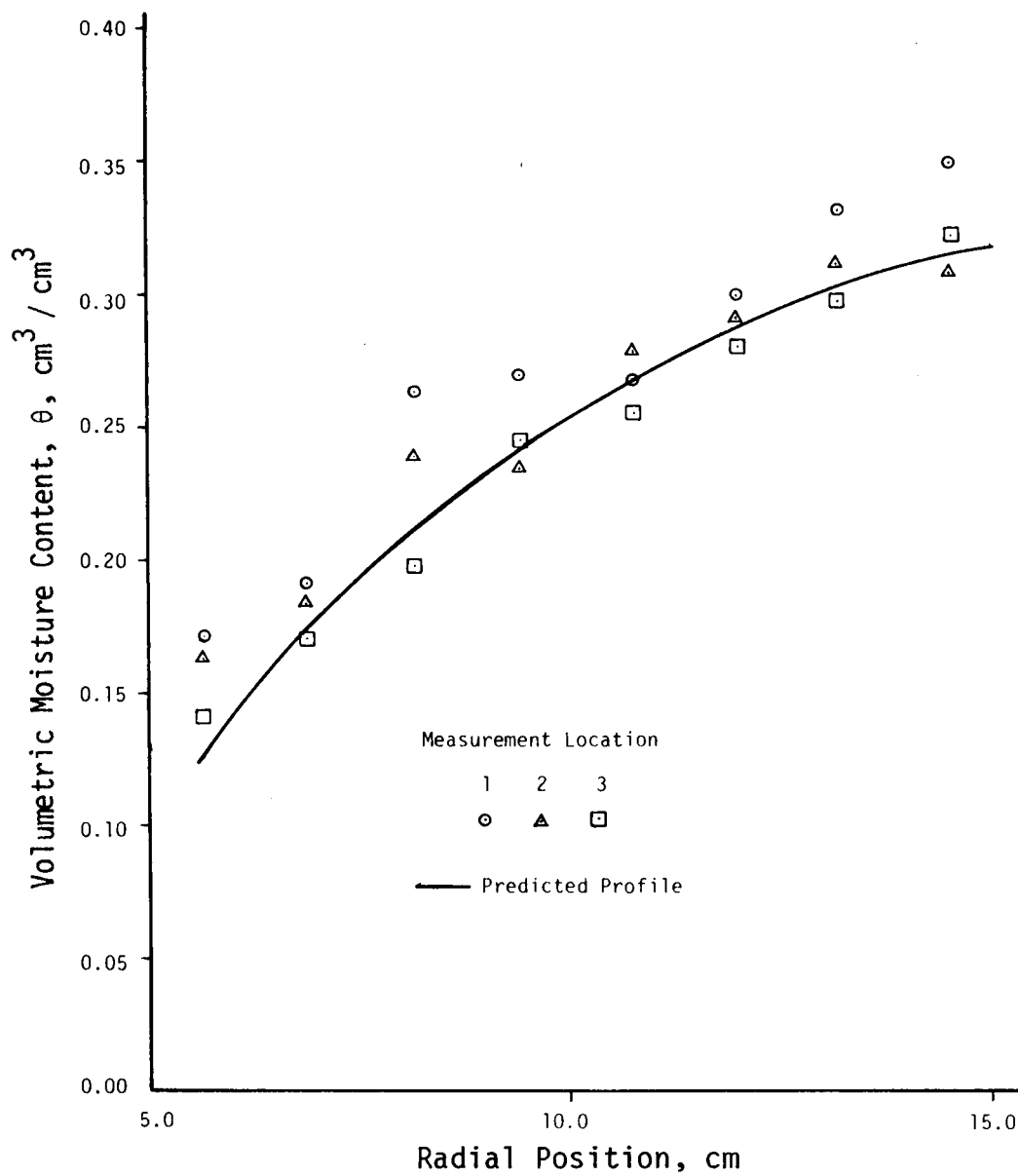
Figure 35.   Local θ vs. Radial Position--Run 8
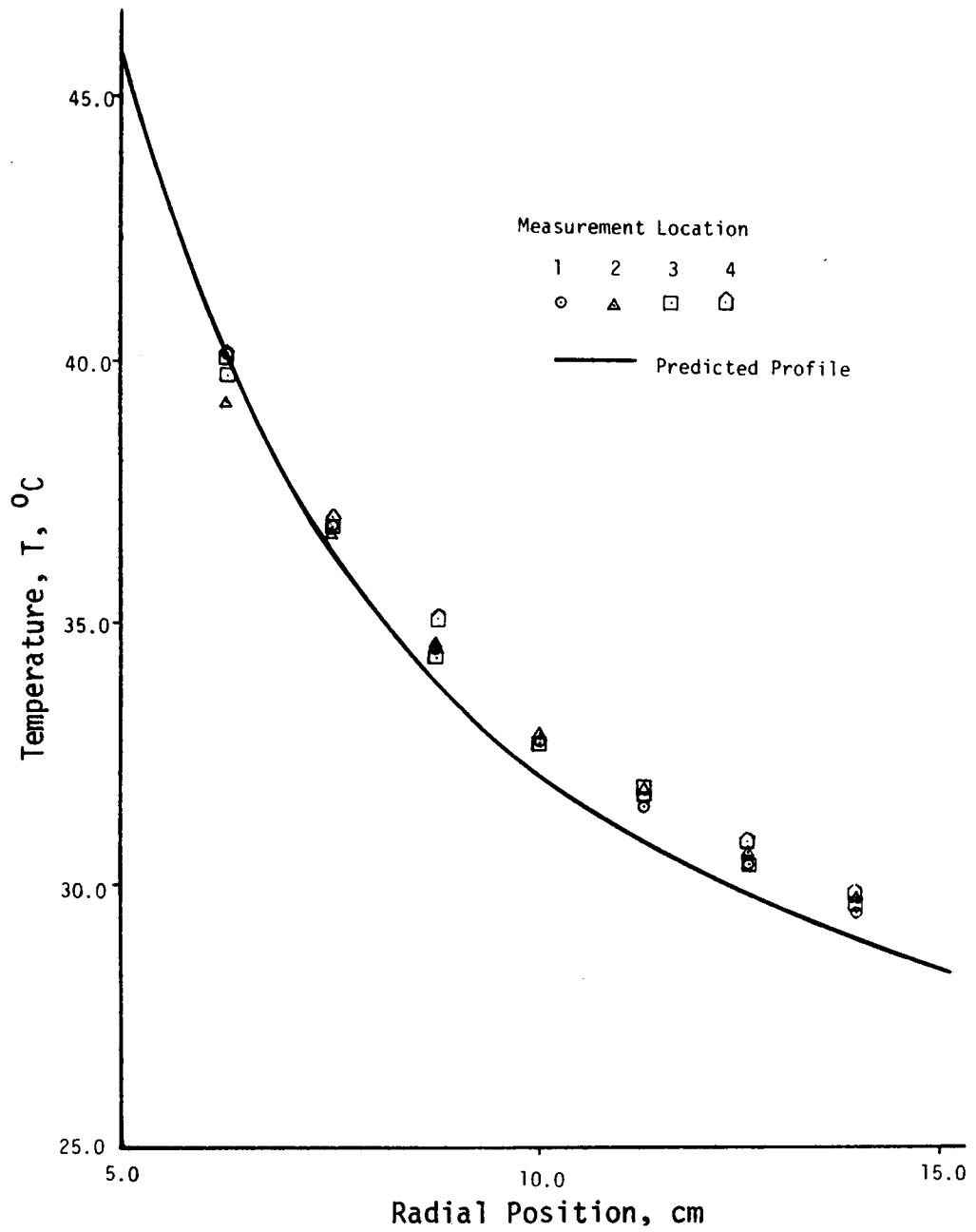
Figure 36. Local T vs. Radial Position--Run 9
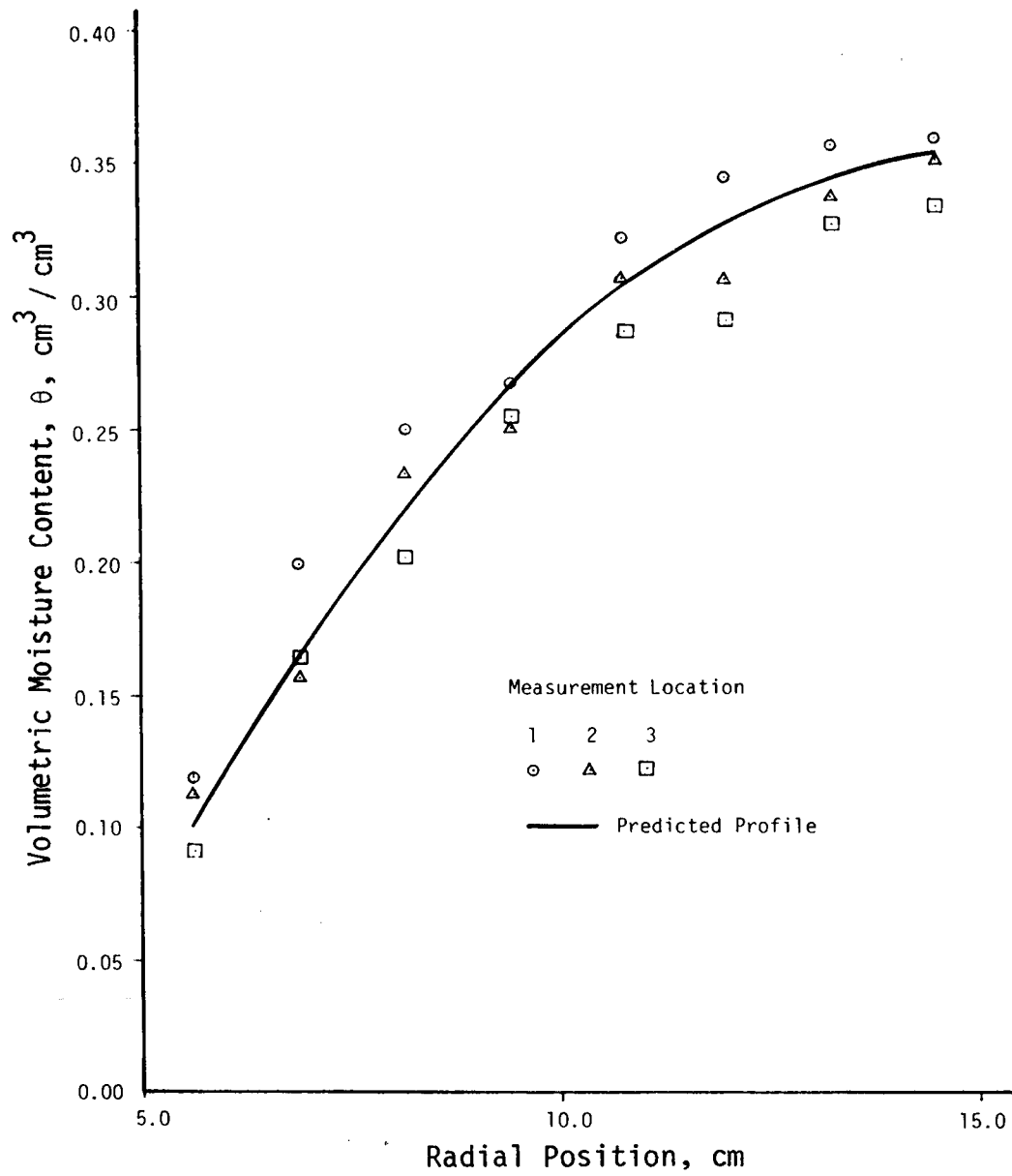
Figure 37. Local θ vs. Radial Position--Run 9
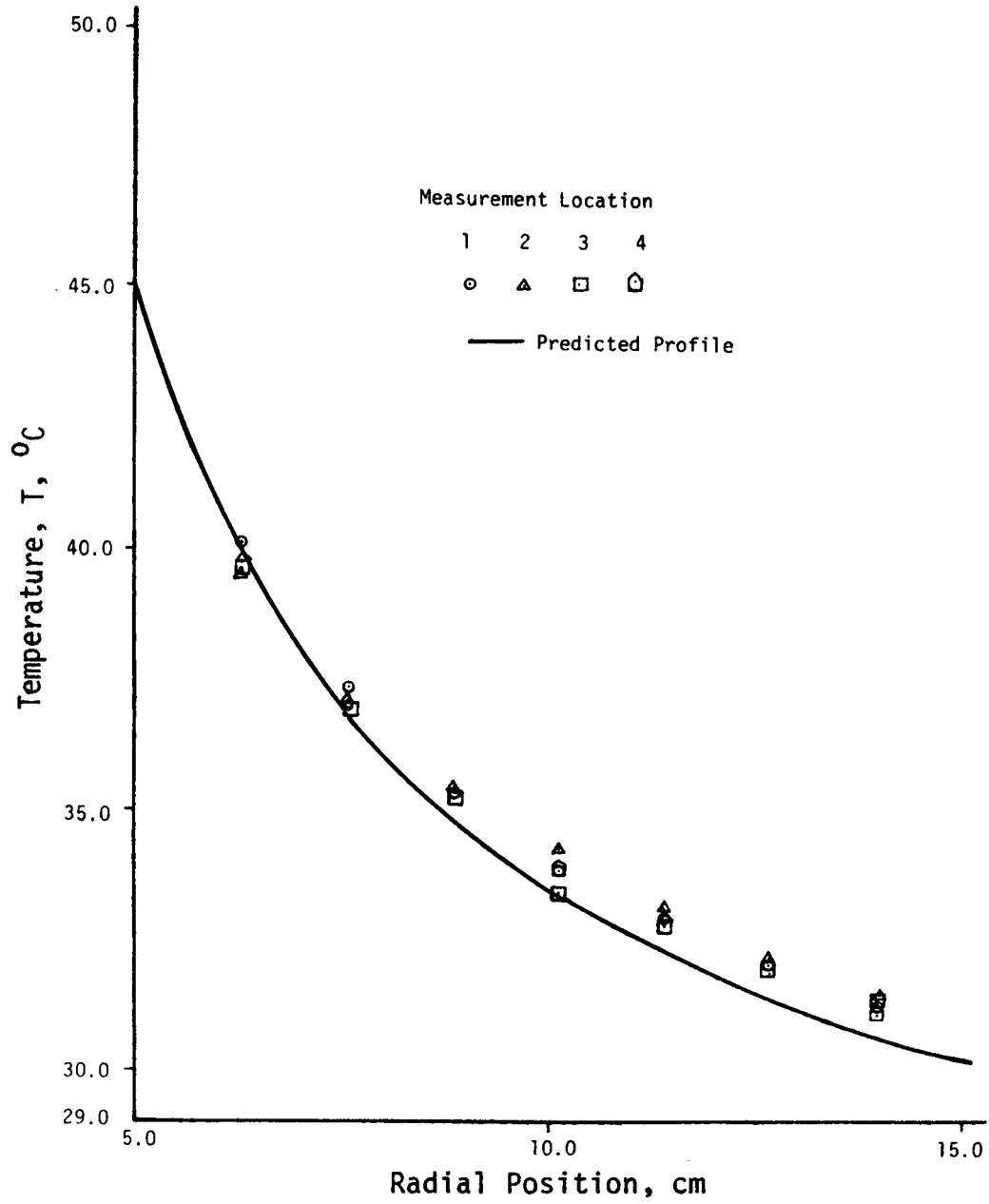
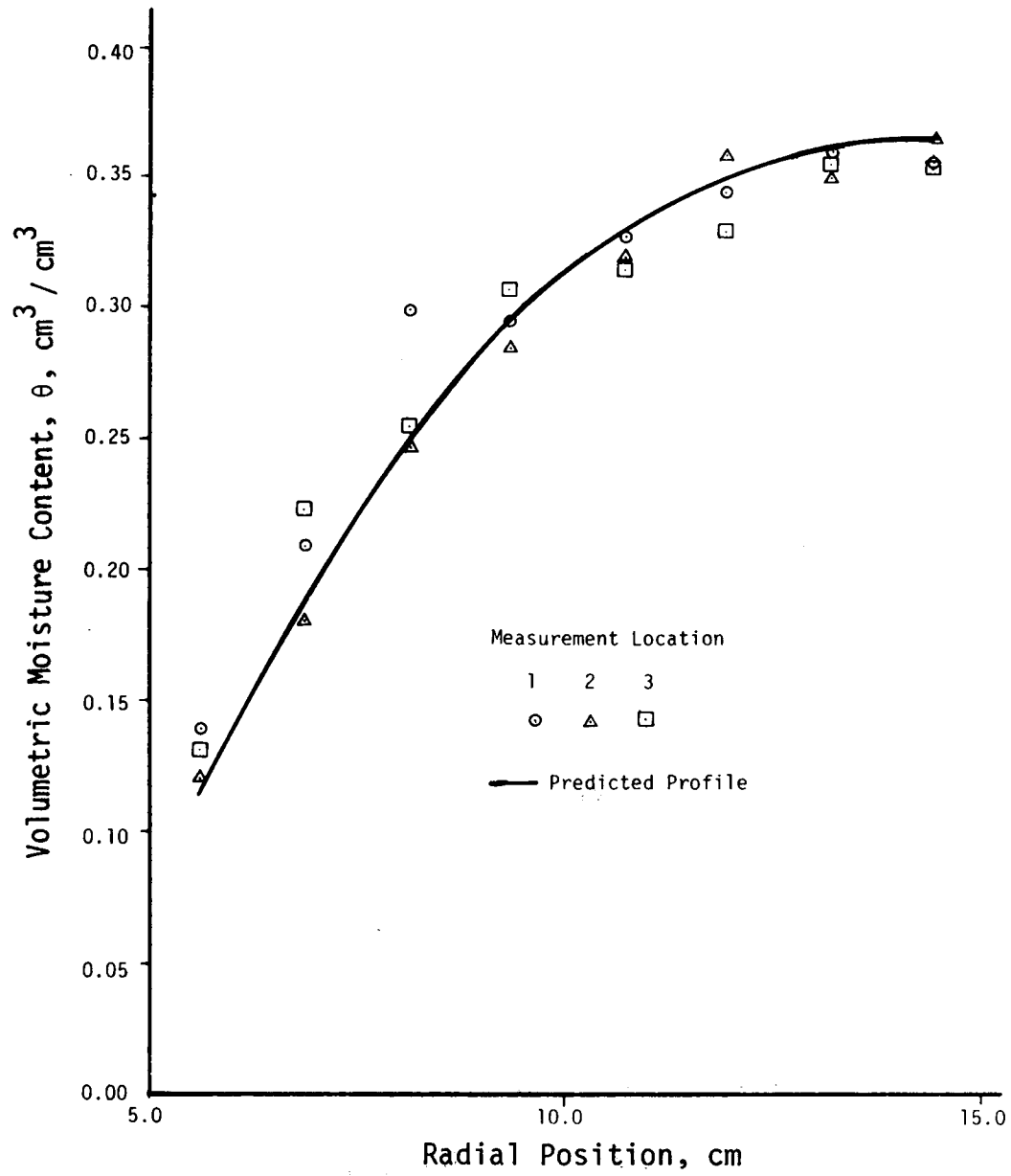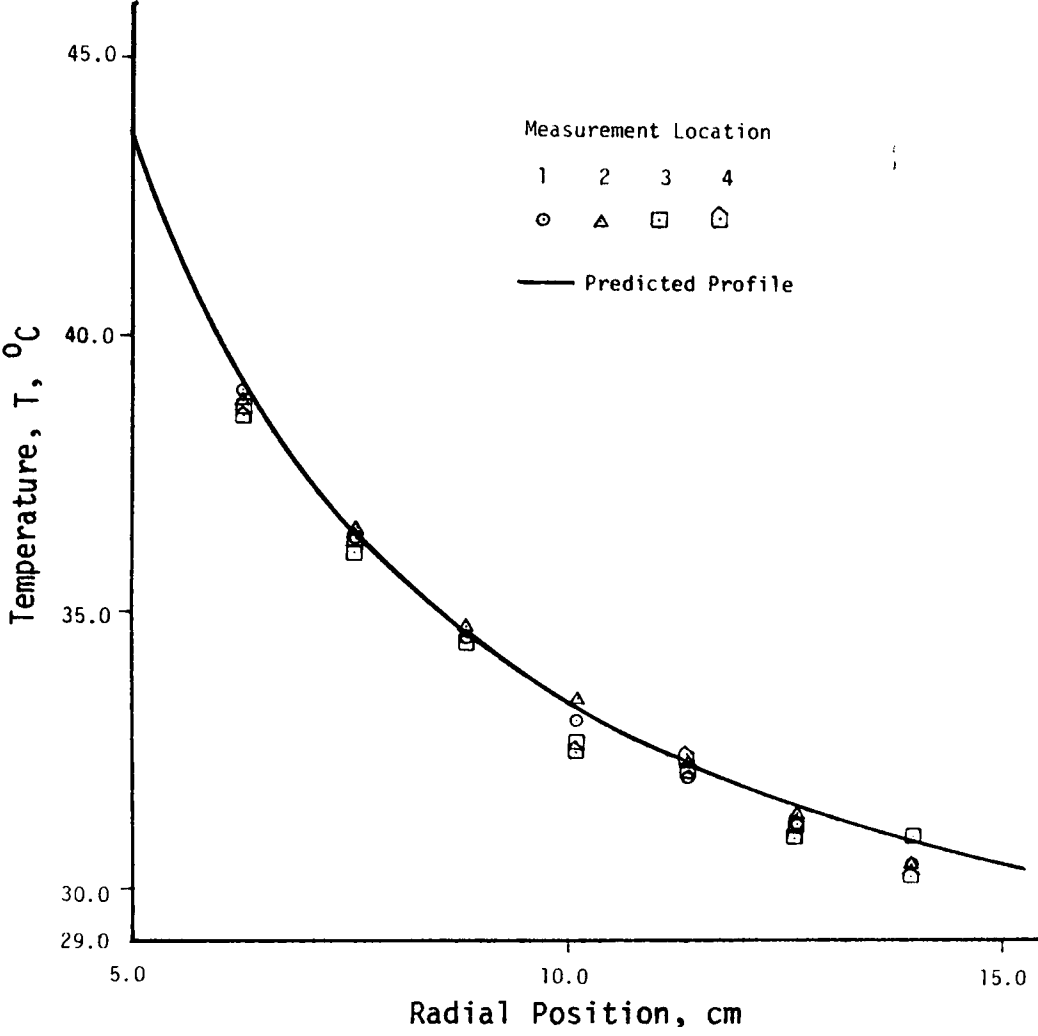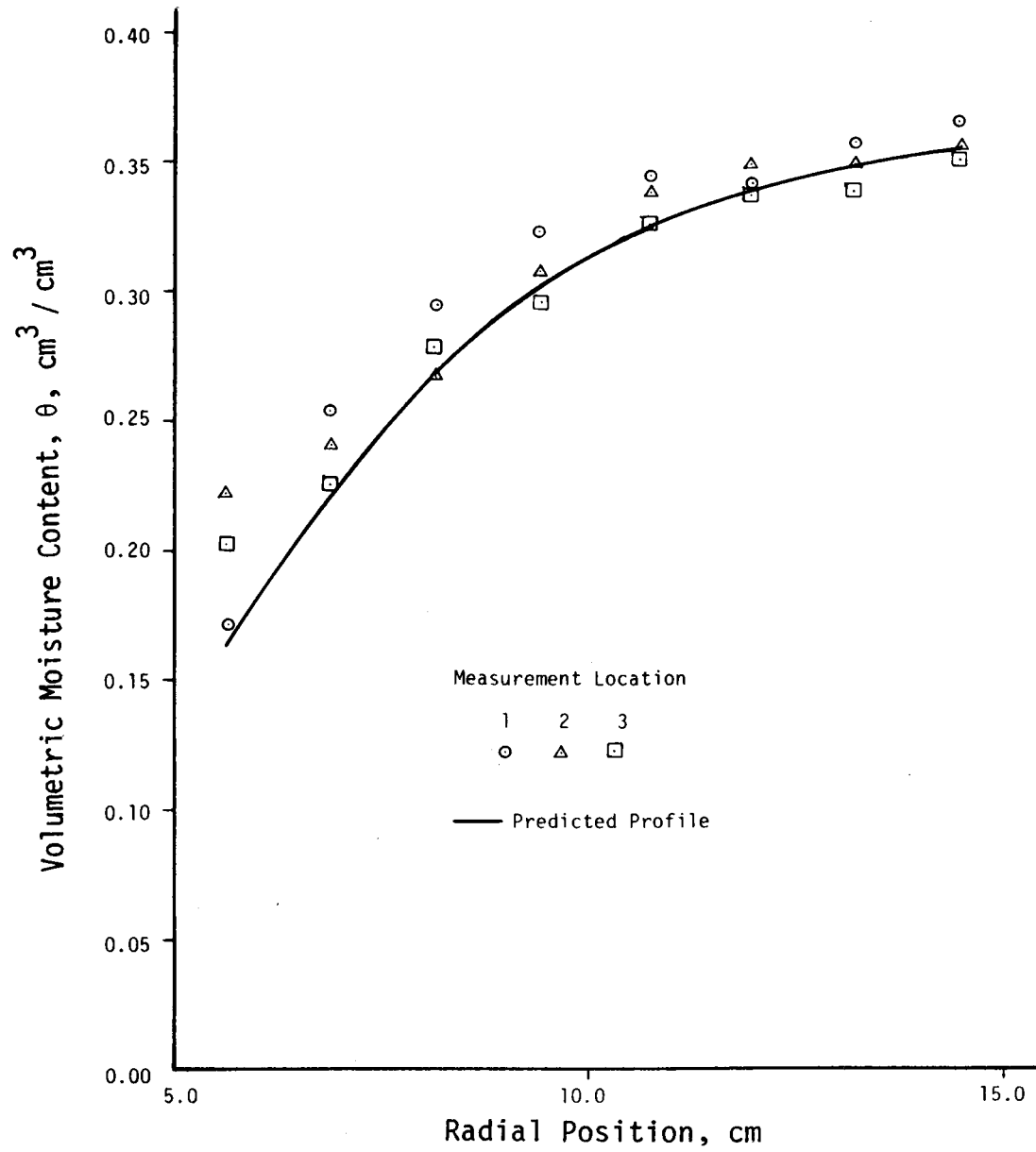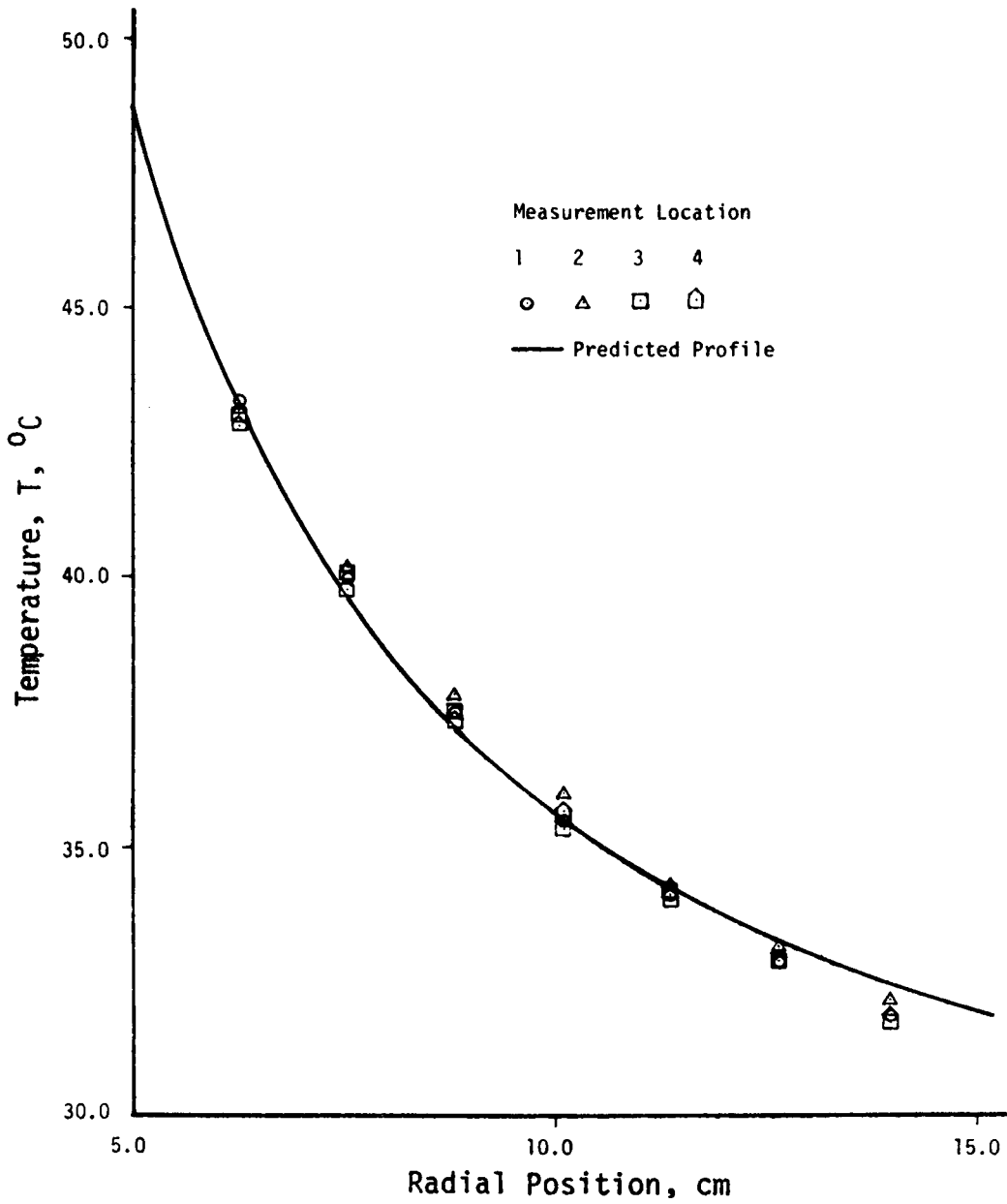Figure 38.   Local T vs. Radial Position--Run 10
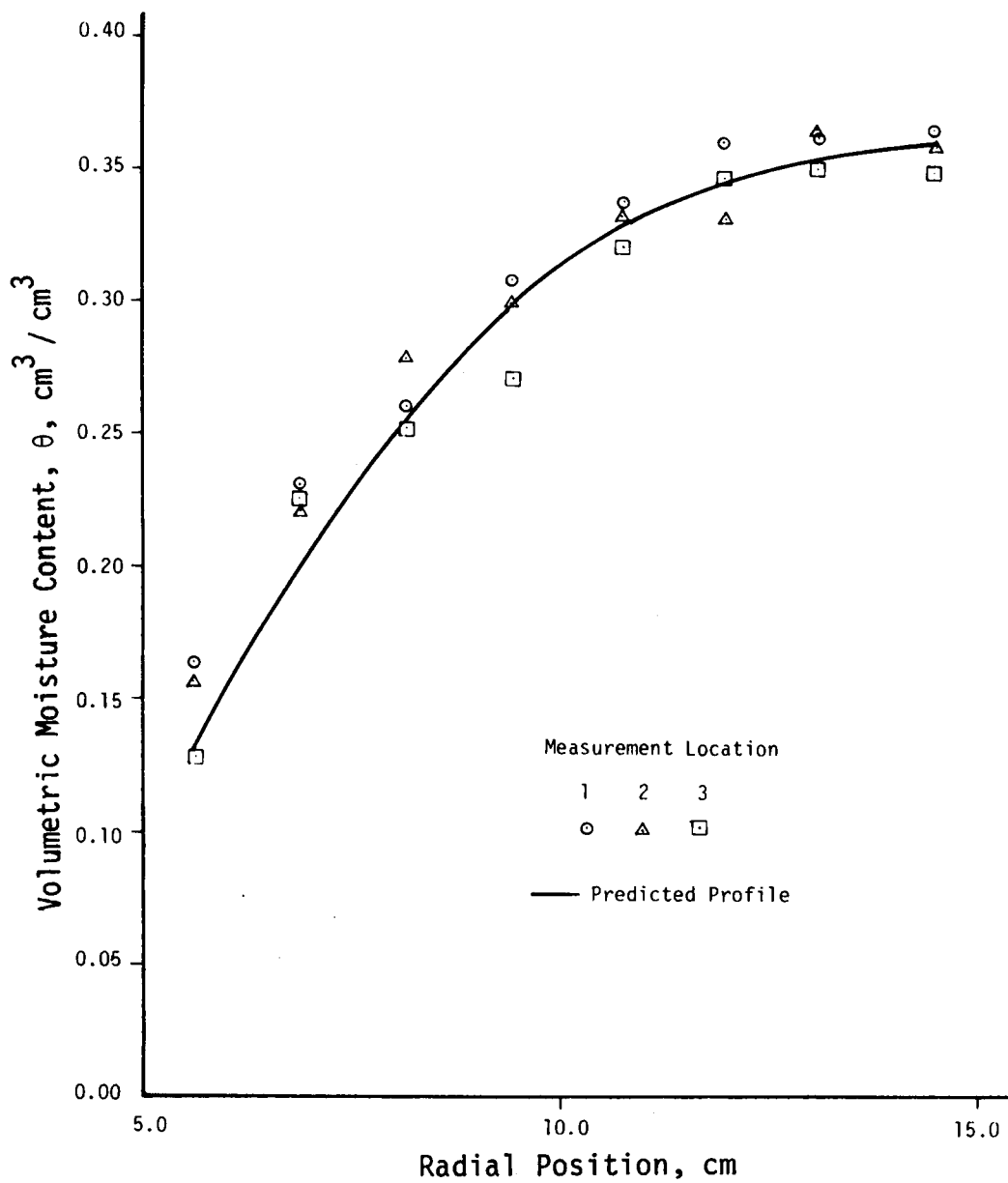
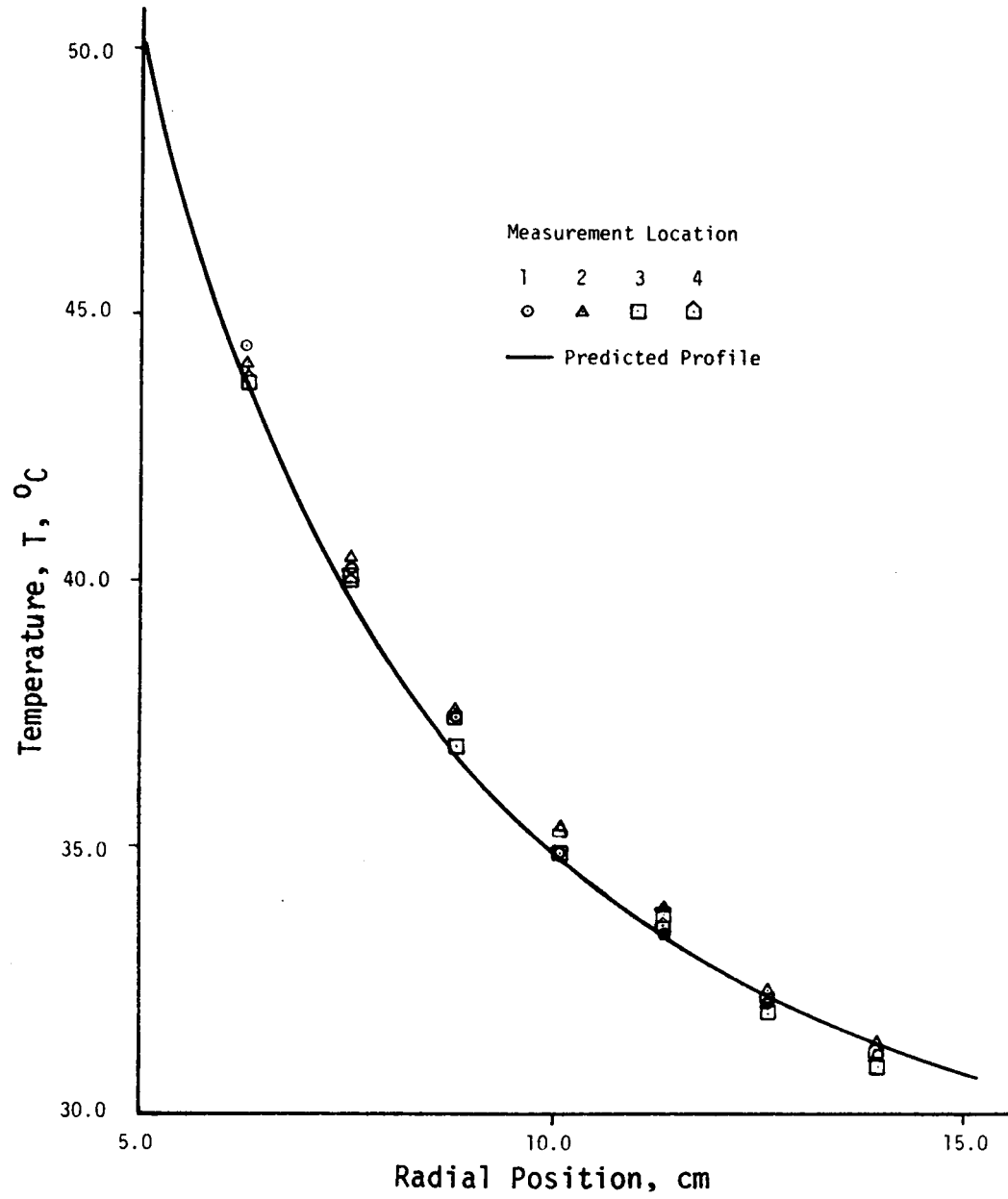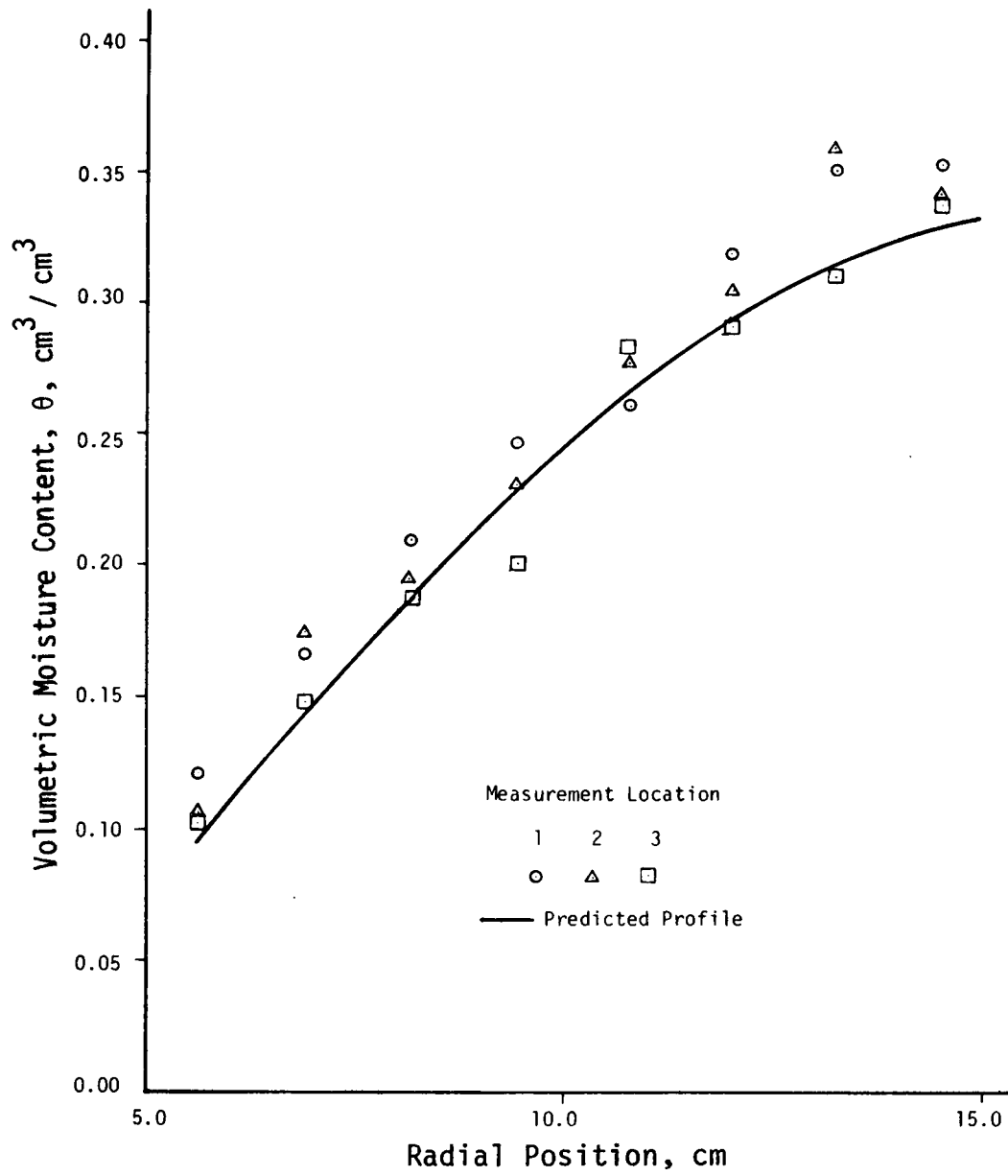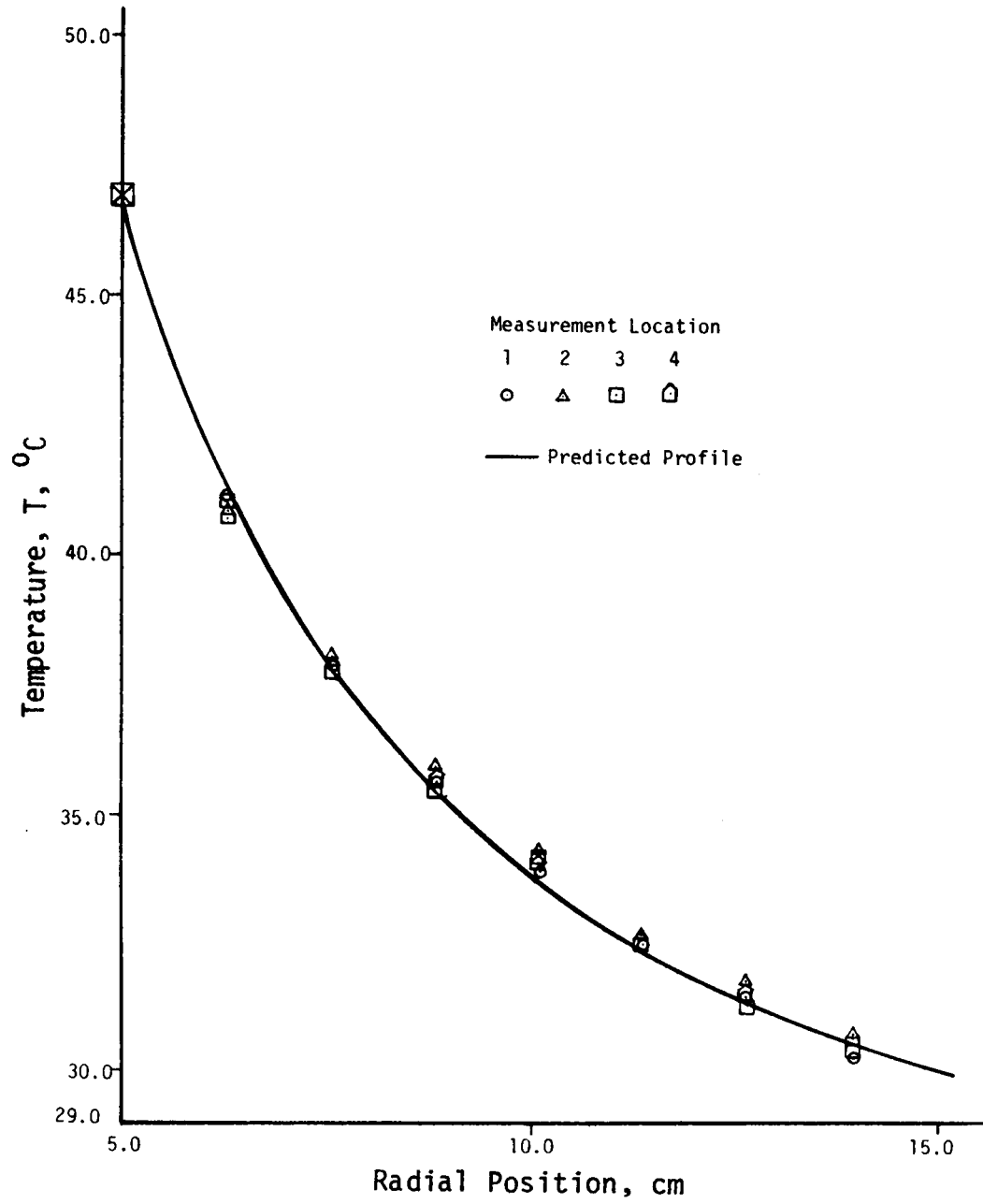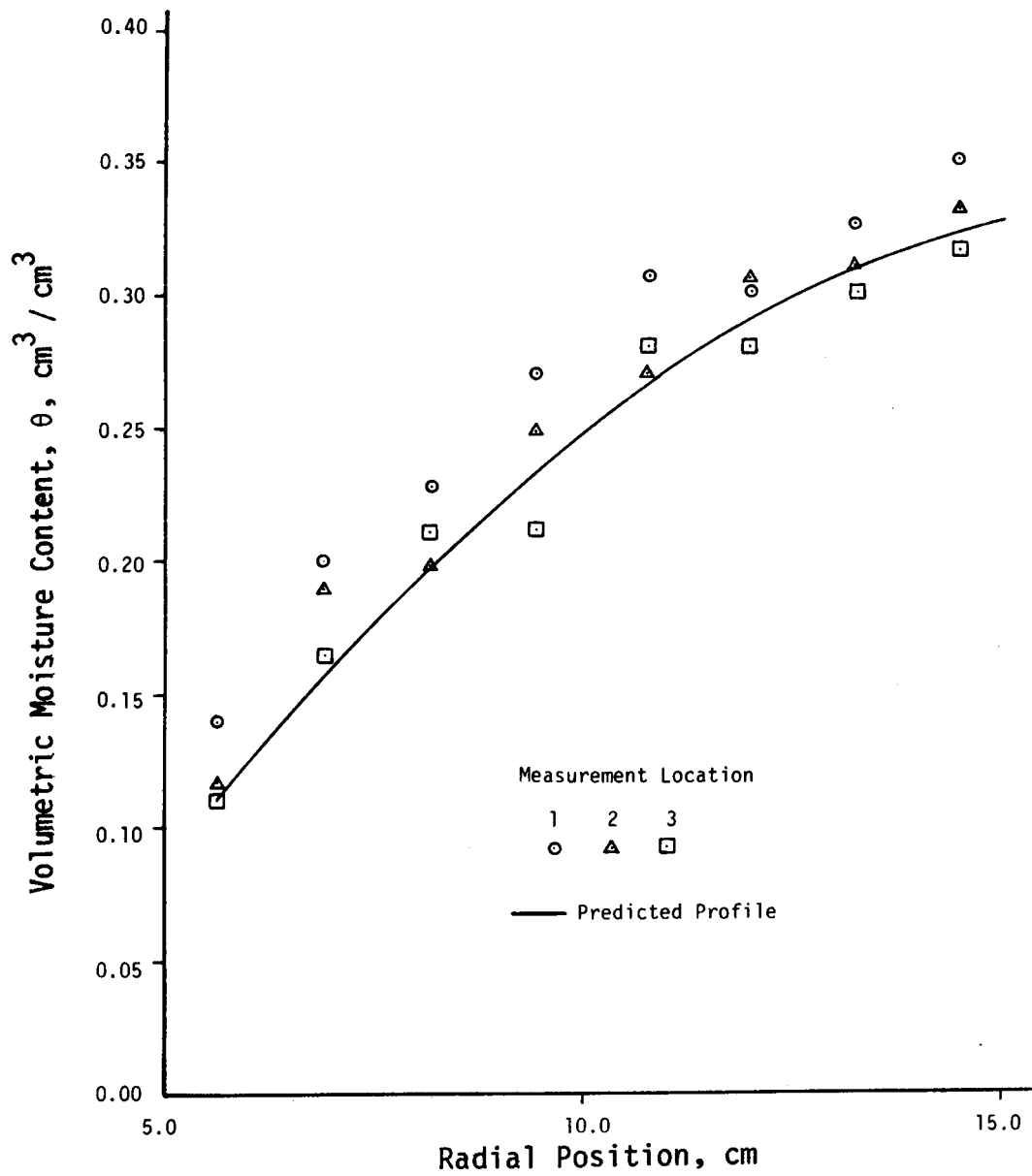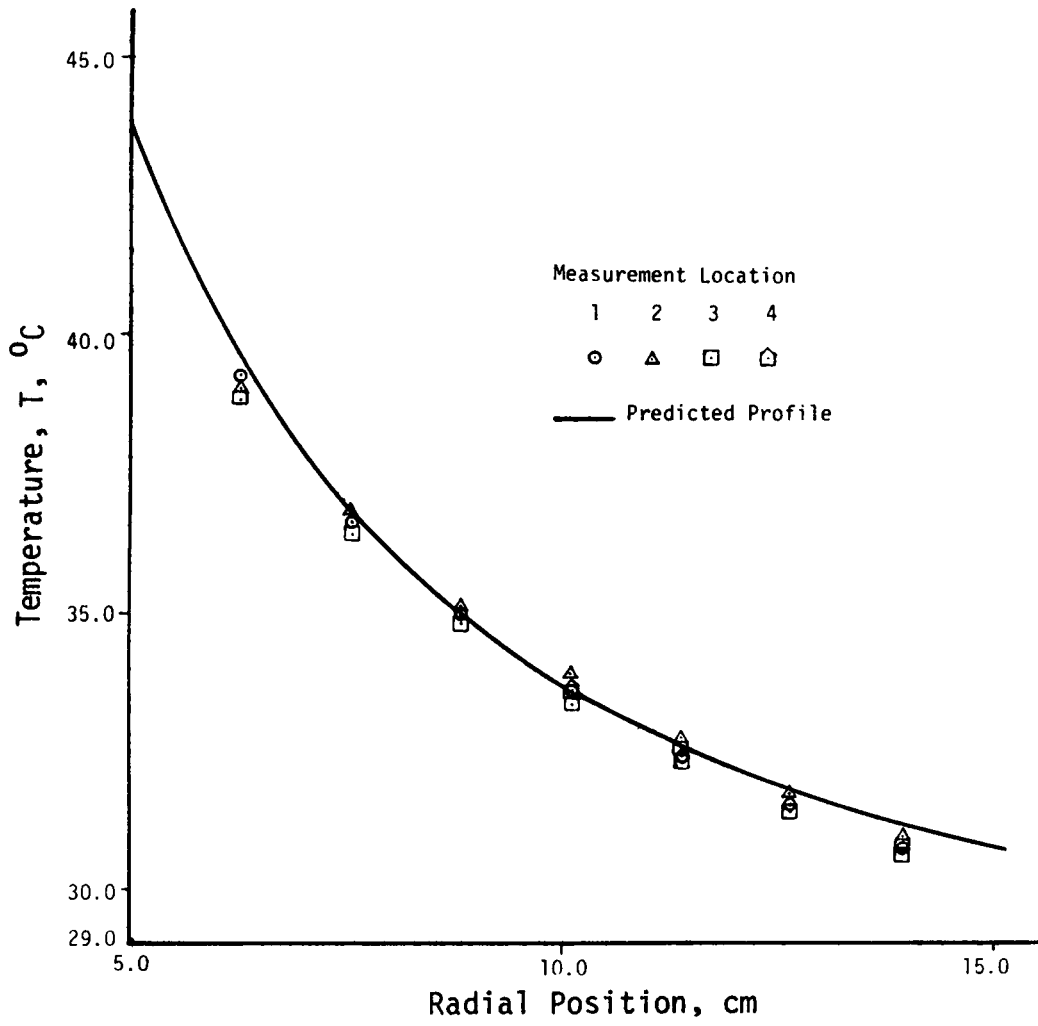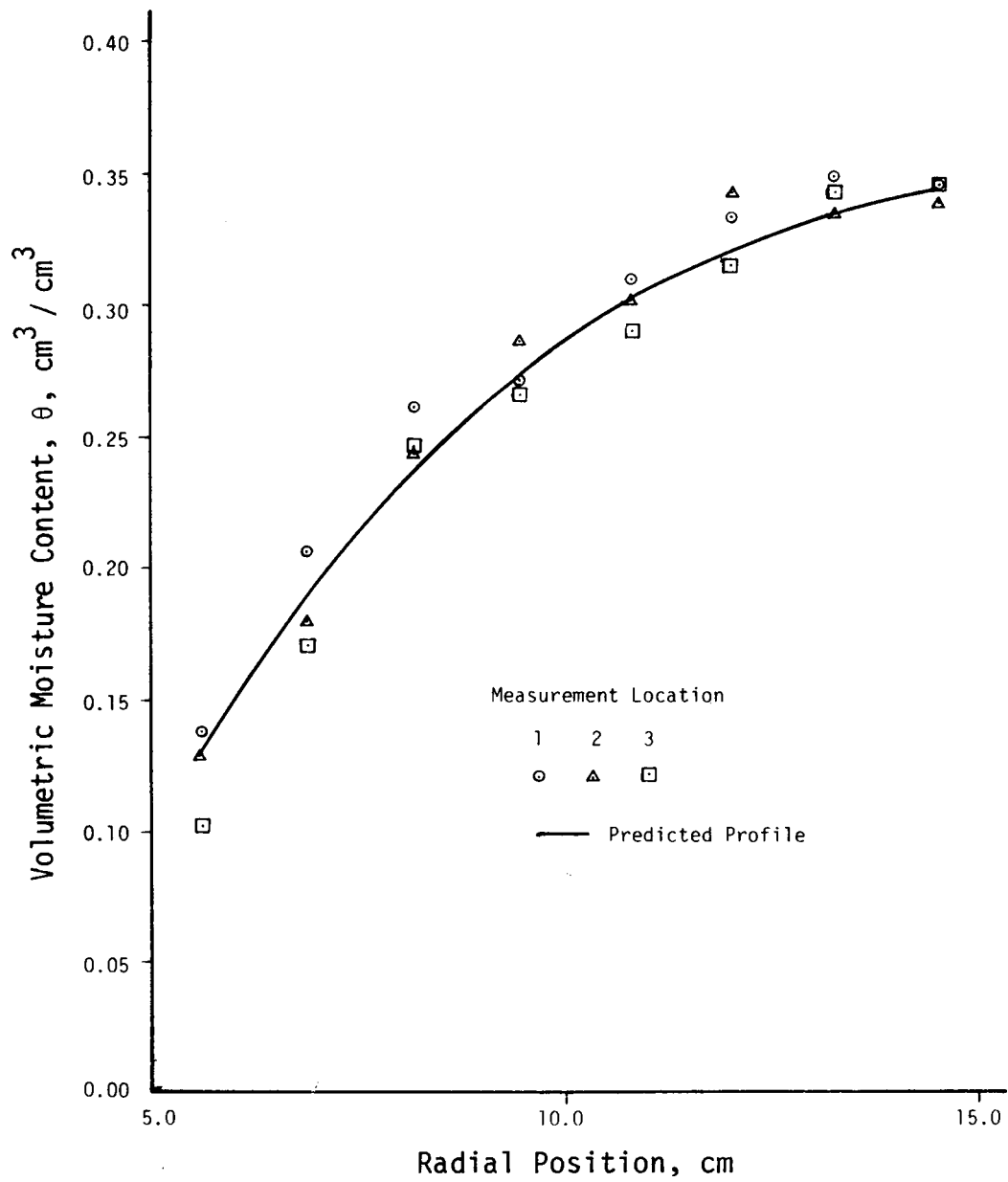Figure 39. Local θ vs. Radial Position--Run 10
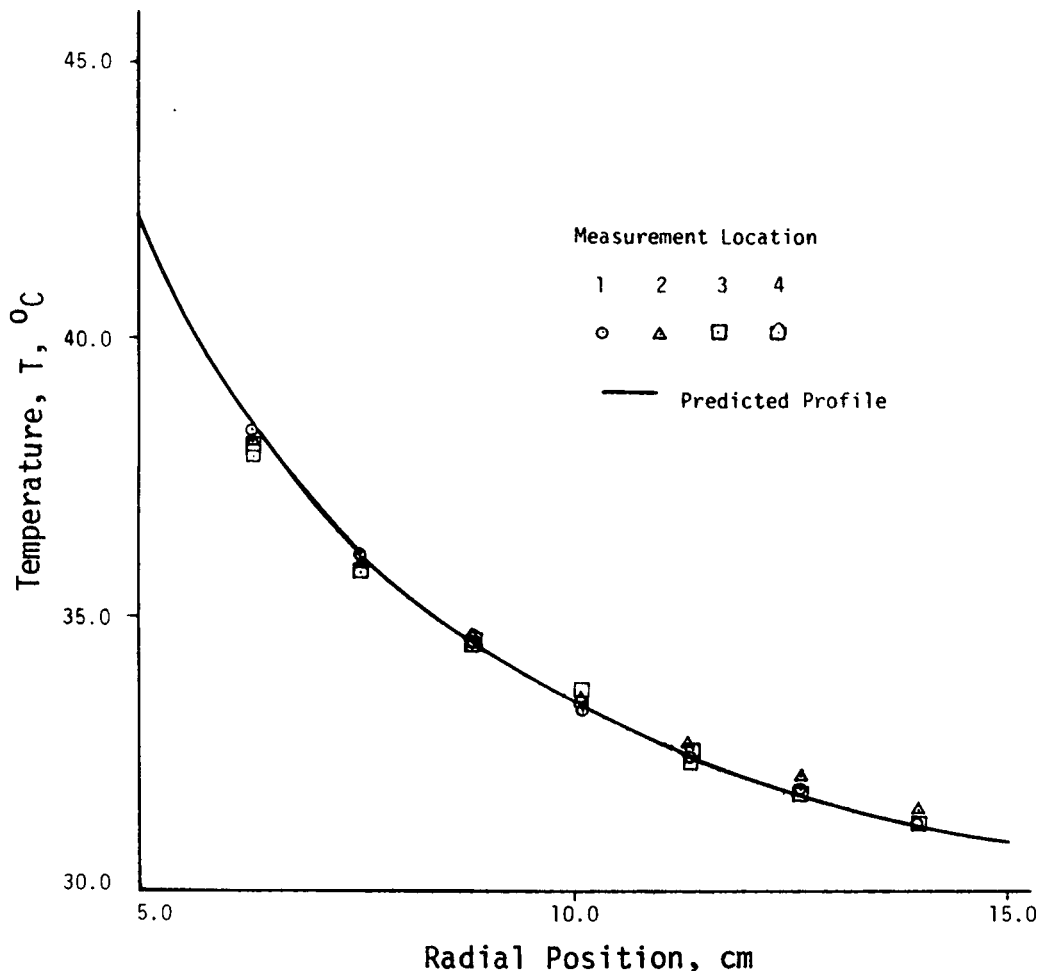
Figure 40.   Local T vs. Radial Position--Run 11
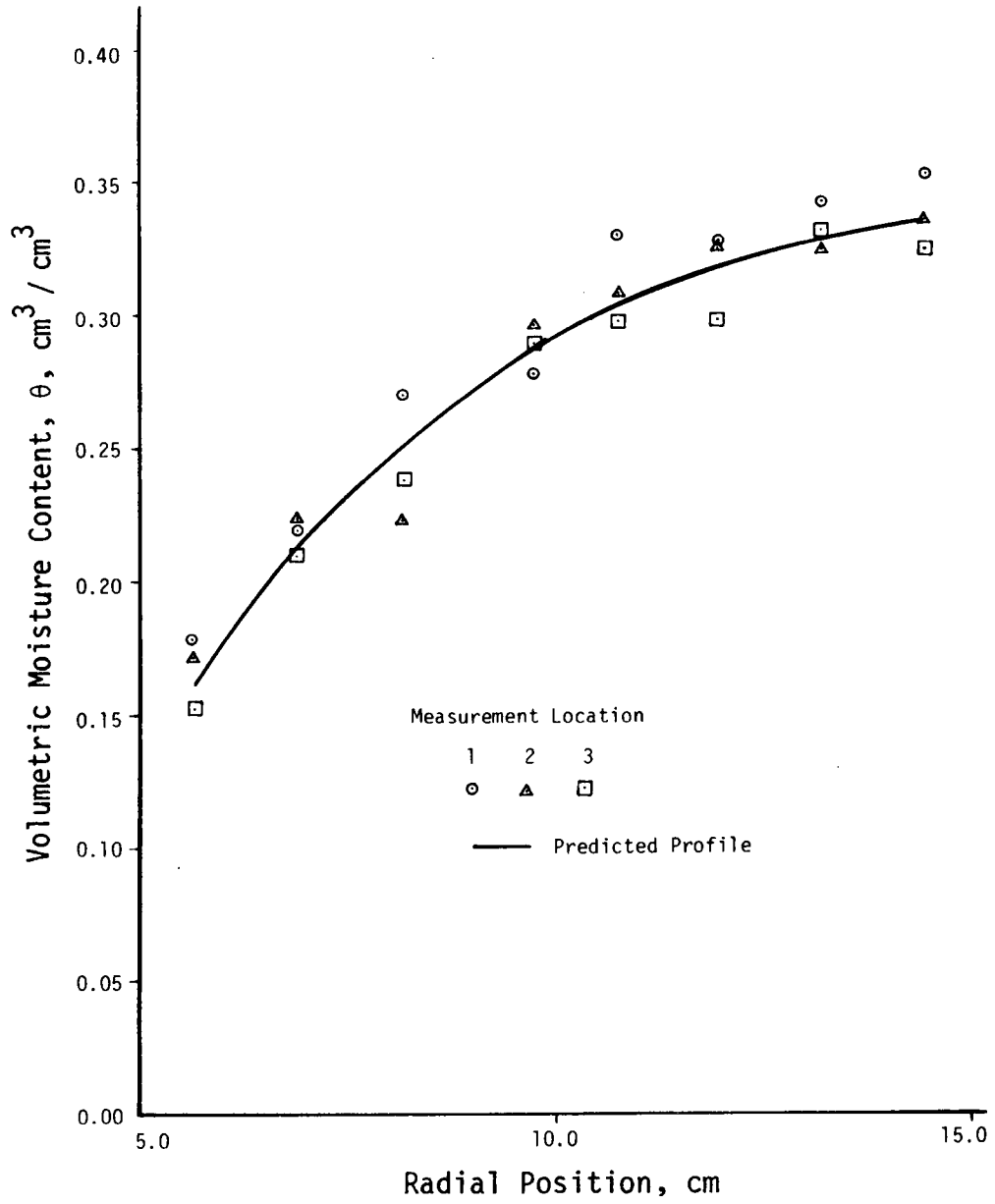
Figure 41. Local θ vs. Radial Position--Run 11

Run 2 had a distribution of moisture content values over the entire wetness range of interest and was therefore selected for calculation of the coupling coefficients, β^*, L_{wq} and β using the methods described in Chapter 6. The dashed curves in Figures 22 and 23, representing "averaged" radial distributions of temperatures and moisture contents for Run 2, were obtained by least-squares fit of the mean local values by second order polynomials. The coefficients calculated from these data were used to predict temperature and moisture content distributions for the other runs.

The solid curves in Figures 20 and 21 and in Figures 24 through 41 are the steady-state profiles of temperature and moisture content predicted by the CSMP simulation program of the model equations. The predicted distributions showed good agreement with the experimentally observed temperature and moisture content profiles.

Independent calculations of β^* values were made with data from Runs 4, 6 and 8, and plotted as functions of moisture content in Figure 42. β^* calculated from Run 2 (see Figure 8), used to predict steady-state profiles, are also shown in Figure 42 for comparison purposes. The different curves for the β^* vs. θ relationship for the four runs show reasonably close agreement, indicating that β^* is a single-valued function of θ for the range of fluxes investigated. The β^* vs. θ curves are similar in appearance to those observed by Gee [38] for soil samples, although Gee's β^* values for the soil media are about 5 to 10 times those in Figure 42. Numerical errors in the evaluation of the temperature and moisture content gradients for subsequent calculation of β^* are probably responsible for the "unsmooth" appearance of these curves.
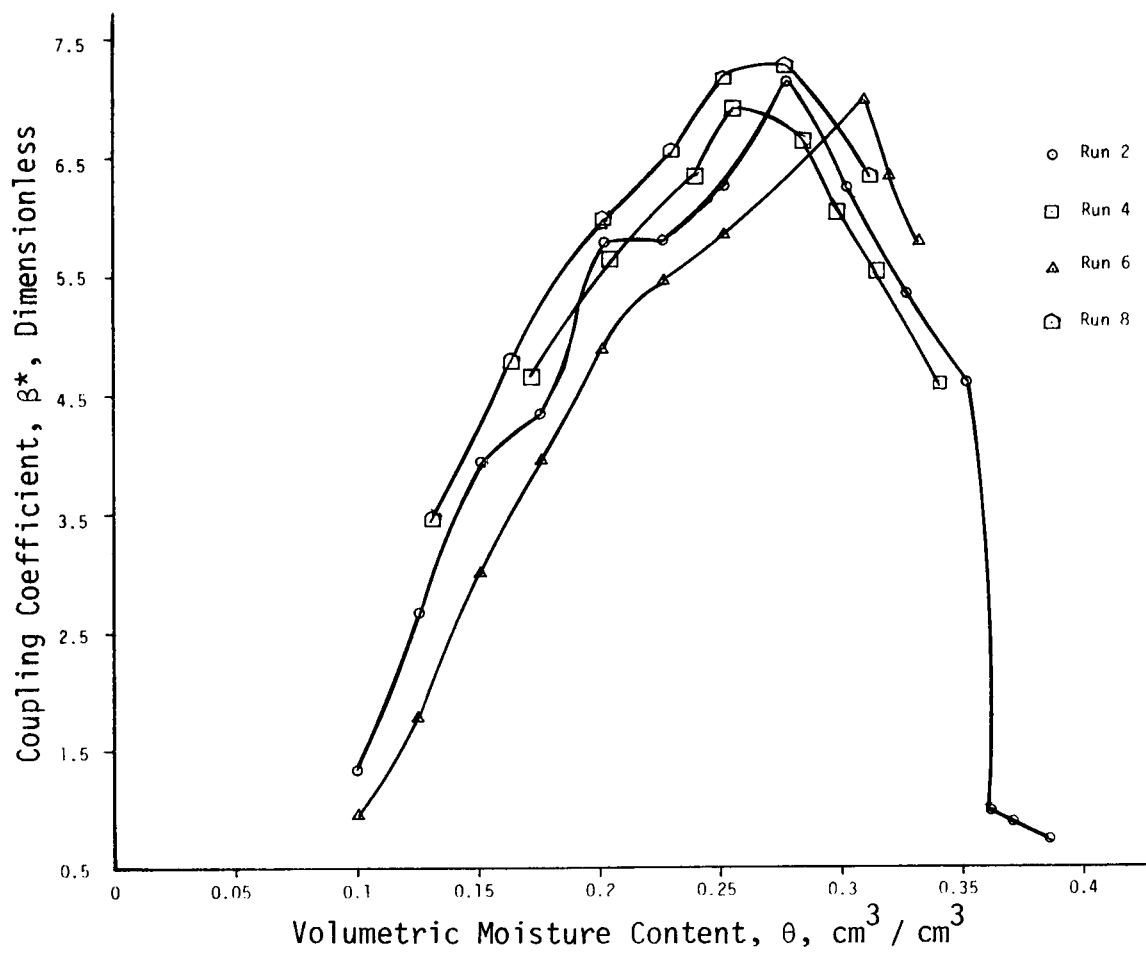
Figure 42. Coupling Coefficient β* vs. Volumetric Moisture
Content θ, for Runs 2, 4, 6, and 8

The extremely small values of the coupling coefficient β (see Figure 10) indicate negligible influence of moisture content gradients on the heat flux. As a numerical check, the model equations were also solved with a zero value for β, and no change was observed in the predicted temperature and moisture content profiles. This constitutes an indirect verification of the Onsager relationship since β was calculated from β^* using the Onsager relation.

Surface temperature uniformity of the two spheres and close agreement of temperatures measured at equal radii for different locations appear to support the assumption of one-dimensional heat transfer. Local moisture content determination by the gravimetric method is subject to greater error than the temperature measurement. Such errors include the spatial averaged nature of the local moisture content values, loss of moisture during handling, and determination of very small differences in mass. The measured values of moisture content, while exhibiting scatter, are in reasonable agreement with predictions utilizing the Cary and Taylor model. The agreement of measured and predicted temperature profiles is better, but this might be attributed to the relative unimportance of coupling of moisture content gradient to heat flux and the greater certainty associated with thermal conductivity values.

The moisture content data indicate, however, that one-dimensional transfer is not strictly satisfied since a general trend toward higher moisture contents is obvious toward the bottom of the annular medium. This observation might be qualitatively associated with gravitational effects.

CHAPTER 9

CONCLUSIONS AND RECOMMENDATIONS

I.   Methods have been developed for obtaining the transport
      coefficients in the Cary and Taylor equations, and a solution tech-
      nique was developed to obtain predictions of the temperature and
      moisture content for a one-dimensional steady-state system with
      zero mass flux.

      A.   A transient method has been used to determine the thermal
            conductivity for the porous medium as a function of moisture
            content. The measurements were made in a time frame which
            precluded significant moisture transfer, thus obviating
            the difficulty of assigning thermal conductivity values which
            do not reflect the coupling between heat and moisture transfer.

      B.   The coupling coefficient β^*, which measures the inde-
            pendent effect of temperature gradient on liquid moisture
            flux, has been determined for a nominally 250 μ glass bead -
            water unsaturated system. β^*, although strongly dependent on
            the moisture content, appears not to be a function of the
            gradients of moisture or temperature for the range of fluxes
            studied. This conclusion is based on comparison of calculated
            values of β^* from runs with heating rates differing by a factor
            of about two, and on the success of prediction of steady-state
            temperature and moisture profiles for different boundary condi-
            tions using β^* determined for one heating rate.

97

C.   The coupling coefficient β, which measures the independent effect of moisture content gradient on heat flux, appears to be essentially zero for this system, based on application of Onsager's relationship and on numerical evaluation of the effect of β on predicted steady-state temperature and moisture content profiles.

D.   The IBM Continuous System Modeling Program has been used to predict the steady-state temperature and moisture profiles in a one-dimensional, spherically symmetric, closed porous medium system. The thermal conductivity, diffusivity, and coupling coefficient β^* are treated as functions of moisture content.

II.   Comparison of steady-state experimental data with model predictions showed reasonable agreement, indicating validity of the Irreversible Thermodynamics model over the range of parameters studied.

III.   Precise guidelines regarding the applicability of the theory of linear Irreversible Thermodynamics to other systems of this nature for both steady-state and transient conditions are not yet known and need to be established.

A.   The importance of hysteresis is not clearly understood and needs investigation.

B.   A theoretical basis is needed for establishing the ranges of moisture contents and temperatures in which liquid-dominated flow, which is assumed in the present formulation of Cary and Taylor model, applies.

C.   For high liquid moisture contents, there is an indication that gravity effects may be important. Extension of the predictive model to include such effects should be instructive.

D.   Validation of the Cary and Taylor model for processes in unsaturated porous media for open systems should be attempted.

E.   Finally, the Irreversible Thermodynamics basis for the Cary and Taylor model needs careful scrutiny. It appears that a more conceptually correct derivation should identify a potential which includes surface effects in the Gibbs Equation and that the identification of chemical potential in the thermodynamic force conjugate to mass flux in this system may not be rigorous.

NOMENCLATURE

A   constant

b   exponent; graphically, the negative of the slope of the log Y-t curve, $\sec^{-1}$

C_i mass concentration of component i, g / g

c   specific heat, cal/g $^{\circ}C$

D   coefficient of diffusivity of liquid water in an unsaturated porous medium, cm^2 / day

g   gravitational constant, cm / $\sec^2$

H   height, cm

h   surface heat transfer coefficient, cal / sec cm^2 $^{\circ}C$

$\bar{H}_i$ partial enthalpy of component i, cal / g

J_i thermodynamic flux of ith species

J_Q thermodynamic heat flux, cal / cm^2 day

J_q heat flux $\left(= J_Q - \sum_{i=1}^{n} J_i \bar{H}_i\right)$, cal / cm^2 day

J_w flux of liquid water, g / cm^2 day

$J_0(x)$ Bessel function of first kind and zero order of x

$J_1(x)$ Bessel function of first kind and first order of x

K   hydraulic conductivity, cm / day

K_s saturated hydraulic conductivity, cm / day

K_{sc} calculated saturated conductivity, cm / day

$K(\theta)_i$ calculated hydraulic conductivity for a specified water
content or pressure

L   length, cm

L_{ik}, L_{iq}, L_{qi},

L_{qq}, L_{qw},   phenomenological coefficients

L_{wq}, L_{ww}

M   mass of system, g

M_i mass of component i, g

n   total number of pore classes

P   pressure, dynes / cm^2

p   parameter that accounts for interaction of pore classes

Q   heat rate, cal / day

Q_w volumetric flow rate, cm^3 / day

R_1, R_2 radial distances, cm

r   radius, cm

r_m radius of cylinder, cm

S   entropy, cal / $^{\circ}C$

$\underline{S}$ specific entropy, cal / g $^{\circ}C$

T   temperature, $^{\circ}K$

T_o initial uniform temperature of sample, $^{\circ}C$

T_1 temperature at radius R_1, $^{\circ}K$

T_a constant ambient water bath temperature, $^{\circ}C$

T_{rm} temperature of cylinder wall

t time variable

$\underline{U}$ specific internal energy, cal / g

$\underline{V}$ specific volume, cm^3 / g

v mass average velocity, cm / sec

v_i velocity of component i, cm / sec

x_1 a constant (= 2.405)

X_i i^{th} thermodynamic force

Y ratio of temperature difference, dimensionless

α thermal diffusivity, cm^2 / sec

β coupling coefficient (= $d\psi$ / d ln T) , cal / g

β^* coupling coefficient (= d 0 / d ln T) , dimensionless

γ colatitude angular coordinate, degrees

Δ notation for change

δ surface tension of water, dynes / cm

ϵ porosity, cm^3 / cm^3

η viscosity of water, g / cm sec

θ volumetric moisture content, cm^3 water / cm^3 medium

θ_1 moisture content at radius R_1, cm^3 water / cm^3 medium

λ thermal conductivity, cal / cm sec $^{\circ}C$

μ chemical potential, cal/g

μ_w chemical potential of water, cal / g

μ_w^0 chemical potential of free water, cal / g

ρ density, g / cm^3

ρ_i density of component i, g / cm^3

ρ_w density of water, g / cm^3

σ rate of entropy production, cal / g ^{o}C day

σ' volumetric rate of entropy production, cal / cm^3 ^{o}C day

ϕ latitude angular coordinate, degrees

ψ water potential, dynes / cm^2

∇ gradient operator, cm^{-1}

LITERATURE CITED

1. Abd-El-Aziz, M. H. and S. A. Taylor, "Simultaneous Flow of Water and Salt through Unsaturated Porous Media," Soil Science Society of America Proceedings, 29(2): 141-143 (1965).

2. Baladi, J. Y., R. J. Schoenhals, and D. L. Ayers, "Transient Heat and Mass Transfer in Soils," 78-HT-31, ASME Publication (1978).

3. Beatty, K. O., Jr. "Phenomenology of 'Coupled' Heat and Mass Transfer," Letters in Heat and Mass Transfer, 1:25-30, Pergamon Press (1974).

4. Boersma, L., "Beneficial Use of Waste Heat in Agriculture," Water Resources Research Conference, 5th, Washington, D. C. (1970).

5. Boersma, L., "Warm Water Utilization, " Proceedings of the Conference on the Beneficial Uses of Thermal Discharge, Albany, New York, New York State Department of Environmental Conservation, Albany, New York: 74-107 (1970).

6. Boersma, L., J. W. Cary, D. D. Evans, A. H. Ferguson, W. H. Gardner, R. J. Hanks, R. D. Jackson, W. D. Kemper, D. E. Miller, D. R. Nielsen, and G. Uehera, Soil Water, American Society of Agronomy, Soil Science Society of America, Madison, Wisconsin (1972).

7. Bolt, C. H. and M. J. Frissel, "Thermodynamics of Soil Moisture," Netherlands Journal of Agricultural Science, 8:57-58 (1960).

8. Bomba, S. J., "Hysteresis and Time-Scale Invariance in a Glass-Bead Medium," Ph.D. Thesis, University of Wisconsin, Madison, Wisconsin (1967).

9. Bondurant, J. L., "Coupled Heat and Moisture Transfer in Soil with Applications to the Design of a Warm Water Subsurface Irrigation System," M.S.Ch.E. Thesis, University of Arkansas, Fayetteville, Arkansas (1975).

10. Bouyoucos, G. J., "The Effect of Temperature on Some of the Most Important Physical Processes of Soils," Michigan Agricultural Experiment Station, Technical Bulletin No. 22, 63 p. (1915).

11. Bouyoucos, G. J., "Effect of Temperature on the Movement of Water Vapor and Capillary Moisture in Soils," Journal of Agricultural Research, 5:141-172, Washington, D. C. (1915).

12. Breyer, W., "Heat Transfer in Porous Media Containing a Volatile Liquid," D. Eng. S. Thesis, Rensselaer Polytechnic Institute, Troy, New York (1968).

13. Buckingham, E., "Studies of the Movement of Soil Moisture," United States Department of Agriculture, Bureau of Soils, Bulletin No. 38, 61 p. (1907).

14. Carnahan, C. L., "Non-equilibrium Thermodynamics of Groundwater Flow Systems: Symmetry Properties of Phenomenological Coefficients and Consideration of Hydrodynamic Dispersion," Journal of Hydrology, 31:125-150 (1976).

15. Cary, J. W. "Onsager's Relation and the Non-isothermal Diffusion of Water Vapor," Journal of Physical Chemistry, 67:126-129 (1963).

16. Cary, J. W., "An Evaporation Experiment and its Irreversible Thermodynamics," International Journal of Heat and Mass Transfer, 7:531-537 (1964).

17. Cary, J. W., "Water Flux in Moist Soil: Thermal Versus Suction Gradients," Soil Science, 100:168-175 (1965).

18. Cary, J. W., "Soil Moisture Transport due to Thermal Gradients: Practical Aspects," Soil Science Society of America Proceedings, 30:428-433 (1966).

19. Cary, J. W. and H. F. Mayland, "Salt and Water Movement in Unsaturated Frozen Soil," Soil Science Society of America Proceedings, 36: 549-555 (1972).

20. Cary, J. W. and S. A. Taylor, "The Interaction of the Simultaneous Diffusions of Heat and Water Vapor," Soil Science Society of America Proceedings, 26:413-416 (1962).

21. Cary, J. W. and S. A. Taylor, "Thermally Driven Liquid and Vapor Phase Transfer of Water and Energy in Soil," Soil Science Society of America Proceedings, 26:417-420 (1962).

22. Cary, J. W. and S. A. Taylor, "The Dynamics of Soil Water: II. Temperature and Solute Effects," In: Irrigation of Agricultural Lands, R. M. Hagan, H. R. Haise, and T. W. Edminster, editors, American Society of Agronomy, Monograph No. 11, Madison, Wisconsin (1967).

23. Cassel, D. K., D. R. Nielsen, and J. W. Bigger, "Soil Water Movement in Response to Imposed Temperature Gradients," Soil Science Society of America Proceedings, 33:493-500 (1969).

24. Childs, E. C. and N. Collis-George, "The Permeability of Porous Materials," Proceedings of the Royal Society, 201A: 392-405 (1950).

25. Chung, P. K. and M. L. Jackson, "Thermal Diffusivity of Low Conductivity Materials," Industrial and Engineering Chemistry, 46(12): 2563-2566 (1954).

26. Coleman, B. D. and C. Truesdell, "On the Reciprocal Relations of Onsager," Journal of Chemical Physics, 33(1): 28-31 (1960).

27. Darcy, H., "Les Fontaines Publique de la Ville de Digon," Dalmont, Paris (1856).

28. Denbigh, K. G., "The Thermodynamics of the Steady State," Methuen and Co., Ltd., London (1951).

29. Deryaguen, B. V. and M. K. Melnikova, "Experimental Study of the Migration of Water Through the Soil Under the Influence of Salt Concentration, Temperature, and Moisture Gradients," International Congress of Soil Science, 6th:305-314, Paris, France (1956).

30. Dewalle, D. R., "An Agro-Power-Waste Water Complex for Land Disposal of Waste Heat and Waste Water," Institute for Research on Land and Water Resources, Pennsylvania State University, Research Publication Number 86 (1974).

31. Dirksen, C. and R. D. Miller, "Closed System Freezing of Unsaturated Soil," Soil Science Society of America Proceedings, 30:168-173 (1966).

32. Edlefson, N. E. and A. B. C. Anderson, "The Thermodynamics of Soil Moisture," Hilgardia, 15:31-299 (1943).

33. Erh, K. T., D. R. Nielsen, and J. W. Biggar, "Two Dimensional Heat Transfer in Porous Media with Steady-State Water Flow," Soil Science Society of America Proceedings, 35:209-214 (1971).

34. Fitts, D. D., "Nonequilibrium Thermodynamics," McGraw-Hill, New York (1962).

35. Fritton, D. D., D. Kirkham, and R. H. Shaw, "Soil Water Evaporation, Isothermal Diffusion, and Heat and Water Transfer," Soil Science Society of America Proceedings, 34:183-189 (1970).

36. Gardner, W. and J. Chatelain, "Thermodynamic Potential and Soil Moisture," Soil Science Society of America Proceedings, 11:100-102 (1946).

37. Gardner, W. R., "Some Steady State Solutions of the Unsaturated Moisture Flow Equation with Application to Evaporation from a Water Table," Soil Science, 85:228-232 (1958).

38. Gee, G. W., "Water Movement in Soils as Influenced by Temperature Gradients," Ph.D. Thesis, Washington State University, Pullman, Washington (1966).

39. Glansdorff, P. and I. Prigogine, "Thermodynamic Theory of Structure, Stability and Fluctuations," John Wiley and Sons, New York (1971).

40. Globus, A. M., "Mechanics of Soil and Ground Moisture Migration and of Water Movement in Freezing Soils Under the Effect of Thermal Gradients," Soviet Soil Science, 2:130-139 (1962).

41. Groenevelt, P. H. and B. D. Kay, "On the Interaction of Water and Heat Transport in Frozen and Unfrozen Soils: II. The Liquid Phase," Soil Science Society of America Proceedings, 38:400-404 (1974).

42. Green, R. E. and J. C. Corey, " Calculation of Hydraulic Conductivity: A Further Evaluation of Some Predictive Methods," Soil Science Society of America Proceedings, 35:3-8 (1971).

43. deGroot, S. R. and P. Mazur, "Non-Equilibrium Thermodynamics," North Holland Publishing Co., Amsterdam (1962).

44. Gurr, C. G., T. J. Marshall, and J. T. Hutton, "Movement of Water in Soil due to a Temperature Gradient," Soil Science, 74:335-345 (1952).

45. Hadas, A., "Simultaneous Flow of Water and Heat under Periodic Heat Fluctuations," Soil Science Society of America Proceedings, 27:263-265 (1963).

46. Hansen, D., W. Breyer, and W. Riback, "Steady State Heat Transfer in Partially Liquid Filled Porous Media," Journal of Heat Transfer, ASME Transactions, pp 520-527 (1970).

47. Harmathy, T. Z., "Simultaneous Moisture and Heat Transfer in Porous Systems with Particular Reference to Drying," Industrial and Engineering Chemistry Fundamentals, 8(1): 92-103 (1969).

48. Havens, J. A., "Thermal Decomposition of Wood," Ph.D. Thesis, University of Oklahoma, Norman, Oklahoma (1969).

49. Havens, J. A. and R. E. Babcock, "Heat and Moisture Conduction in Unsaturated Soils," Arkansas Water Resources Research Center, Publication No. 28 (1975).

50. Hillel, D., "Soil and Water, Physical Principles and Processes," Academic Press, New York (1971).

51. Hutcheon, W. L., "Moisture Flow Induced by Thermal Gradients Within Unsaturated Soils," In: Water and Its Conduction in Soils, Highway Research Board, Commission on Physico-Chemical Phenomena in Soils, Special Report No. 40, 113 p (1958).

52. Jackson, R. D. and D. Kirkham, "Method of Measurement of the Real Diffusivity of Moist Soil," Soil Science Society of America Proceedings, 22:479-482 (1958).

53. Jackson, R. D., D. A. Rose, and H. L. Penman, "Circulation of Water in Soil Under a Temperature Gradient," Nature, 205:314-316 (1965).

54. Jakob, Max, "Heat Transfer," Vol. I, John Wiley, New York (1949).

55. Jury, W. A., "Simultaneous Transport of Heat and Moisture Through a Medium Sand," Ph.D. Thesis, University of Wisconsin, Madison, Wisconsin (1973).

56. Jury, W. A. and E. E. Miller, "Measurement of the Transport Coefficients for Coupled Flow of Heat and Moisture in a Medium Sand," Soil Science Society of America Proceedings, 38:551-557 (1974).

57. Kay, B. D. and P. H. Groenevelt, "On the Interaction of Water and Heat Transfer in Frozen and Unfrozen Soils: I. Basic Theory; The Vapor Phase," Soil Science Society of America Proceedings, 38:395-400 (1974).

58. Kendrick, J. H., "Heat Budget of a Subsurface, Water Pipe, Soil Warming System," M.S.Ch.E. Thesis, University of Arkansas, Fayetteville, Arkansas (1972).

59. Kendrick, J. H., "Economic Analysis of a Subsurface Water Pipe, Soil Warming System," Chemical Engineering Department Report, University of Arkansas, Fayetteville, Arkansas (1973).

60. Kendrick, J. H. and J. A. Havens, "Heat Transfer Models for a Subsurface, Water Pipe, Soil-Warming System," Journal of Environmental Quality, 2(2):188-196 (1973).

61. Kuzmak, J. M. and P. J. Sereda, "The Mechanism by Which Water Moves Through a Porous Material Subjected to a Temperature Gradient, I: Introduction of Vapor Gap into a Saturated System," Soil Science, 84:291-299 (1957).

62. Kuzmak, J. M. and P. J. Sereda, "The Mechanism by Which Water Moves Through a Porous Material Subjected to a Temperature Gradient, II: Salt Tracer and Streaming Potential to Detect Flow in the Liquid Phase," Soil Science, 84:419-422 (1957).

63. Lavenda, B. H., "Thermodynamics of Irreversible Processes," John Wiley and Sons, New York (1978).

64. Letey, J., "Movement of Water Through Soil as Influenced by Osmotic Pressure and Temperature Gradients," Hilgardia, 39: 405-418 (1968).

65. Matthes, R. K., Jr. and H. D. Bowen, "Steady-State Heat and Moisture Transfer in an Unsaturated Soil," ASAE Transactions (1968).

66. Meixner, J., "Thermodynamik der Irreversible Prozesse," Aachen (1954).

67. Miller, D. G., "Thermodynamics of Irreversible Processes. The Experimental Verification of the Onsager Reciprocal Relations," Chem. Rev., 60:15-37 (1960).

68. Moench, A. F. and D. D. Evans, "Thermal Conductivity and Diffusivity of Soil Using a Cylindrical Heat Source," Soil Science Society of America Proceedings, 34:377-381 (1970).

69. Moore, N. R., Jr., "Simultaneous Heat and Mass Transfer in Moist Porous Media," Ph.D. Thesis, University of Arkansas, Fayetteville, Arkansas (1972).

70. Moore, N. R., Jr., "Simultaneous Heat and Mass Transfer in Moist Porous Media," Research Report Series--No. 16, Engineering Experiment Station, University of Arkansas, Fayetteville, Arkansas (1972).

71. Moore, R. E., "The Relation of Soil Temperature to Soil Moisture, Pressure, Potential, Retention, and Infiltration Rate," Soil Science Society of America Proceedings, 5:61-64 (1940).

72. Morrow, N. and C. Harris, "Capillary Hysteresis in Porous Materials," Society of Petroleum Engineering Journal, 5:15-24 (1965).

73. Nagpal, N. K. and L. Boersma, "Air Entrapment as a Possible Source of Error in the Use of a Cylindrical Heat Probe," Soil Science Society of America Proceedings, 37:828-832 (1973).

74. Onsager, L., Physical Review, 37:405 (1931), and 38:2265 (1931).

75. Parikh, R. J., J. A. Havens, and H. D. Scott, "Thermal Diffusivity and Conductivity of Moist Porous Media," Soil Science Society of America Journal, 43:1050-152 (1979).

76. Peck, A. J., "Change of Moisture Tension with Temperature and Air Pressure: Theoretical," Soil Science, 89:303-310 (1960).

77. Perry, R. H., C. H. Chilton, and S. D. Kirkpatrick, "Chemical Engineers' Handbook," 4th, McGraw-Hill, New York (1963).

78. Philip, J. R., "Evaporation, Moisture, and Heat Fields in the Soil," Journal of Meteorology, 14:354-366 (1957).

79. Philip, J. R. and D. A. deVries, "Moisture Movement in Porous Materials under Temperature Gradients," Transactions, American Geophysical Union, 38(2):222-232 (1957).

80. Prigogine, I., "Thermodynamics of Irreversible Processes," John Wiley and Sons, New York (1967).

81. Raats, P. A. C., "Transformation of Fluxes and Forces Describing the Simultaneous Transport of Water and Heat in Unsaturated Porous Media," Water Resources Research, 11(6):938-942 (1975).

82. Riback, W., "Simultaneous Heat and Mass Transfer in Porous Media," D. Eng. S. Thesis, Rensselaer Polytechnic Institute, Troy, New York (1968).

83. Rollins, R. L., M. G. Spangler, and D. Kirkham, "Movement of Soil Moisture Under a Thermal Gradient," Highway Research Board Proceedings, 33:492-508 (1954).

84. Rose, C. W., "Water Transport in Soil with a Daily Temperature Wave. I: Theory and Experiment," Australian Journal of Soil Research, 6:31-44 (1968).

85. Rose, C. W., "Water Transport in Soil with a Daily Temperature Wave. II: Analysis," Australian Journal of Soil Research, 6:45-57 (1968).

86. Sliepcevich, C. M. and H. T. Hashemi, "Irreversible Thermo-dynamics," Chemical Engineering Education, Summer:109-113 (1968).

87. Smith, W. O., "Temperature Transfer of Moisture in Soils," American Geophysical Union Transactions, 24:511-523 (1943).

88. Spanner, D., "The Active Transport of Water Under a Temperature Gradient," Society of Experimental Biology VIII, Active Transport: 76-93 (1954).

89. Srivastava, R. C. and P. K. Avasthi, "Non-Equilibrium Thermo-dynamics of Thermo-Osmosis of Water through Kaolinite," Journal of Hydrology, 24:111-120 (1975).

90. Taylor, S. A. and J. W. Cary, "Analysis of the Simultaneous Flow of Water and Heat with the Thermodynamics of Irreversible Processes," Transactions, International Congress of Soil Science, 7th, (1):80-90, Madison, Wisconsin (1960).

91. Taylor, S. A. and J. W. Cary, "Linear Equations for the Simul-taneous Flow of Matter and Energy in a Continuous Soil System," Soil Science Society of America Proceedings, 28:167-172 (1964).

92. Taylor, S. A. and L. Cavazza, "The Movement of Soil Moisture in Response to Temperature Gradients," Soil Science Society of America Proceedings, 18:351-358 (1954).

93. Topp, G. C., "Soil Water Hysteresis Measured in a Sandy Loam and Compared with the Hysteretic Domain Model," Soil Science Society of America Proceedings, 33:645-651 (1969).

94. Topp, G. C. and E. E. Miller, "Hysteretic Moisture Characteristics and Hydraulic Conductivities for Glass Bead Media," Soil Science Society of America Proceedings, 30:156-162 (1966).

95. Trezak, G. J. and D. Obeng, "An Analytical Consideration of Undersoil Heating," Journal of Environmental Quality, 2(4): 458-462 (1973).

96. Van Wijk, "Physical of Plant Environment," John Wiley and Sons, New York 1963).

97. deVries, D. A., "Some Remarks on Heat Transfer by Vapour Movement in Soils," Transactions, International Congress of Soil Science, 4th, (2):38-41 (1950).

98. deVries, D. A., "Simultaneous Transfer of Heat and Moisture in Porous Media," Transactions, American Geophysical Union, 39(5):909-916 (1958).

99. deVries, D. A., "Thermal Properties of Soils," In: Physics of Plant Environment, Van Wijk, editor, John Wiley and Sons, New York (1963).

100. deVries, D. A., "Heat Transfer in Soils," In: Heat and Mass Transfer in the Biosphere, I. Transfer Processes in Plant Environment, deVries, D. A. and N. H. Afgan, editors, Scripta Book Company (1975).

101. Waldron, L. J., J. L. McMurdie, and J. A. Vomocil, "Water Retention by Capillary Forces in an Ideal Soil," Soil Science Society of America Proceedings, 25:265-267 (1961).

102. Wechsler, A. E., "Glass Beads--A Standard for the Low Thermal Conductivity Range?", In: Thermal Conductivity Conference, 7th, editors, Flynn, D. R. and B. A. Peavy, Jr., National Bureau of Standards Special Publication 302 (1968).

103. Weeks, L. V., S. J. Richards, and J. Letey, "Water and Salt Transfer in Soil Resulting from Thermal Gradients," Soil Science Society of America Proceedings, 32:193-197 (1968).

104. Wei, J., "Irreversible Thermodynamics in Engineering," Industrial and Engineering Chemistry, 58(10):55-60 (1966).

105. Wescott, D. W. and P. J. Wierenga, "Transfer of Heat by Conduction and Vapor Movement in a Closed Soil System," Journal Article No. 456, Agricultural Experimental Station, New Mexico State University (1972).

106. Wierenga, P. J. and C. T. DeWit, "Simulation of Heat Transfer in Soils," Soil Science Society of America Proceedings, 34:845-848 (1970).

107. Wierenga, P. J., D. R. Nielsen, and R. M. Hagan, "Thermal Properties of a Soil Based Upon Field and Laboratory Measurements," Soil Science Society of America Proceedings, 33:354-360 (1969).

108. Wilkinson, G. E. and A. Klute, "The Temperature Effect on the Equilibrium Energy Status of Water Held by Porous Media," Soil Science Society of America Proceedings, 26:326-329 (1962).

109. Winterkorn, H. F., "Mass Transport Phenomena in Moist Porous Systems as Viewed from the Thermodynamics of Irreversible Processes," In: Water and Its Conduction in Soils, Highway Research Board, Commission on Physico-Chemical Phenomena in Soils, Special Report No. 40:324-337 (1958).

110. Woodside, W. and J. M. Kuzmak, "Effect of Temperature Distribution on Moisture Flow in Porous Materials," Transactions, American Geophysical Union, 39:676-680 (1958).

111. Sliepcevich, C. M., K. Starling, and J. A. Havens, "Thermodynamics of Continuous Systems," Air Force Office of Scientific Research Rpt. 563-66 (1969).

APPENDIX

CSMP PROGRAM FOR NUMERICAL INTEGRATION
OF IRREVERSIBLE THERMODYNAMICS
MODEL EQUATIONS

```
* CSMP PROGRAM FOR NUMERICAL INTEGRATION OF TAYLOR AND CARY EQUATIONS
*  FOR SPHERICALLY SYMMETRIC, STEADY STATE, HEAT TRANSFER IN A CLOSED
*  (JW=0.0), WATER UNSATURATED, GLASS BEAD POROUS MEDIA
*
* EQUATIONS SOLVED ARE FROM THIS REPORT, EQS. (5.4) AND (5.5)
*      JW=0.0=-RHOW*L22*(DTHETA+(BSTAR/T)*DT)
*      JQ=Q/(4*3.14*R**2=-RHOW*L22*B*DTHETA-L11*DT
*          WHERE   JQ=HEAT FLUX,CAL/CM**2 DAY
*                  RHOW=DENSITY OF WATER,GM/CM**3
*                  L22=DIFFUSIVITY,CM**2/DAY
*                  DTHETA= DERIVATIVE OF THETA WITH RESPECT TO R
*                  BSTAR=BETASTAR (EQ. 4.27)
*                  B=BETA (EQ. 4.23)
*                  DT=DERIVATIVE OF T WITH RESPECT TO R
*                  Q=HEAT FLOW RATE,CAL/DAY
*                  R=RADIUS,CM
*                  L11=THERMAL CONDUCTIVITY,CAL/CM DAY
*                  T=TEMPERATURE,K
*
RENAME TIME=R
INITIAL
FIXED I
* THE FOLLOWING FUNCTIONS SPECIFY THE FOUR PHENOMENOLOGICAL
*  COEFFICIENTS AS A FUNCTION OF MOISTURE CONTENT THETA
*      LL11=THERMAL CONDUCTIVITY,CAL/CM C DAY
*      LL22=DIFFUSIVITY,CM**2/DAY
*      LL21=CROSS COEFFICIENT LWQ,CM**2/DAY, (L22*BSTAR)
*      LL12=CROSS COEFFICIENT LQW,CAL/CM DAY, (RHOW*L22*B)
*
* THERMAL CONDUCTIVITY VERSUS MOISTURE CONTENT
FUNCTION LL11=(0.0,45.8),(0.05,116.6),(0.10,127.9),...
     (0.15,137.4),(0.20,144.3),(0.25,152.9),(0.30,162.4),...
     (0.35,170.2),(0.38,176.8)
*
* DIFFUSIVITY VERSUS MOISTURE CONTENT
FUNCTION LL22=(0.035,321.4),(0.045,573.1),(0.065,991.9),...
     (0.085,2486.5),(0.1,3388.1),(0.115,4424.0),...
     (0.13,5734.7),(0.15,7291.6),(0.17,8176.2),...
     (0.18,8268.6),(0.19,6500.1),(0.201,6450.6),...
     (0.215,6518.7),(0.235,9050.2),(0.255,15113.0),...
     (0.275,22654.6),(0.3,40894.1),(0.32,56896.1),...
     (0.345,82925.4),(0.36,134406.8),(0.375,216722.3),...
     (0.385,563266.3)
*
* COUPLING COEFFICIENT LWQ VERSUS MOISTURE CONTENT
FUNCTION LL21=(0.1,4506.2),(0.125,13802.0),(0.15,28728.9),...
     (0.175,35670.0),(0.2,38187.6),(0.225,44840.0),...
     (0.25,82500.0),(0.275,161980.4),(0.3,255179.2),...
     (0.325,330792.0),(0.35,381150.0),(0.36,131718.7),...
     (0.37,153720.0),(0.38,240000.0)
```

```
* COUPLING COEFFICIENT LQW VERSUS MOISTURE CONTENT
FUNCTION LL12=(0.1,4.04),(0.125,3.18),(0.15,2.42),(0.175,1.67),...
      (0.2,0.93),(0.225,0.68),(0.25,0.89),(0.275,1.1),(0.3,1.27),...
      (0.325,1.21),(0.35,0.95),(0.36,0.19),(0.37,0.13),...
      (0.38,0.08)
*
CONSTANT N=1,MIN=0.0,MAX=0.4
*
* HEAT TRANSFER RATE, CAL/DAY
CONSTANT Q=158000.0
*
* BOUNDARY CONDITIONS
* INNER SPHERE SURFACE TEMPERATURE
CONSTANT TO=315.5,T=315.5
*
* CONSERVATION OF MASS CONSTRAINT
CONSTANT MASS1=4082.0
*
* INITIAL GUESS OF THETA 1
CONSTANT TH1=0.1
      TH=TH1
DYNAMIC
*
* TRANSPORT PHENOMENOLOGICAL COEFFICIENTS TABLE LOOKUP
NOSORT
IF (R.EQ.0.0) THETA=TH1
      L11=AFGEN(LL11,THETA)
      L12=NLFGEN(LL12,THETA)
      L21S=NLFGEN(LL21,THETA)
      L21=L21S/T
      L22=NLFGEN(LL22,THETA)
SORT
*
* EQUATIONS (5.4) AND (5.5) ABOVE CAN BE SOLVED FOR DTHETA AND DT
*  TO GIVE THE FOLLOWING DIFFERENTIAL EQUATIONS
      DT=L22*Q/(4.0*3.14*(R+5.0)**2*(L21*L12-L11*L22))
      DTHETA=L21*Q/(4.0*3.14*(R+5.0)**2*(L11*L22-L21*L12))
*
* TEMPERATURE DISTRIBUTION
      T=INTGRL(TO,DT)
*
* MOISTURE CONTENT DISTRIBUTION
      THETA=INTGRL(TH,DTHETA)
*
* MASS OF WATER
      DMASS=4.0*3.14*(R+5.0)**2*THETA
      MASS=INTGRL(0.0,DMASS)
TERMINAL
```

```
*  SHOOTING METHOD FOR BOUNDARY VALUE DETERMINATION (SEE PAGE 26)
        N=N+1
        IF(N.GT.20) GO TO 3
        DIF=MASS-MASS1
        IF(ABS(DIF)-1.0) 3,3,4
4       IF(DIF) 2,3,5
2       MIN=TH
        TH1=MIN+0.618*(MAX-MIN)
        GO TO 6
5       MAX=TH
        TH1=MIN+0.382*(MAX-MIN)
6       CALL RERUN
*
3       CONTINUE
TIMER FINTIM=10.0
END
TIMER PRDEL=1.0,OUTDEL=1.0
PRTPLT T,THETA,MASS
END
STOP
ENDJOB
```